UNIVERSITY OF MANITOBA
WINNIPEG, MANITOBA

ULTIMATE STRENGTH ANALYSIS OF REINFORCED CONCRETE GRILLAGES

by

Wesley W. Dolhun, B.Sc. (C.E.)

A Thesis Submitted in Partial Fulfilment
of the Requirements for the Degree of Master of Science

Faculty of Graduate Studies and Research

Department of Civil Engineering

February, 1970

TABLE OF CONTENTS

TABLE OF CONTENTS CONTINUED

ABSTRACT

This dissertation deals with the assessment of the ultimate strength of conventionally reinforced concrete grillages, as occur in buildings and bridges, under concentrated loads and with particular emphasis on plastic hinge theory for grillages.

Two identical, $\frac{1}{4}$-scale models, were built in the laboratory for two tests. The first test involved applying a concentrated load at the center of the grillage. This test was performed in two sections. The first part proceeded until yielding occurred, and the second part proceeded to destruction. The second test involved applying a pair of concentrated loads to the interior longitudinal of the second grillage. This test continued until the mode of loading changed.

In the first test the collapse load was 1.30 times the load predicted by the method of combined ultimate design and plastic hinge theory. In the second test the collapse load was 1.23 times the predicted load. Increased concrete and steel strengths partially explained the increase in the collapse loads. Membrane and arching action in the interior grillage beams was also used to explain additional increase in the collapse loads. The concept of a hanging network of steel reinforcement was used to explain the large deflections. The behaviour of the two grillages under static load to destruction was also compared and discussed.

The test results from this study indicate that the combined ultimate strength and plastic hinge theory for reinforced concrete grillages is valid and safe, within certain limitations.

ACKNOWLEDGMENTS

The writer would like to thank all of those who have assisted in making this thesis possible. He is most grateful to the National Research Council of Canada for providing financial assistance for the laboratory investigation. Special consideration must be given to Dr. A. M. Lansdown, M.E.I.C., M.I.A.B.S.E., Head of the Civil Engineering Department, University of Manitoba, for his guidance and assistance throughout this project.

Sincere thanks are extended to the writer's collegue Mr. S. Teerachaichyuti for his help in testing the models.

To those in the Materials Testing Laboratory, Messrs. E. Lemke, D. Drul, R. Muir and H. Brooks the author expresses his thanks for their assistance in building equipment, test models, and in the actual testing.

LIST OF TABLES

LIST OF FIGURES

LIST OF FIGURES CONTINUED

LIST OF FIGURES CONTINUED

NOTATION

A_{cage} .....cross-sectional area enclosed by reinforcing cage

A_{sc} .....area of compression steel in beam

A_{st} .....area of tensile steel in beam

b .....width of beam

b'.....width of reinforcing cage

C .....circumference or perimeter of reinforcing cage

d .....overall depth of beam

d'.....depth of reinforcing cage

d_n .....depth of neutral axis of beam

$d_1, d_2 \ldots d_3$.depth to steel in levels 1,2....3

f'_c .....crushing strength of 6 x 12-in. concrete cylinders

f'_{pr}.....crushing strength of concrete prism

f_y, σ_y.....yield stress in steel

f_{st} .....stress in tensile steel

f_{yc} .....yield stress in compression steel

f_{yt} .....yield stress in tensile steel

F_y .....yielding strength in one steel bar

K .....coefficient

M .....bending moment in a beam

M_u .....ultimate moment of a beam

M_{IP} .....ultimate moment of an interior beam

M_{EP} .....ultimate moment of an exterior beam

M_T .....torsional moment in a beam

M_{ET} .....torsional moment in an exterior beam

$M_{T_{st}}$ .....total torsional moment developed by yielding steel (and its associated compressive concrete)

n .....integer

NOTATION CONTINUED

n_x.....number of helices in reinforcing cage

p .....pitch of transverse reinforcement

P .....concentrated load

P_u .....ultimate concentrated load

R .....yielding strength per unit width, in torsional reinforcement

u .....crushing strength of 6 x 6-in. concrete cubes

V .....shear stress

δ .....deflection

θ .....rotation

α .....empirical coefficient

β .....angle of helices in torsional reinforcement; empirical coefficient

$\emptyset$ .....diameter of steel bar

ε_c .....ultimate compressive strain in concrete

E.....modulus of elasticity

CHAPTER I

INTRODUCTION AND REVIEW

1.1 Introduction.

With the constant introduction of new and better construction materials, engineering research is, to a greater extent, playing an important part in developing new analytical theories and building techniques. The goal of any research is to develop a logical analytical system which ensures that a structure will have sufficient strength to resist a system of loads imposed upon it, and to transmit these loads safely to its foundations.

In the past the method of ensuring the strength of a structure was by means of linear elastic analysis, which limited the maximum elastic stresses to a desired fraction of the stress at which elastic behaviour terminated. The maximum allowable stress for mild steel was set at a percentage of the yield stress, whereas for concrete, a percentage of the cylinder or cube crushing strength determined the "allowable working stress". Thus for several decades the Theory of Elasticity governed engineering analysis.

In conjunction with the Theory of Elasticity, laboratory investigation helped to formulate empirical methods of design and analysis. These methods often required simplifying assumptions in order to develop a practical design method and, because of this, they were rather conservative and uneconomical.

The elastic method of analysis proved most efficient for simple determinate structures where the elastic strength and the real strength were related linearly. However, this linear relationship was not valid for indeterminate structures unless they were made of an elastic, brittle material

such as glass. In indeterminate structures constructed of mild and intermediate grades of steel, or where this type of steel is used as reinforcement in concrete, the "plastic" behaviour of this material permits the redistribution of stress at high loads. The ability of a ductile material such as mild steel, with its reserved strength, to redistribute load from high stress regions to less highly stressed areas was not readily recognized in practice, except in such classical examples as steel rivet groupings and fillets.

In the 1920's and 1930's it was recognized that elastic analysis of indeterminate structures produced excess strengths and investigations began to find the true ultimate strengths of such structural systems. However, it was not until after the Second World War, when building materials were in short supply, particularly in Europe, that the popularity of ultimate strength methods of analysis gathered momentum.

The use of Ultimate Strength Design for reinforced concrete has finally been recognized as more consistent than Elastic Design. Ultimate Strength Design recognizes the actual behaviour of a reinforced concrete member at ultimate capacity, and it is the only method that predicts the strength of a section. A specified overload factor is applied to each service load to obtain the desired ultimate load capacity. As the overload factor is used to design for the actual ultimate strength, a uniformly consistent, more accurate, safety factor will be obtained for all units of a structure. Elastic Design, or Working Stress Design, uses allowable stresses with the straight-line theory and the actual factor of safety is obscured and may vary widely with different types of members. With Ultimate Strength

Design it is permissible to apply a lower load factor to dead load than to live load, which is logical and desirable, as the dead loads to which a member is to be subjected are usually known with greater precision than live loads. Different load factors for live and dead load lead to a more realistic safety factor. Another advantage of Ultimate Strength Design is that it generally will result in more economical structures with safety uniform at all points. It allows full utilization of higher strength steels and concretes, whereas Working Stress Design underestimates the contribution of higher strength steels. Under Ultimate Strength Design, strength is of prime importance and serviceability and appearance are secondary.

Even though Ultimate Strength Design is slowly replacing Working Stress Design for simple designs, North American building codes still prescribe an elastic analysis for all indeterminate concrete structures. For buildings of the usual type of construction, spans, and story heights, codes permit the use of approximate methods of analysis for the determination of elastic moments and shears within certain ranges of variation in span lengths and loads. When the external moments and forces in a structure have been determined by the theory of elastic frames, the design of sections can proceed using Ultimate Strength Design.

Engineers are increasingly becoming aware that the behaviour of individual members in any composite structure is that of the structure as a whole, rather than that of separate units. The importance of considering the composite behaviour of the complete structure under load in both elastic and ultimate analyses is evident. It is easy to see that this type of analysis is rather difficult and it is only comparitively recently that composite action in structures has been studied in detail.

In understanding the strength of composite reinforced concrete structures, the study of flexural grillages in-

creases our knowledge of the subject as it plays an important part in both buildings and bridges. In the past, however, in the analysis of buildings the skeletal framework has been isolated from the structure as a whole and then calculations have been made on the framework alone. In bridge work, where the main and transverse beams more clearly define a grillage, composite action between beams and slab has quite frequently been considered. However, where composite action has been used in analysis of bridge decks the usual method has been the equivalent T-beam system, which is in effect the grillage approach.

The strength analysis of a plastic grillage is governed by the principles of limit analysis[a]. A correct solution is found when coincident upper and lower bound solutions have been obtained. The analysis of grillages by the plastic hinge method is dependent on the existence of sufficient plastic rotational capacity at each hinge to enable the complete mechanism to form without premature failure. Sufficient plastic rotational capacity exists in hinges of under-reinforced concrete beams. However, for beams having high flexural steel ratios or when considering torsion hinges, extreme caution must be exercised. Also it is not permissible to include the brittle strength of a member in such an analysis unless it can be shown that the "brittle hinge" is the last to form[b]. In cases where brittle "hinges" are included in the strength analysis, failure will be catastrophic. Due to the high load factor recommended in cases of this nature[c], it may be preferable to assume a plastic hinge strength of zero at the brittle hinges and calculate the smaller but non-catastrophic plastic failure strength.

1.2 Review.

The amount of experimental work done on the composite action of reinforced concrete grillages has been extremely small. The earliest work done in this field was by Nylander[d]. He performed two tests on reinforced concrete grillages in 1945. Each of the grillages was comprised of five beams and was supported at four points. The grillages were tested by loading the secondary beam at two central points. The results indicated that a failure load greater than that predicted by limit analysis was obtained and that torsional rotations in the grillages were from three to six times those observed in torsional control tests.

Work related to this study was also done by Heyman[e,f], who described a method for the limit design of transversely loaded square grids. He made the usual assumptions of plastic theory as applied to steel structures. However, the fundamental assumption that full moment redistribution occurs may lead to error if applied to concrete grillage structures where torsion failures are possible. A.L.L. Baker[g], in considering the design of reinforced and prestressed concrete frames, considered it necessary to calculate rotations in plastic hinges and proposed a method of doing this.

Another series of tests on concrete grillage bridges, known to the writer, was performed by Reynolds[b]. In his research Reynolds used nine small scale prestressed bridges, comprising a preliminary structure, six right bridges, and two skew bridges. Good agreement was found between analytical results and experiment, with the ultimate load of each of the bridges tested slightly in excess of the estimated

ultimate load. In Reynolds' analysis, however, the strength of brittle torsion "hinges" was included. These hinges were fortunately the last to form and the calculated load was realized. For all of the grillage bridges there was a decrease in strength after the maximum load was reached. This decrease was most severe in one of the skew grillages tested and was to be expected as a skew structure carries more load through torsion than does a right grillage. Reynolds' tests also serve to show that in order to develop a plastic failure, adequate shear strength is required.

More recently a series of concrete grid frame and beam tests, similar to those conducted in this study, were performed by Klus and Wang[h]. Using computer analysis and model tests, it was indicated that moment distribution in grid frames could be predicted within ± 15 percent using the displacement method analysis and including the effects of torsion. If torsion was neglected in the analysis, it was found large errors could occur for certain loading conditions.

1.3 Object of the Tests.

The purpose of this study was to examine the design of right-angled concrete grillages using ultimate strength analysis in combination with a plastic hinge theory and to compare the theoretical with the actual test results. Certain contingencies were accounted for; the main beams were made rigid enough so that plastic hinges would form in the secondary interior beams, and also enough shear reinforcement was placed in all beams so as to ensure adequate shear strength. The behaviour of the structure was also to be observed.

It was hoped that the results of this study would aid in the understanding of reinforced concrete beam and slab composite structures. In conjunction with research done by Lansdown[i] and other studies initiated at the University of Manitoba[j,k], a valid method of predicting the ultimate strength of composite structures could, in time, be achieved.

The study itself included the building and testing of two identical $\frac{1}{4}$-scale model grillages. The results of the two tests to destruction, under different loading conditions, were then analyzed.

HISTORICAL BIBLIOGRAPHY

(a) Greenberg, H.J. and Prager, W. — "Limit Analysis of Beams and Frames". Proceedings A.S.C.E., v. 77, St. 59, Feb. 1951, pp.12.

(b) Reynolds, G.C. — "The Strength of Prestressed Concrete Grillage Bridges". London, Cement and Concrete Association, TRA/268, June 1957.

(c) — Report of a Committee on Structural Safety. The Structural Engineer, v. 33, n. 6, June 1955.

(d) Nylander, H. — "Torsion and Torsional Restraint of Concrete Structures". Statens Kommitte for Byggnadsforskning, Meddelanden No. 3, 1945, pp.138.

(e) Heyman, J. — "The Limit Design of Space Frames". Journal of Applied Mechanics, v. 18, n. 2, June 1951, pp.157-162.

(f) Heyman, J. — "The Limit Design of a Transversely Loaded Square Grid". Journal of Applied Mechanics, v. 19, n. 2, June 1952, pp.153-158.

(g) Baker, A.L.L. "The Ultimate-Load Theory Applied to the Design of Reinforced and Prestressed Concrete Frames". 1st. Edition, London, Concrete Publications Ltd., 1956.

(h) Klus, J.P. and Wang, C.K. "Torsion in Grid Frames". Torsion of Structural Concrete, A.C.I. Publication SP-18, 1968, pp. 89-101.

(i) Lansdown, A.M. "An Investigation into the Ultimate Behaviour of Reinforced Concrete Beam and Slab Structures, in particular Bridge Decks". Ph.D. Thesis, University of Southampton, June 1964.

(j) Yih, J.C. "Model Studies of Reinforced Concrete Skew Slab and Beam Bridges Under Ultimate Loads". M.Sc. Thesis, University of Manitoba, March 1967.

(k) Teerachaichayuti, S. "A Study of Reinforced Concrete Beam and Slab Bridge Decks under Ultimate Loads". M.Sc. Thesis, University of Manitoba, April 1968.

CHAPTER II

DESIGN OF GRILLAGES

2.1 General Considerations.

In order to test further the validity of the proposed method of analysis for reinforced concrete grillage systems, two $\frac{1}{4}$-scale models of a typical simply supported grillage system were built and tested. These grillage models could represent either a two-lane highway bridge or a structural framework in a building.

The two structures were tested to destruction under two different loading conditions. The first model was tested using a single concentrated load applied at the center. The second model was tested using two concentrated loads applied along the interior longitudinal. These concentrated loads were applied through steel blocks, 3 inches square. It was considered that concentrated loads represented the most severe loading condition that any beam and girder structure would be required to resist. The locations of the load points for each of the tests are shown in Figures 1 and 2, page 11.

In designing the grillage models, the main exterior beams were purposely made extremely rigid. This was done so that all of the plastic hinges would form in the interior secondary beams. In this way, plastic hinge formation and beam deflections could be observed fairly easily in locations predicted by the collapse theory. A layout for both grillages is shown in Figure 3, page 12.

2.2 Description of Grillage.

The two grillage models were not intended to be examples

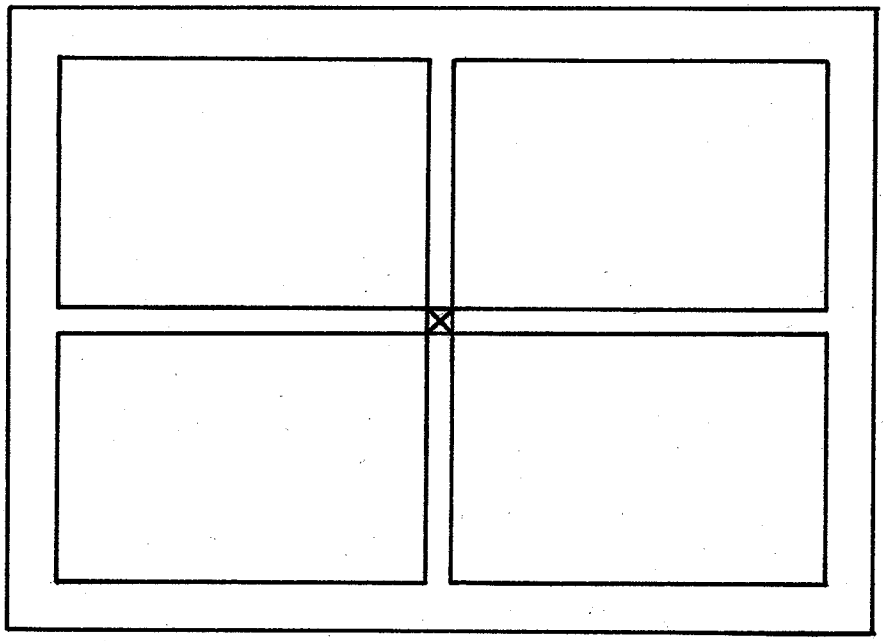

Figure 1. Load Point, Test No. 1

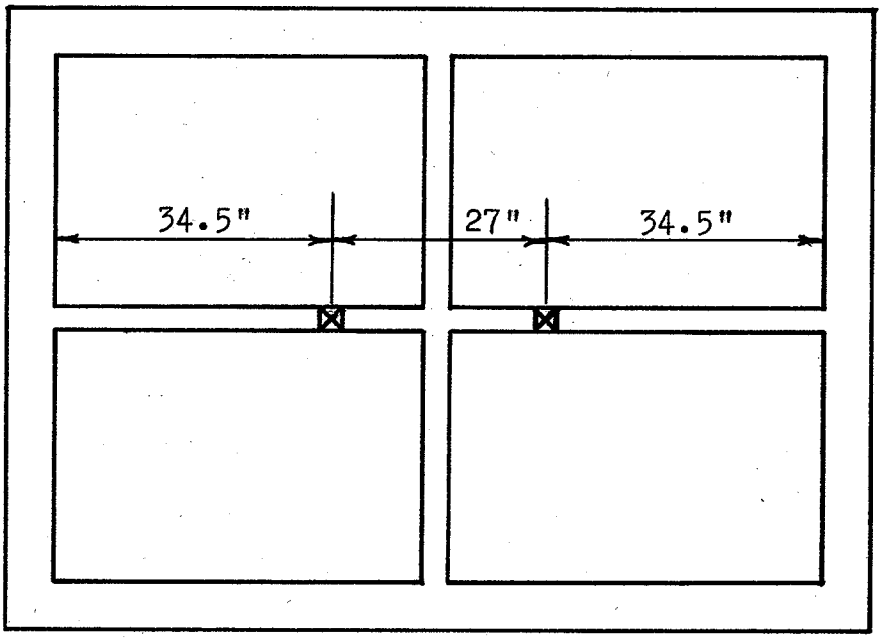

Figure 2. Load Points, Test No. 2

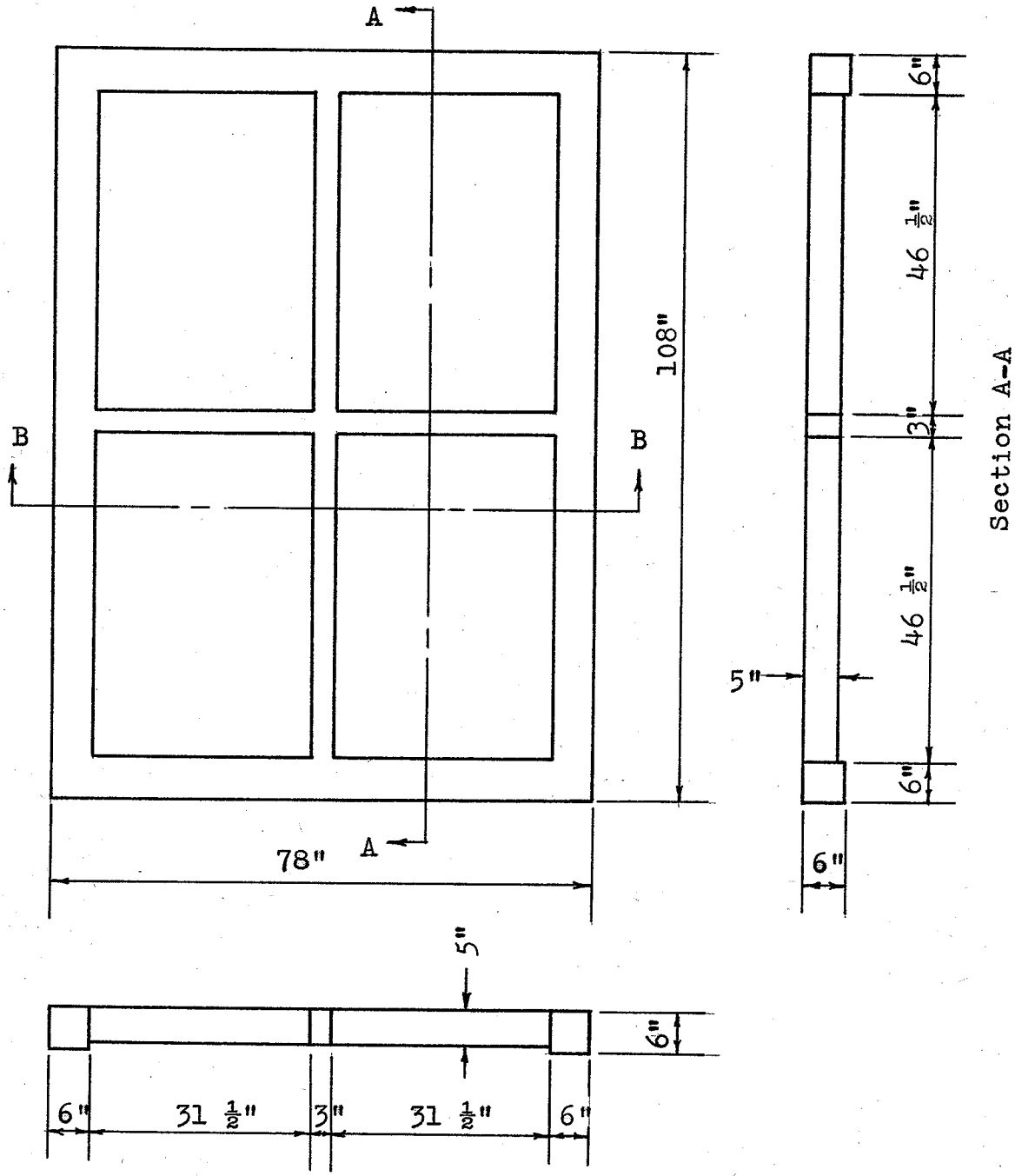

Figure 3. Model Diagram.

of a particular structure. They were chosen to represent simple cases of grillages with rigid edge beams. The models were designed independently and were not scaled down from any prototype. Scale relations are important in model tests, however, and in the next section various relationships are listed.

A framework of this type could be used either in bridge or building construction. It is apparent, however, that in most cases a floor or roadbed system will cover this type of frame in practice. Two types of systems could be used. The covering could be either integral with the frame or it could be precast units which are essentially self-functioning. The type of covering would dictate the type of analysis such a composite structure would require.

2.3 Scale Relations.

When testing a model of a full scale structure, the factors governing the collapse of the model such as stress, strain, and loading do not scale down as readily as linear dimension.

The scale relationships between the model and a full scale structure are as follows:

(a) All linear dimensions are $\frac{1}{4}$ as large in the model as in the actual structure.

(b) Concentrated loads are $(\frac{1}{4})^2$ as large for the model as for the actual structure.

(c) Beam dead loads are computed from the model.

(d) Steel cross-sectional areas are computed from the model.

The various relationships between a full scale structure and the models are shown in Table I, page 14.

Table I. Scale Relationships.

	Model	Prototype
Span Length	102"	34'
Width	78"	26'
Main Beam Spacing	72"	24'
Beam Sections	6"x 6"	24"x 24"
	3"x 5"	12"x 20"
Concentrated Load	$(\frac{1}{4})^2 P$	P

2.4 Design of Models.

Ultimate Strength Design of Models.

Both of the grillage models used in the tests were designed using a combination of ultimate strength analysis and plastic hinge theory. The ultimate strength analysis of reinforced concrete beams is well established[1,2,3,4]. A method of analyzing beam systems for steel structures has been well established and published by Professor J.F. Baker and his colleagues at Cambridge[5]. This work has done a great deal to promote the use of ultimate load analysis in the design of steel structures, but so far this type of analysis has rarely been applied to reinforced concrete structures. The reason for this is that doubt still exists as to whether or not sufficient rotation can be obtained from a reinforced or prestressed concrete structure to allow all the plastic hinges to form before failure of one of these hinges occurs. This is no problem in a steel structure which has ample plasticity. One of the main aims

of this study is to show that enough ductility can be achieved in reinforced concrete structures to permit plastic hinges.

Several methods can be used to increase the ductility of a concrete section. One method of achieving this is to insure that bars are adequately anchored. Another method is to have sufficient shear reinforcing in the form of spirals and closed ties or stirrups.

If therefore, in the analysis, it is assumed at failure that the resistance moment at each plastic hinge is the ultimate moment of that section, this presumes that sufficient rotation will occur to allow the last hinge to form before any of the other hinges fail. A series of tests devised and carried out by Ernst[6] seem to indicate that sufficient rotation will always be achieved with reinforced concrete sections; and a further extensive series of tests initiated by the European Committee for Concrete is already under way. As mentioned earlier, doubt still exists as to whether the above assumptions are valid. Researchers such as Mattock[22] emphasize that the strains that can be developed in the concrete and reinforcing steel in a reinforced concrete member are considerably less than those which can be developed in a mild steel member. Consequently, instances can occur in which the strain capacity of a reinforced concrete hinging section is exhausted before full redistribution of bending moments is achieved in the structure as a whole. Mattock believes that it is necessary to consider the deformation of the hinging regions and to limit their rotation to known safe values. If, however, we proceed on the assumption that all hinges can rotate sufficiently, ultimate load analysis can be carried out in two ways -- virtual work and equilibrium.

As with beams, a plane frame is analyzed when it is subjected to the working load multiplied by an appropriate

load factor. Under the loading configuration a system of hinges is selected which will allow the structure, or part of the structure, to fail. This is equivalent, in slab analysis, to selecting a yield-line pattern. Some point of the structure is then given a virtual displacement and by the method of virtual work an equation is obtained relating the moments in the plastic hinges to the value of the applied loads. With slabs, this equation is regarded as the solution, since except in the simplest cases it is not possible to prove that this solution is the most critical. However, with frames, it is possible to find if this solution is the most critical. The solution obtained by virtual work can therefore be regarded as the upper bound value of the collapse load.

In order to investigate whether the selected pattern of hinges is the most critical, the equilibrium of the frame can be checked to find whether or not the collapse mode is a statically admissible system. This merely entails checking by equilibrium that the ultimate strength of the various sections is not exceeded. The solution thus obtained by equilibrium is a lower bound value of the collapse load. If the lower bound has the same value as the upper bound, this solution is the correct one or an admissible system, if it is not, the selected hinge pattern is incorrect and the process must be repeated with a new system of hinges. Any bending moment distribution such that at no cross-section does the bending moment exceed the limit moment for the cross-section is called an "admissible" distribution of bending moments. It is for this reason that in the analysis of the grillages under consideration, the end moments in the exterior beams have been assigned a value of zero rather than some other arbitrary value.

When planning this study, the prime consideration in designing the model grillages was to have all of the plastic

hinges forming in the secondary interior members. With the one concentrated load at the center, the failure mode that was desired can be seen in Figure 4, page 18. The exterior longitudinals and transversals were designed to remain rigid and strong enough so that neither torsional nor bending hinges would appear at connecting points with the interior members. Upon completion of the first test it was seen that the exterior members were perhaps too rigid and repetition of the first loading mode would serve no useful purpose. It could readily be seen that the same collapse mechanism would form and no new information would be obtained. It was at this time that a double concentrated load system along the interior longitudinal was considered. The expected failure mode for this loading combination can be seen in Figure 5, page 18.

In general the plastic design of the beams followed the British system with particular reference to Jones[7]. In his work Jones uses the test results of Hognestad, Hanson and McHenry[4] in dealing with the distribution of stress in the compression zone of reinforced concrete beams, as well as the ultimate compressive strain at beam failure. The torsional strength of the exterior beams was based on a method by Lansdown[8]. Although some investigations by Nylander[9] and by Cowan and Armstrong[10] indicate that small amounts of bending do not materially decrease torsional strength, the exterior beams were made strong enough in torsion to take into account any unknowns.

Current design codes were used to determine the properties of the concrete and steel. In the initial calculations a cylinder compressive strength of 3000 psi. was used for the concrete and the steel was assumed to have a yield stress of 40,000 psi.

Moments and steel percentages were calculated for individual beams. When the various failure modes were examined,

it was necessary to check if beam strengths were adequate. Detailed calculations for the various beams are shown in Appendix A, page 107.

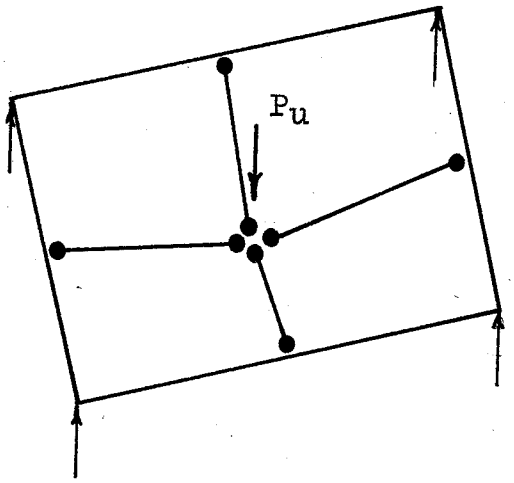

Figure 4.
Probable Failure Mode for Test No. 1.

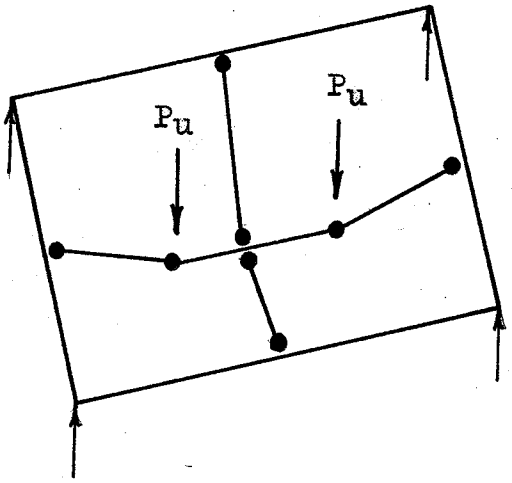

Figure 5.
Probable Failure Mode for Test No. 2.

CHAPTER III

MODELS AND LOADING APPARATUS

3.1 Construction of Models.

Two reinforced concrete grillage models were constructed for testing. As previously mentioned, both models were designed using ultimate strength techniques and were identical in all respects. Details concerning model size and appearance were given in the previous chapter. Table I, page 14, gives data on model scale relations and Figure 3, page 12, shows a plan of the models.

Preparation for the pouring of concrete was started by building a collapsible wooden form for the grillage models. The form was constructed of 3/4 inch plywood cut to size and held together by steel angles and screws. The design of the form allowed for easy dis-assembly so that the same form could also be used for the second grillage. All of the form's interior construction joints were covered with masking tape in order to help retain moisture during the curing period. The interior of the form was also shellacked and just prior to the pouring of concrete, the form was lightly oiled. The assembled form appears in Figure 6, page 20.

The steel reinforcing cage was identical for both models. Figure 7, page 20, shows a completed cage. The steel reinforcing was assembled outside the wooden form and close checks were kept on dimensions to ensure that the cage would fit into the form when completed. The building of the reinforcing cage was a very delicate operation as tolerances were very small.

Exterior beam reinforcing consisted of four #4 bars top and bottom as the main steel. A cross-section of an

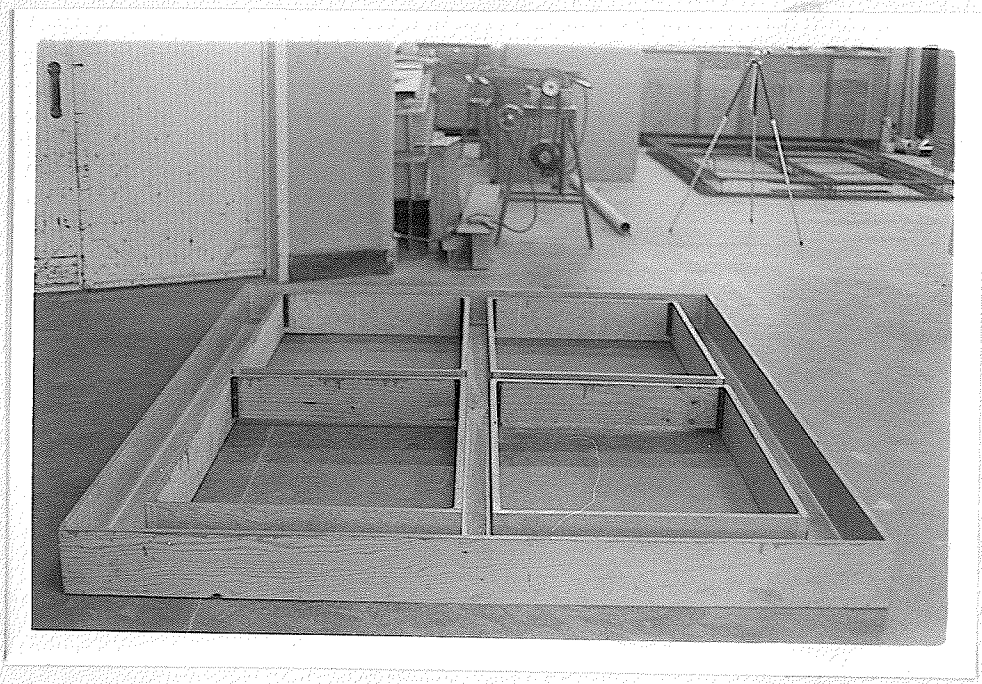

Figure 6. Plywood Form for Grillage Model.

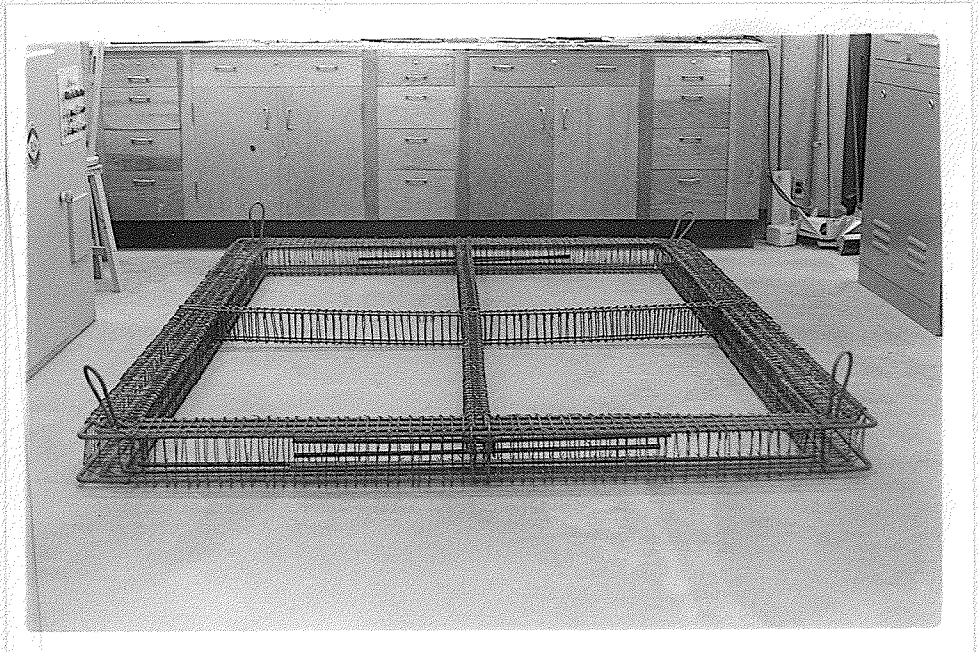

Figure 7. Reinforcing Cage for Grillage Models.

exterior beam showing main steel and ties can be seen in Figure 8, page 22. Two #4 bars, with two 90° bends in each, formed closed loops in the exterior beams. Eight such sets, four top and four bottom, constituted the main steel reinforcing for the main beams. The splices in these loops were located in regions where moments were considered to be minimal or nil. The 90° bar bends did not conform to standard practice as the actual bends were much sharper than those recommended by the American Concrete Institute[16]. A plan view of a corner detail can be seen in Figure 10, page 24. The sharp bends were required because of the relatively small cross-sectional area and the large amount of steel. It was felt that for test purposes, this procedure would not effect test results to any great extent. Figure 10, page 24, also shows the #10 wire ties used diagonally at all corners.

The interior beam reinforcing consisted of two plain #2 bars top and bottom. Figure 9, page 23, shows a cross-section of the interior beams. The #2 bars were all well anchored in the exterior beams. The top #2 bars were wrapped, in stirrup fashion, around the main exterior beam steel as shown in Figure 11, page 24. The bottom #2 bars were bent around four #4 dowel bars which generated enough bond strength to guarantee against pull-out. These dowel bars can be seen in Figure 7, page 20. This elaborate procedure was followed to ensure that bond failure would be no problem at beam junctions, as well as to increase the ductility of the section at the connection. Figure 12, page 25, gives an excellent plan view of the center of the grillage where the transversal and longitudinal cross. The figure shows tie spacing as well as the amount of clearance between the steel cage and the form.

The shear steel in both the exterior and interior beams consisted of #11 gauge steel wire ties at intervals of one

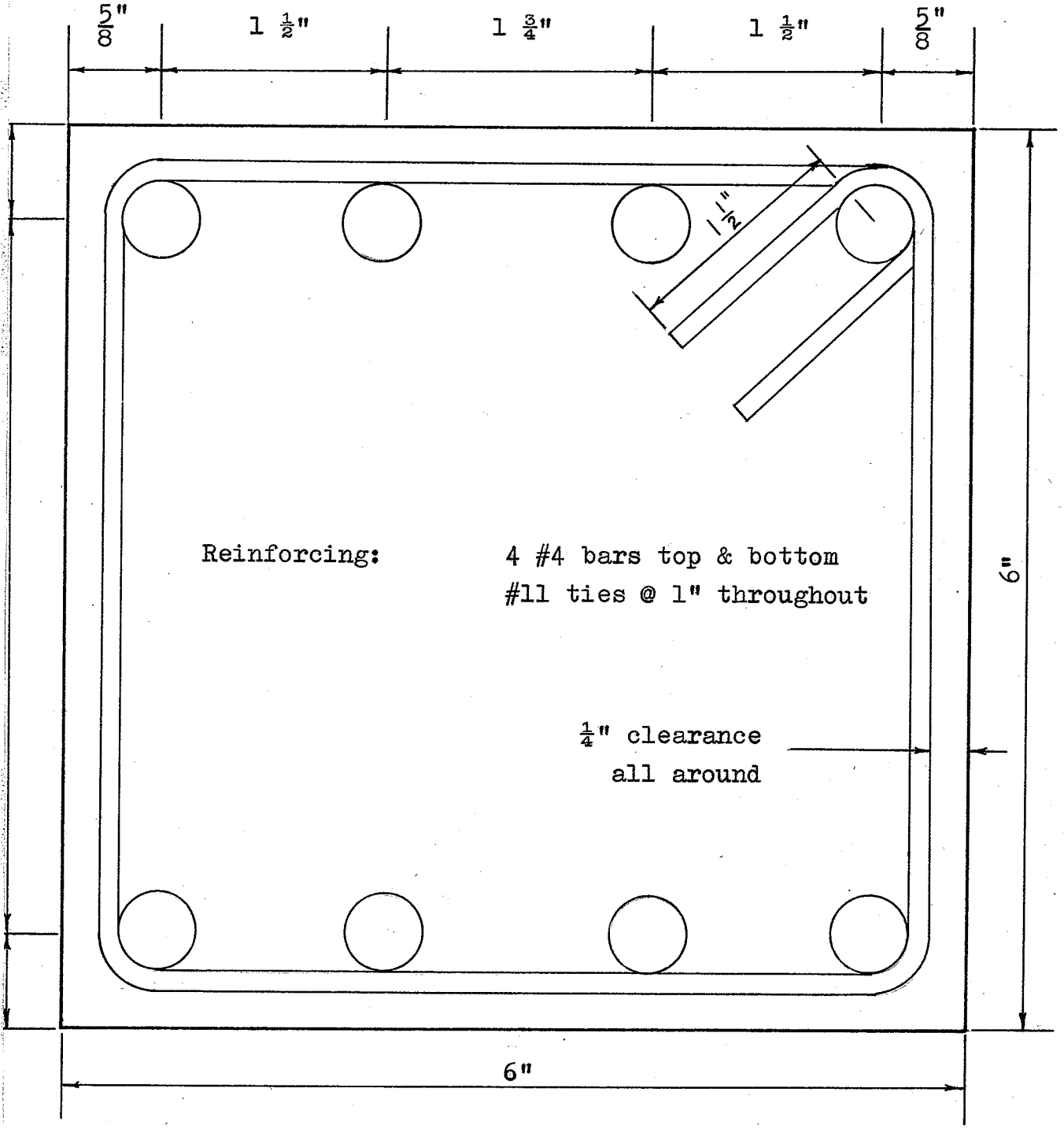

Figure 8. Cross-Section of Exterior Beams.

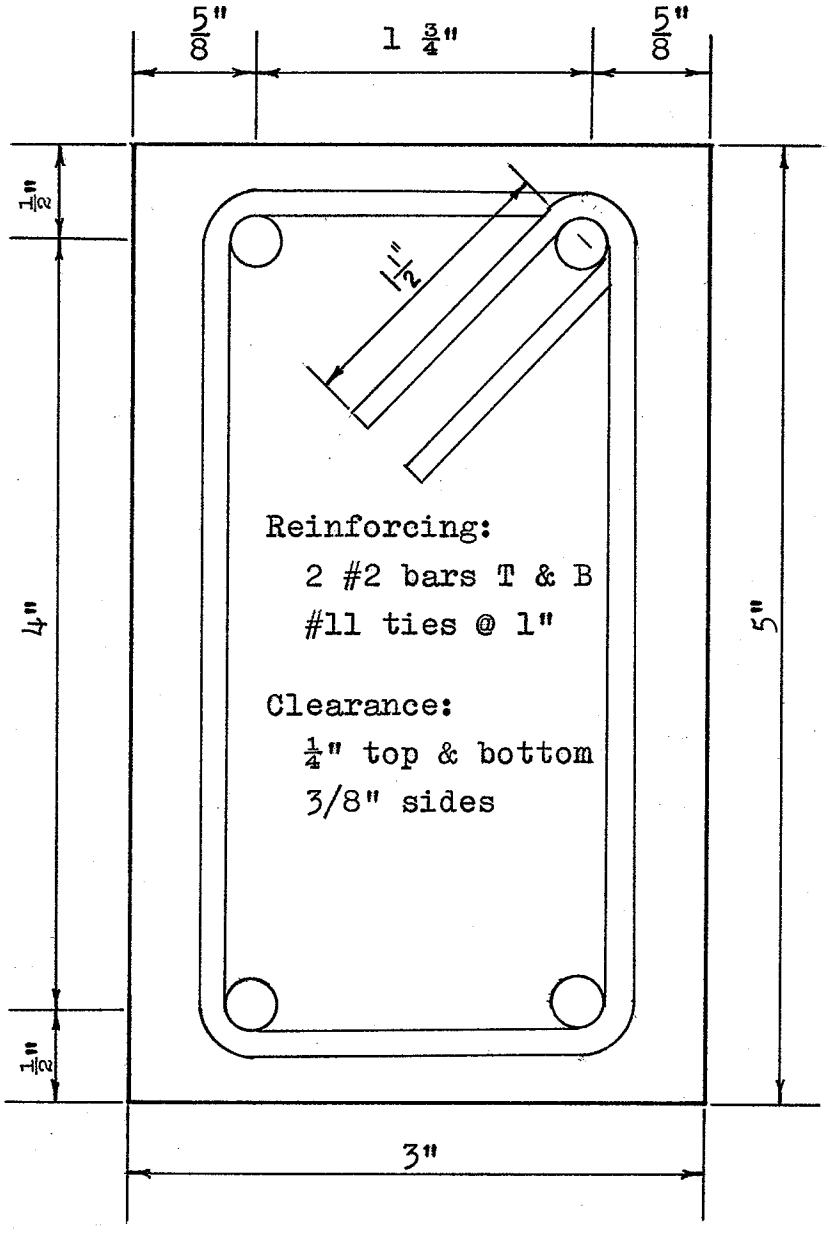

Figure 9. Cross-Section of Interior Beams.

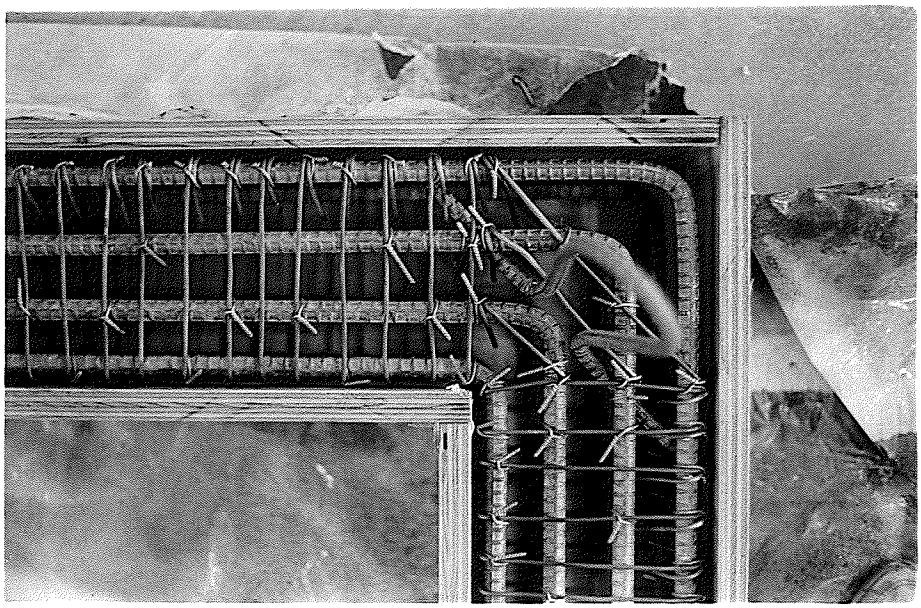

Figure 10. Plan View of Corner Detail.

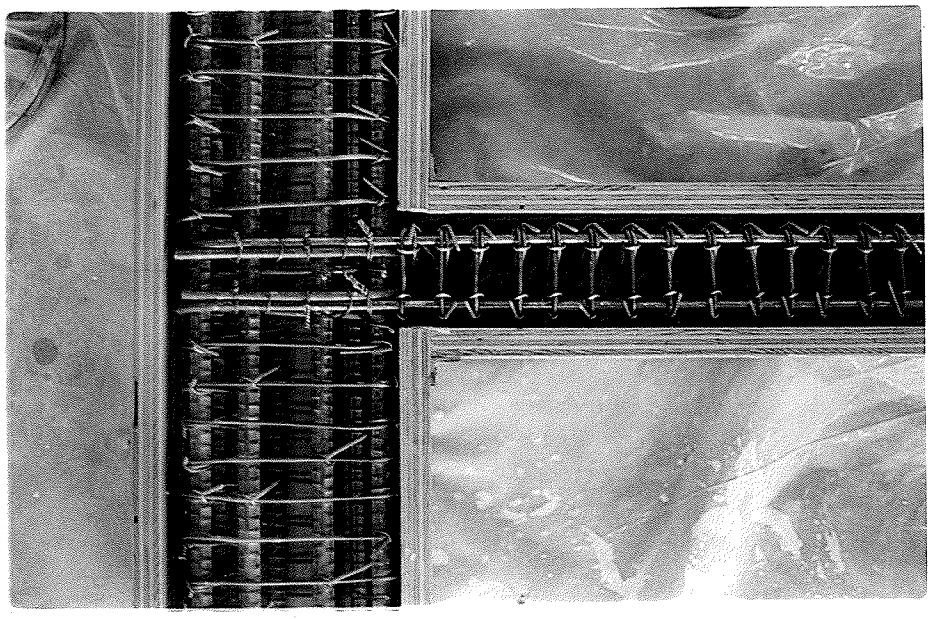

Figure 11. Anchorage of Interior Beam Top Bars.

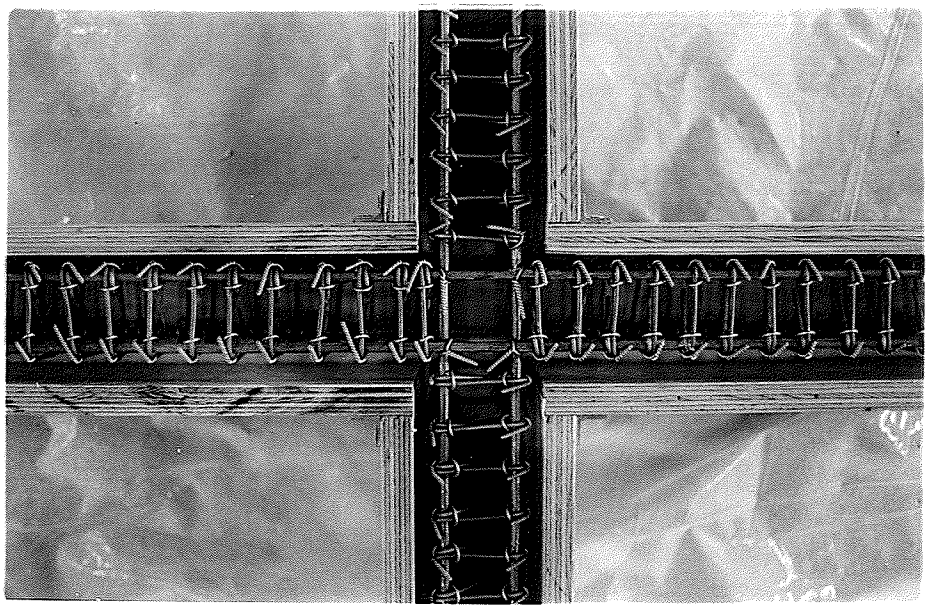

Figure 12. Plan View of Grillage Centre.

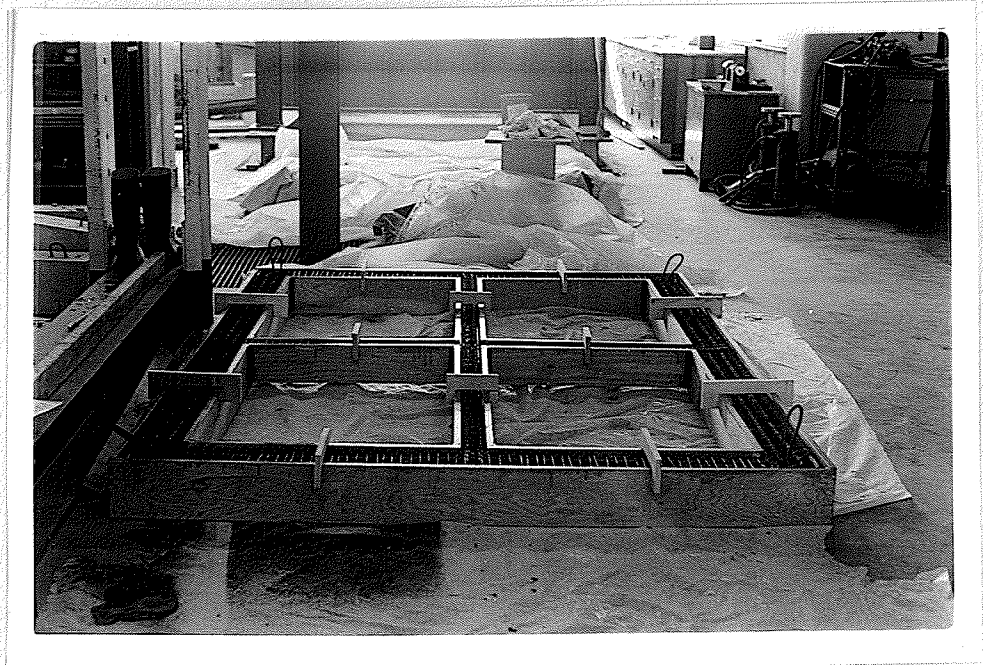

Figure 13. Grillage Model Ready for Concrete.

inch. Such close stirrup or tie spacing was used to ensure that shear failure would not occur before the collapse load. As mentioned previously, #10 gauge wire ties were also used at the corners. In order to facilitate handling, #3 bars, in the form of hooks, were placed in each corner of the models. These handling hooks can be seen in Figure 13, page 25, which shows a grillage model ready for concrete. The brackets, also appearing in this figure, were used to prevent the plywood form from bulging due to the concrete.

The concrete mix design used for the two test models was the same. In general, a 3000 psi., non-air-entrained concrete with a slump of 5 to 6 inches was selected. The water/cement ratio of the mix was 0.55. The maximum aggregate size was limited to 3/8 of an inch. High early strength Portland Cement was also used for both models.

The concrete was mixed in a laboratory counter-current rapid mixer in batches of 3.5 cubic feet. Three batches were required for each grillage model, and two standard cylinder samples were taken from each batch. The concrete was trucked from the mixer to the form in wheelbarrows and the concrete then shovelled into the form. Because of the close knit steel cage, the concrete had to be thoroughly vibrated into place using a 3/4 inch, square head vibrator. The vibrator fitted quite well between the main steel and the ties and even though a great deal of vibration was required, later cuts through the members showed that there was no noticeable segregation.

Slight trowelling was required to get an even top surface, and after several hours when the concrete had set slightly, the curing process began. Curing involved covering the entire model with wet burlap and plastic sheeting for a period of seven days. The burlap was watered down every day in order to ensure that it remained moist. After the seven day period, the models were removed from

the form and cured in the open air until the tests were run.

3.2 Properties of Materials.

Tension tests were performed on samples of each reinforcing bar used in both grillages. Tension tests were also performed on samples of the #11 gauge wire used as ties on the beams and the #10 gauge wire used as ties at the corners. The properties of the steel are shown in Table II, page 28. The wire, $\frac{1}{4}$-inch and $\frac{1}{2}$-inch bars all exhibited a horizontal yield plateau followed by considerable strain hardening and elongation before failure. Yield points for all bar specimens were found by the "half of the pointer" method. All steel specimens tested showed sufficient ductility and percent elongation over an 8 inch length averaged over 20 percent.

The concrete mix design for the two grillages was the same. The concrete had an aggregate/cement ratio of 5.4 and a water/cement ratio of 0.55. Slight differences in the amounts of water used for different batches were necessary to compensate for free moisture in the aggregate and to keep the workability of the various batches approximately the same. Two standard test cylinders were cast from each 3.5 cubic foot batch. The properties of the concrete were obtained from compression tests and split cylinder tension tests of the 6" x 12" cylinders. Tests for concrete strength were made at 7 days and at the time of testing of each model. The results of the tests are listed in Table III, page 29.

3.3 Loading Apparatus and Instruments.

The steel loading frame used for the tests was a free standing, stiff structural-steel reaction frame. The frame appears in Figure 17, page 34. This reaction frame, in ef-

TABLE II. Properties of Steel.

Model No.	No. Tested	Mean Diameter (in.)	Mean Area (in^2)	Av. Yield Load per bar(lb.)	Av. Ultimate Load per bar(lb.)	Av. Yield Stress per bar(psi.)	Av. Failure Stress per bar(psi.)	% Av. Elong. over 8"
No. 1								
½" Ø	16	.500	.200	9,850	15,140	49,250	75,700	22
¼" Ø	8	.250	.050	1,920	2,580	38,400	51,600	20
11 Ga.	6	.116	.010	341	566	34,100	56,600	26
No. 2								
½" Ø	16	.500	.200	10,050	15,265	52,500	76,300	21
¼" Ø	8	.250	.050	3,265	3,970	65,300	79,400	23
11 Ga.	11	.117	.010	396	577	39,600	57,700	19.6
Both								
10 Ga.	2	.126	.0125	490	730	39,200	58,400	18.5

TABLE III. Properties of Concrete.

Structure	Days	Average Compressive Strength (psi.), fc. 6" x 12" Cylinder	Average Tensile Strength (psi.), ft. 6" x 12" Cylinder
No. 1	7	3,830	----
	At time of testing (76 days)	6,060	440
No. 2	7	3,890	412
	At time of testing (155 days)	5,290	652

fect a portal frame, consisted of two columns connected at the top by four channels, two on each side, and anchored at the bottom to two heavy steel beams, which comprised the base of the frame. The two large welded steel beam abutments, upon which the model was supported, were also anchored to the beams forming the base of the frame. Load was applied to the model by a hydraulic, hand-operated jack with a maximum capacity of 200 kips. Two methods were required to indicate the applied load. For the lower applied loads a hydraulic pressure cell, attached to the hydraulic line, and used in conjunction with a Budd strain indicator gave the desired load readings. When the pressure cell's capacity was exceeded, a valve was turned to keep it from becoming damaged and a pressure dial gauge was used to indicate applied load. The pump, Budd strain indicator and pressure dial gauge can be seen in Figure 14. Both of these systems were calibrated against a 200 kip testing machine in order to obtain the relationship between the applied load and gauge readings. The calibration curve of the pump and hydraulic strain equipment is shown in Figure 15, page 31. Figure 16, page 32, shows the calibration curve of the pump and pressure dial gauge.

Figure 14. Pump and Load Indicating Apparatus.

Figure 15.

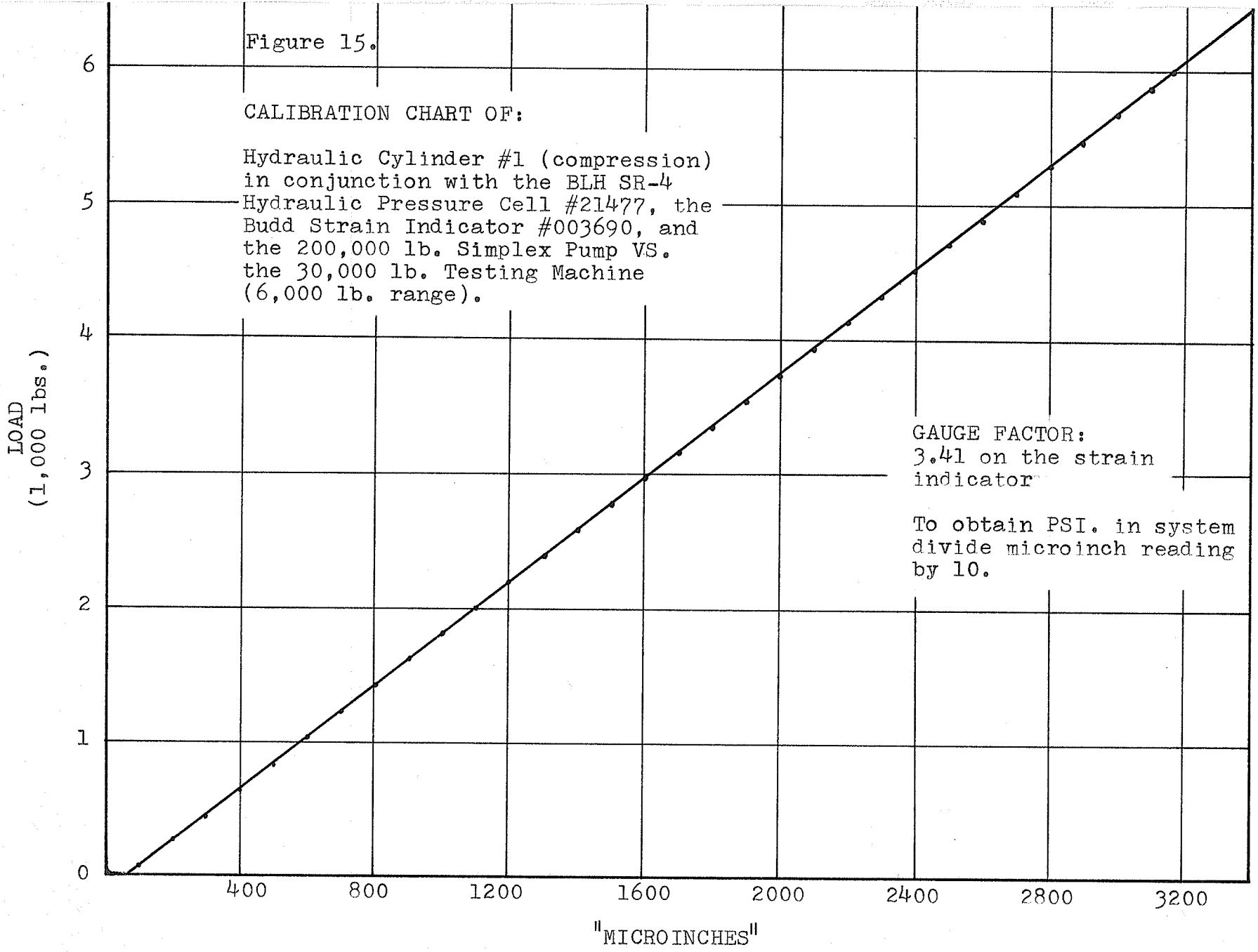
CALIBRATION CHART OF:
Hydraulic Cylinder #1 (compression) in conjunction with the BLH SR-4 Hydraulic Pressure Cell #21477, the Budd Strain Indicator #003690, and the 200,000 lb. Simplex Pump VS. the 30,000 lb. Testing Machine (6,000 lb. range).
GAUGE FACTOR: 3.41 on the strain indicator
To obtain PSI. in system divide microinch reading by 10.
LOAD (1,000 lbs.)
0
1
2
3
4
5
6
400
800
1200
1600
2000
2400
2800
3200
"MICROINCHES"

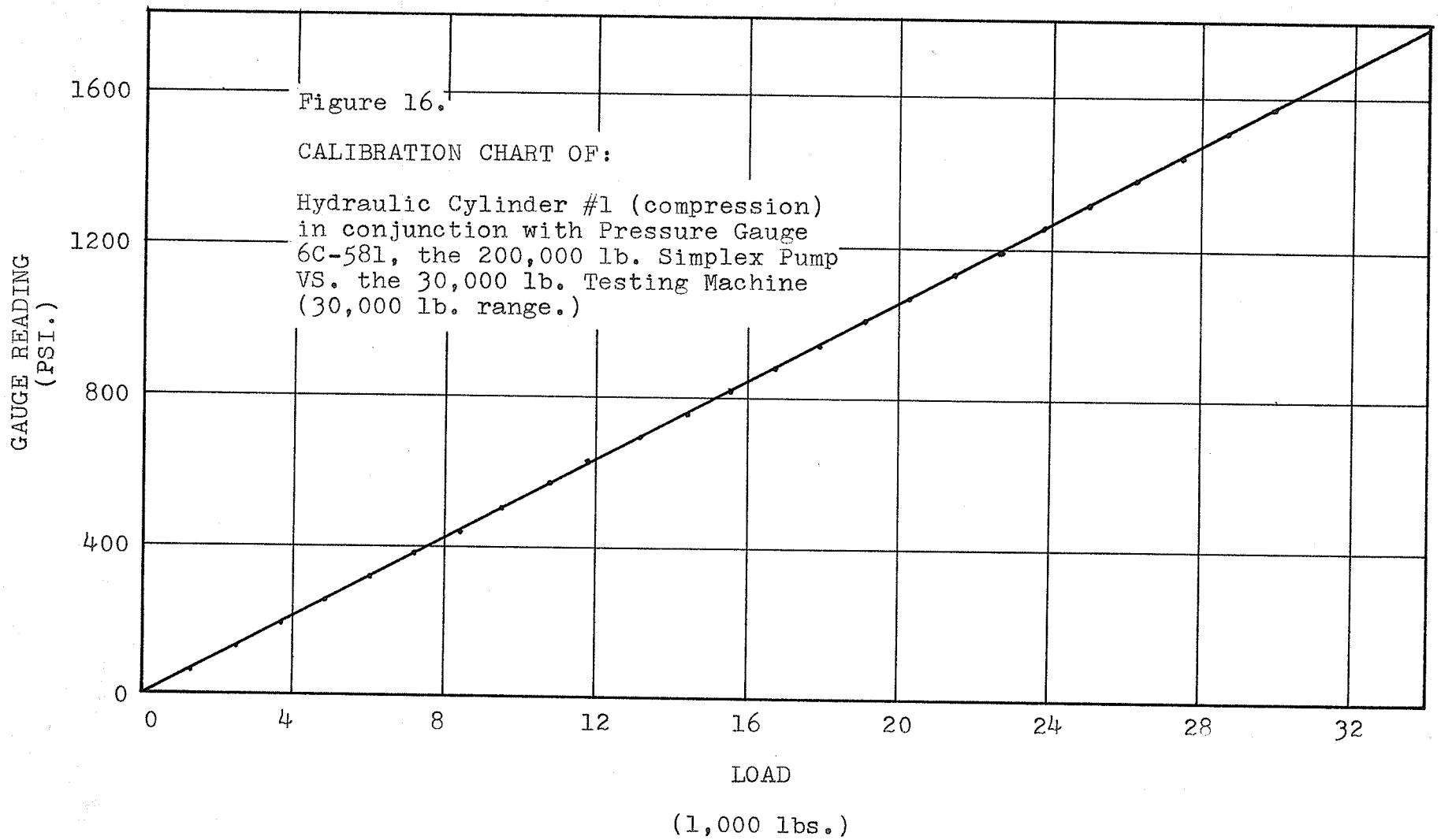

Figure 16.

CALIBRATION CHART OF:

Hydraulic Cylinder #1 (compression) in conjunction with Pressure Gauge 6C-581, the 200,000 lb. Simplex Pump VS. the 30,000 lb. Testing Machine (30,000 lb. range.)

The load was applied to the models in a different manner for each of the two tests. Figure 17, page 34, shows the testing arrangement for the first test. In the first test the single load was applied to the grillage using a roller bearing consisting of two grooved, 3 inch square, steel blocks with a ball bearing in between. The head of the jack rested on the top block and the base of the jack was clamped to the channels forming the portal frame. Figure 18, page 34, shows this arrangement clearly.

For the second test two equal point loads were applied to the interior longitudinal. As before, the base of the jack was attached to the channels of the portal frame, but this time the head of the jack rested on the center of a stiffened I spreader-beam. The point loads were transferred from the spreader-beam to the concrete beam by means of two roller bearings identical to the one used in the first test. Figure 19, page 35, shows the overall test set-up for the second grillage, while Figure 20, page 35, shows in detail the loading arrangement with the spreader-beam.

The grillage model rested upon four supports standing on the heavy steel beam abutments. An arrangement of three different kinds of supports was used to ensure simple support for the grillage model at each end. These supports consisted of one fixed support, two supports that allowed movement in two directions and one support that allowed movement in one direction. The various supports and their actual positioning can be seen in Figures 21, 22, 23 and 24 on pages 36 and 37. The layout of the supports was planned to give the model stability under deflection caused by the loading as well as some freedom of movement to adjust to loading conditions. In case the model shifted from its supports during loading, safety precautions were taken. Large steel angles were attached to the abutments to prevent the grillage model from slipping beyond the abutments and four wood-

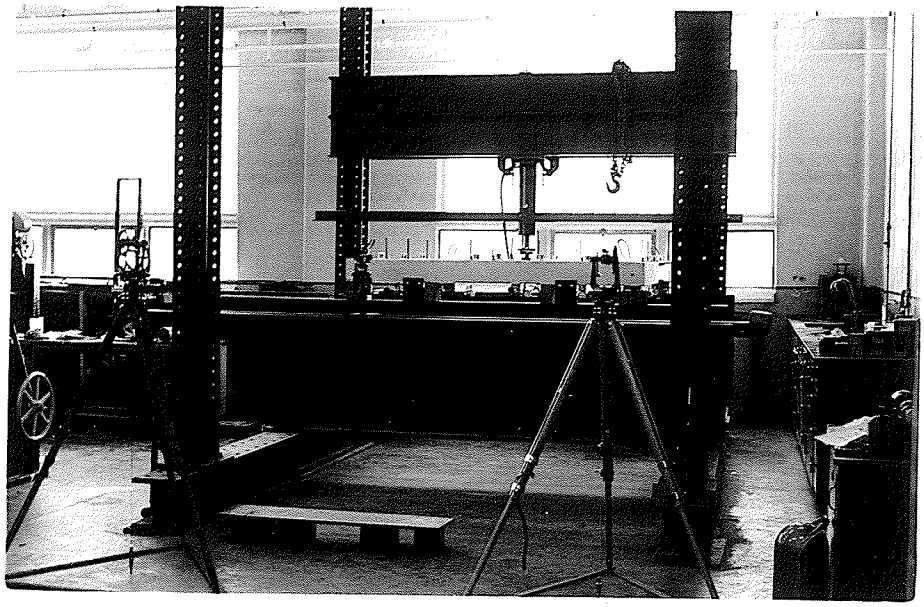

Figure 17. Testing Arrangement for First Test.

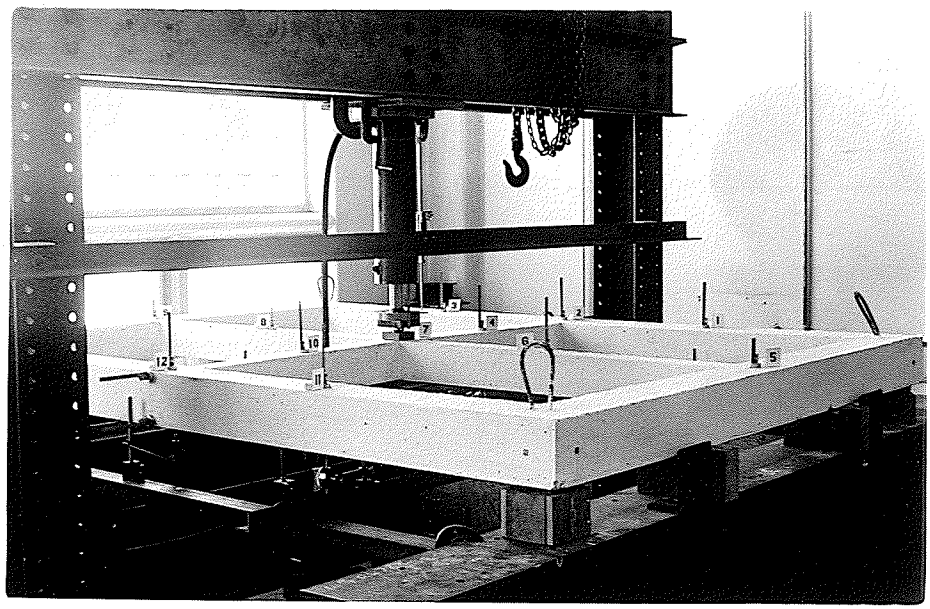

Figure 18. Loading Arrangement for First Test.

Figure 19. Testing Arrangement for Second Test.

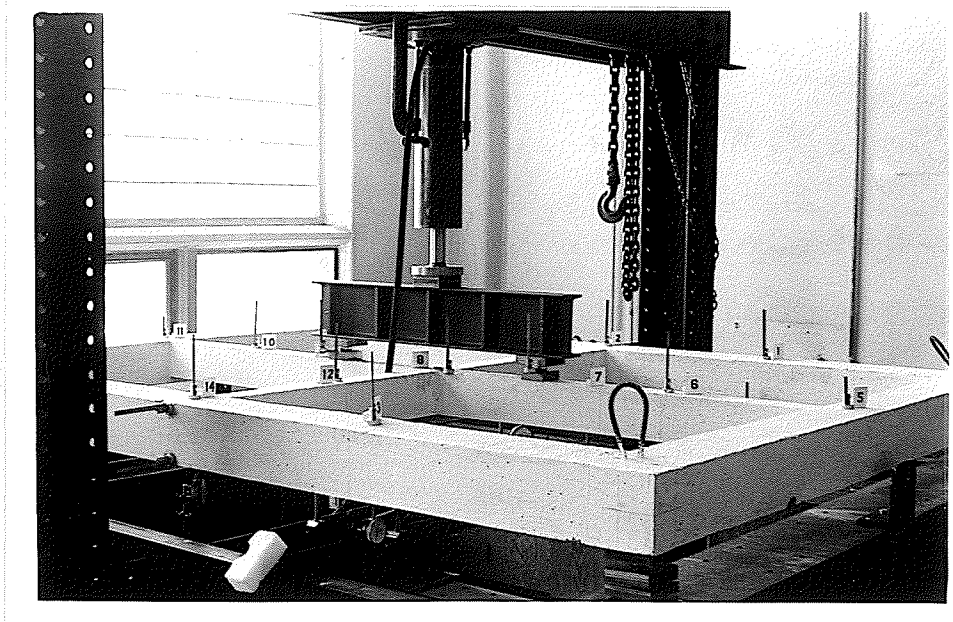

Figure 20. Loading Arrangement for Second Test.

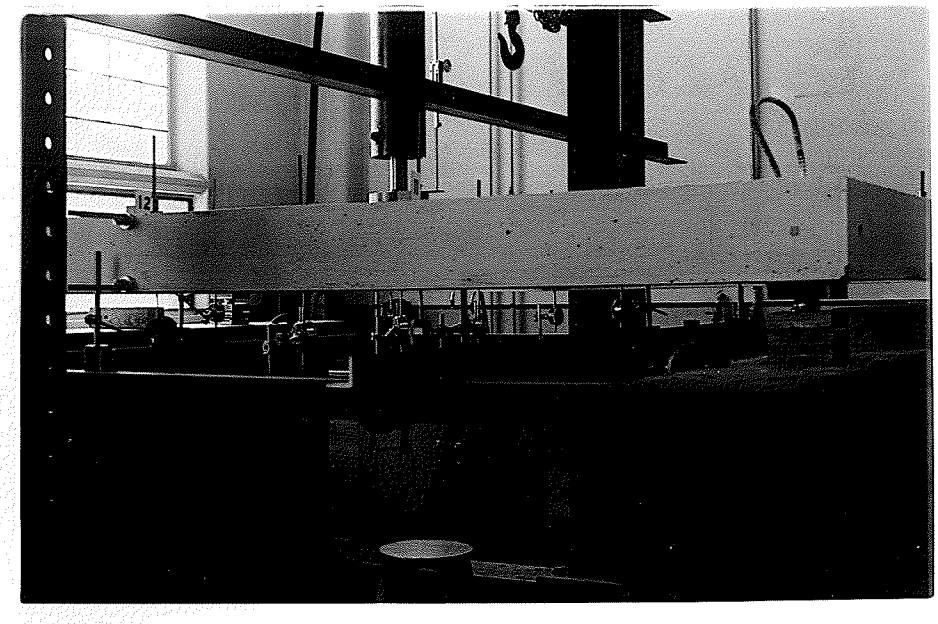

Figure 21. "Two-Direction" Grillage Supports.

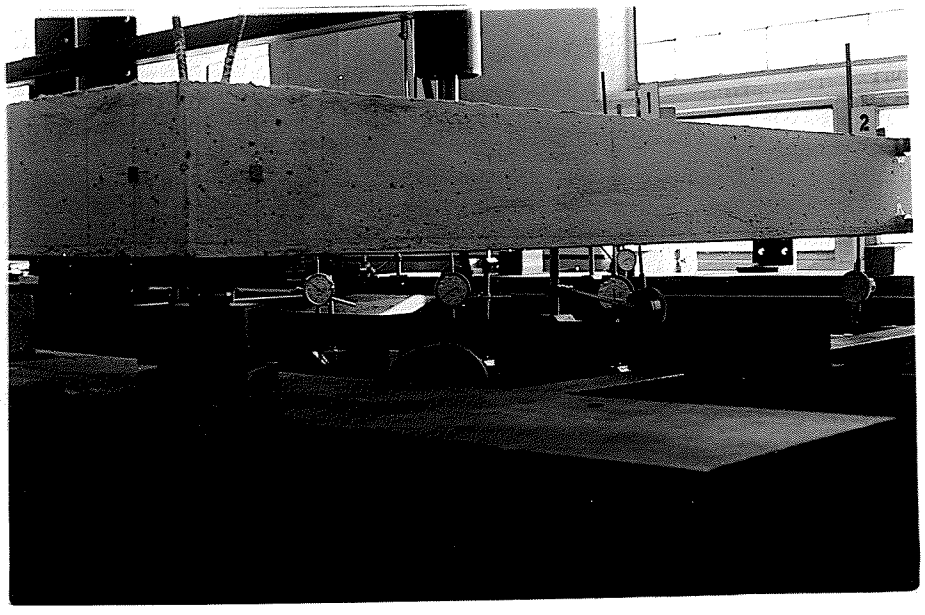

Figure 22. "One-Direction" Grillage Support.

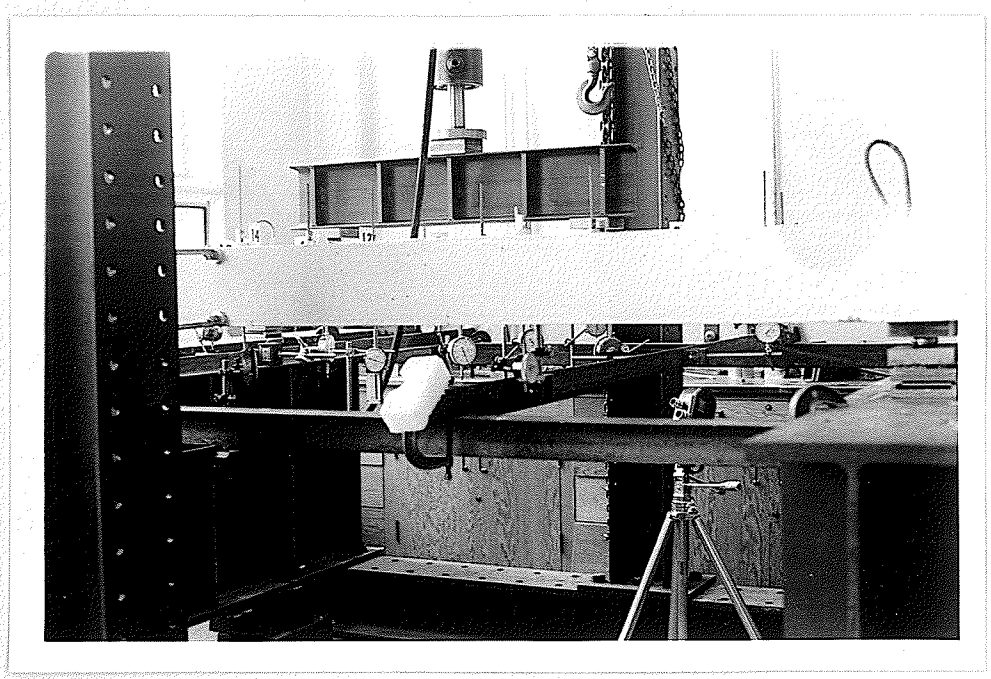

Figure 23. Dial Gauge Support Framework.

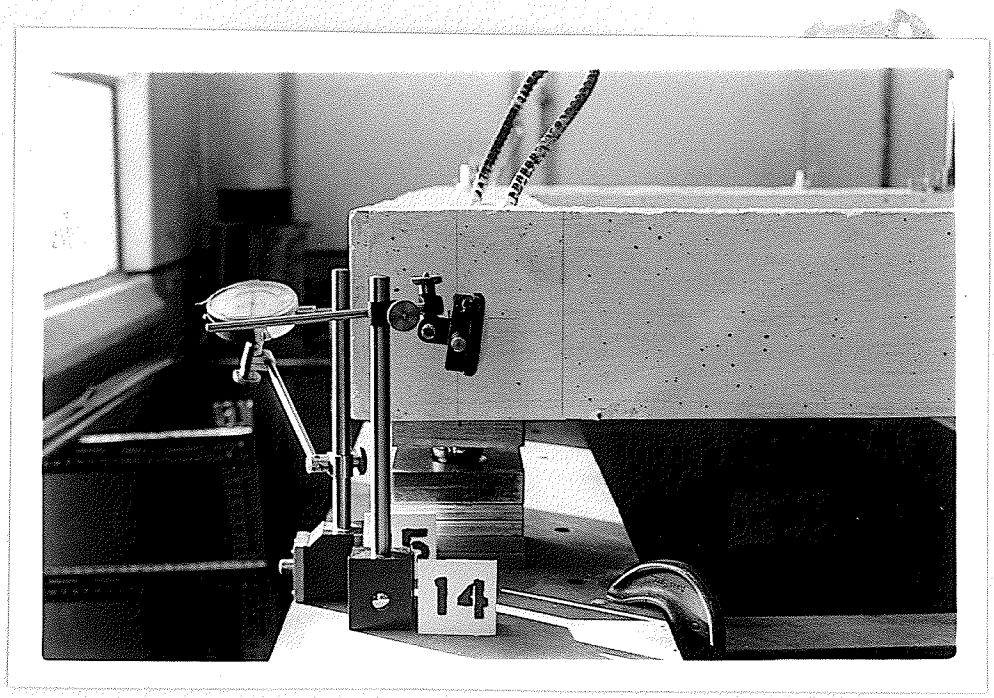

Figure 24. Fixed Support with Lateral Deflection Gauges.

en wedges, two on each end, were also placed on the abutments to arrest any unforeseen large movements. Both the steel angles and the wooden wedges remained clear of the model during the actual testing. The wooden wedges, however, were used to prop up the model when the supports were being put into place. The same arrangement of supports was used for both grillage model tests.

Three types of readings were made during the tests -- deflection, rotation and lateral movement. To measure lateral movement, two dial gauges mounted on magnetic stands attached to the steel beam abutment, and bearing on small steel pads on the grillage model, were used. This arrangement was located at the fixed support and is shown in Figure 24, page 37.

To measure rotation, scales mounted on aluminum bases, were attached to the sides of the exterior longitudinals so that one was even with the top of the longitudinal and the other with the bottom. These scales were placed at the center of the longitudinals where they connected with the interior transversals. Rotation was then measured by means of two transits, one for each longitudinal. The horizontal scales and the transits can be seen in Figures 17, 18, 19 and 20 on pages 34 and 35.

Deflection measurements of the grillage beams were made in two ways. One method consisted of using dial gauges accurate to 1/1000 of an inch. These dial gauges were attached to an independent steel framework by magnetic stands, and small steel pads provided bearing for the gauges on the concrete beams. The framework for the gauges, which was below the model, consisted of steel angles clamped firmly to the large steel beam abutments. During testing some of the dial gauges were reset when their length of travel was exceeded. The gauges and the framework can be seen in Figures

21, 22 and 23 on pages 36 and 37.

Steel scales, six inches in length, were also attached to the top surface of the grillage to measure deflection. The scales, set in aluminum bases, were attached to the beams by means of glue in identical positions to the dial gauges beneath the grillage. An engineering level was used to read the scales to an accuracy of 1/100 of an inch. The level was set upon a special support which was fixed to a pair of angles anchored to two vertical columns. The level and transit arrangement can be seen in Figure 17, page 34, and Figure 19, page 35.

The combination of methods for reading deflections allowed readings over a wide range. The dial gauges fell into two categories -- those with a range of 1 inch and those with a range of 2 inches. When deflections reached a critical stage for individual gauges, they were reset. This procedure continued as long as feasible. When the deflections became quite large, the dial gauges and their supporting framework had to be removed.

Level readings of the steel scales were taken from the beginning of the tests. Some of the scales could no longer be read when deflections became large. There was also slight error in some of the scale readings in that the scales on the interior beams did not remain vertical. However, in the total amount of travel of the scales, six inches, the error induced was considered negligible. It was believed that even if each reading were corrected, the load-deflection curve would appear unchanged.

In the first test a hydraulic point gauge was also used to measure center deflection. It was set up to measure the length of piston travel. However, final readings could only give an approximation of the total deflection due to several difficulties which will be explained in the next

chapter. The point gauge and its supporting member are shown in Figure 18, page 34.

CHAPTER IV

STATIC TESTS OF MODELS AND RESULTS

4.1 Testing Procedure.

Each test was planned to be carried out in one run lasting approximately four hours. However, the first test had to be completed over a two day period, as on the first run, the jack's piston reached its maximum length of travel before total collapse of the grillage. This turn of events required extending the length of travel of the piston by inserting a section of steel beam between the base of the jack and the channels of the portal frame. It can readily be seen that this procedure made deflection readings not entirely accurate for the second run. Other than this instance, the testing procedures were basically the same for both grillages.

The placing of the grillage models onto the loading frame followed a fairly simple procedure. One of the large steel abutments was removed from the frame using a movable hoist and the concrete model was wheeled into position under the portal frame on dollies. By means of a block and tackle, attached to the channels of the portal, the model was raised to a suitable height and the abutment was moved back into place and anchored. The grillage was then lowered onto its supports which were enclosed in wooden jackets to prevent movement. An example of this enclosure can be seen in Figure 18, page 34. Instrument frames were then assembled and gauge placement could commence when desired. At this point the concrete was painted with a watered down white latex paint so that cracks forming during the test would be readily visible.

On the morning of the test all of the instrumentation was set up. This included the dial gauges, the steel scales, the level, the transits and the strain indicator which measured load through a hydraulic pressure cell. In the afternoon the actual testing proceeded until completion.

During the test, besides the deflection and rotation readings that were being taken, observations as to the cracking and ultimate behaviour of the structure were also noted. A series of black and white still pictures, as well as 16 mm. motion pictures* were taken to show the progress of each test.

The method of loading both grillages was different. As mentioned previously, the first grillage was loaded with a concentrated load at the center. The second grillage was loaded with two concentrated loads along the interior longitudinal by means of a spreader-beam. In each test the loads were applied to the concrete model through 3 inch square steel blocks. The arrangement of loading for the two tests can be seen in Figures 18 and 20, on pages 34 and 35 respectively.

For both tests deflections were measured by dial gauges, as well as scales read by level. In the first test, a total of fifteen dial gauges was used to measure deflection including two gauges that were used to measure lateral movement at one of the corners. Thirteen steel scales, set on aluminum bases, were also used to read vertical deflection. In the second test, the two dial gauges used to measure lateral movement were eliminated and fifteen dial gauges and fifteen steel scales were used to measure vertical deflection. In both tests four steel scales, two per beam, were also used to measure rotation of the external longitudinals.

---

* The motion pictures are kept on file at the Civil Engineering Department, University of Manitoba.

Dial gauges were removed when deflections were such that readings could no longer be taken. Gauge positions, load points and support arrangement can be seen in Figures 25 and 26, on pages 44 and 45.

Before actual loading commenced, an initial jack load was applied to both grillage models and then released. This test load was used as a check to ensure that the load was centered properly, that the grillage sat well on the supports and that the instruments were functioning properly. When this initial loading was completed, all of the dial gauges were "zeroed" and the readings on the steel scales, taken by level, were recorded.

In the two grillage tests the basic load increment was 200 lbs. This increment was varied to meet specific conditions in each test.

At each load increment, for both tests, as much data as possible was gathered. This included dial gauge readings, level readings, as well as transit readings in order to monitor rotation of the main exterior beams. Cracks were marked, with various colour felt marking pens, as they developed and can clearly be seen on all photographs taken of the tests. Numbers marked along side crack patterns indicate approximately the loads at which the crack lines appeared. The marked loads vary slightly from the true loads listed in the observations and used in all load-deflection curves.

4.2.1. Observations from Test #1a.

The first grillage, with the single concentrated load at the center, was to be tested to destruction in one run. However, as the length of travel of the piston ran out before total destruction of the grillage, a second run had to be carried out. To achieve sufficient length of piston

TEST #1

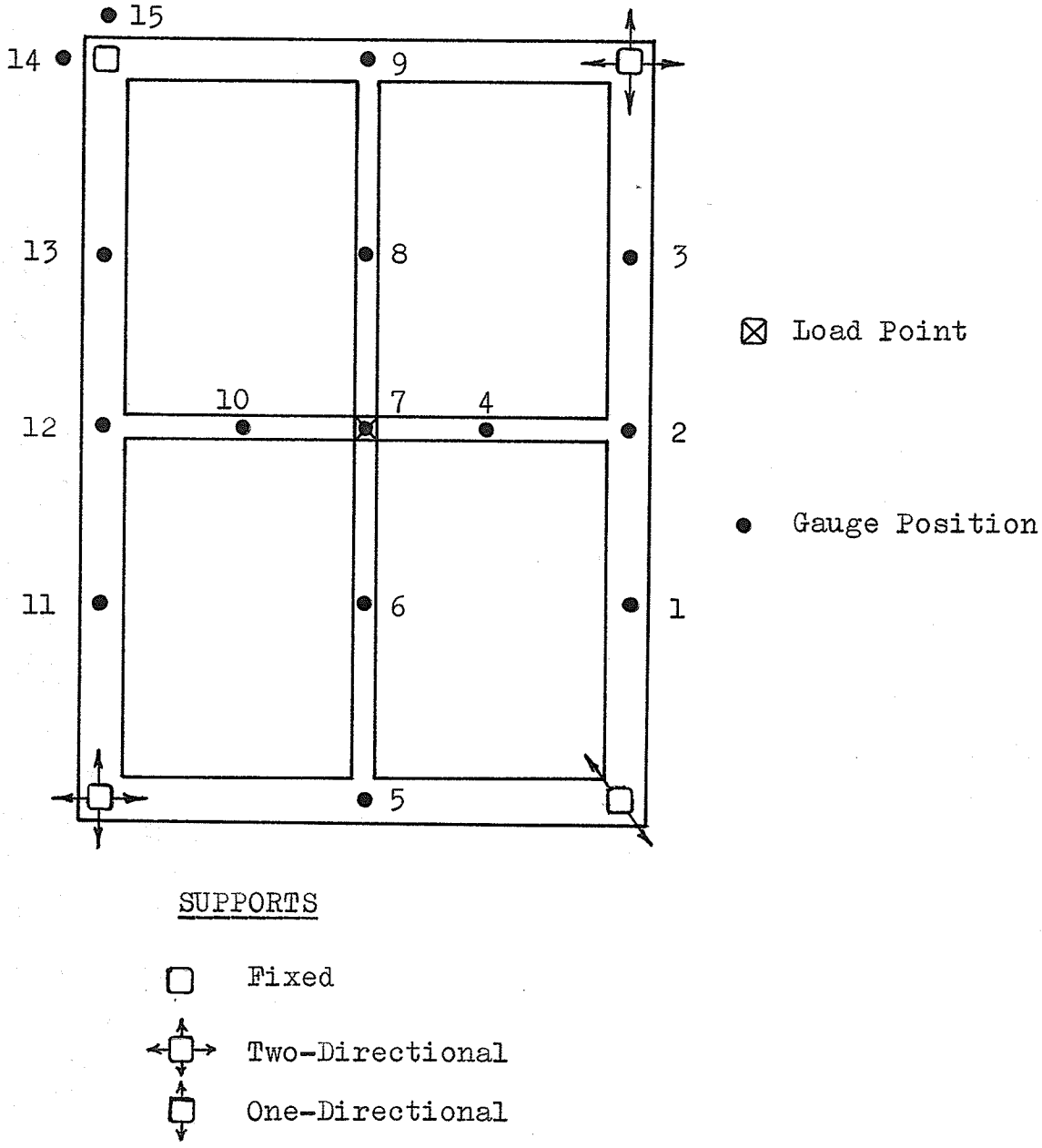

Figure 25. Gauge Positions and Support Arrangement.

TEST #2

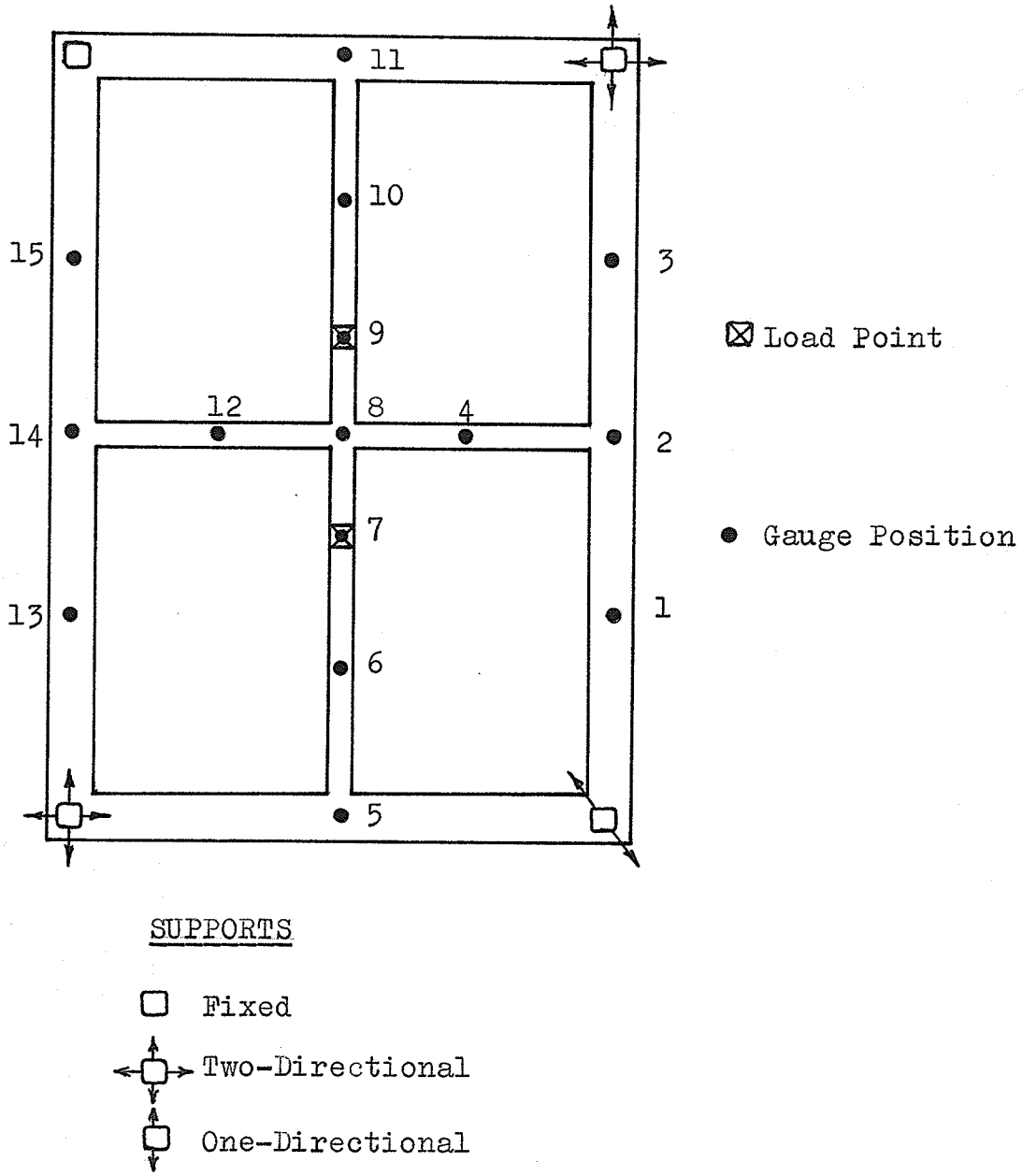

Figure 26. Gauge Positions and Support Arrangement.

travel for the second run, a WF-beam was inserted between the base of the jack and the portal channels. Also additional steel blocks were placed between the head of the piston and the roller bearing through which load was applied to the grillage model. This arrangement can be seen in Figure 35, page 56.

The first run progressed very smoothly. The grillage model sat on its supports very well as load was applied and cracks did not appear for some time. It was not until a load of 1060 lbs. that the first cracks appeared at the center of the grillage and at the beam junction in the vicinity of gauge 5. At a load of 1260 lbs. no new cracks occurred, but the cracks immediately under the load propagated. All cracks increased in length as the load reached 2050 lbs. At this point new cracks appeared near the center of the grillage on the interior beams at predicted hinge locations. From a load of 2250 lbs. to 2430 lbs., new cracks appeared on the interior beams near their junctions with the exterior members. These cracks were also in predicted hinge areas.

When loading reached 2630 lbs., the load began to drop off slightly and this was thought to indicate first yield. The grillage continued to take increased loading and between 2830 and 3220 lbs. cracks at the center of the grillage increased in length. Also two new cracks appeared on the interior longitudinal member between gauge locations 6 and 7.

As loading progressed from 3420 lbs. to 4000 lbs., no new developments occurred except for the cracks at the center, which began opening up and continued to do so with each load increment. At 4200 lbs. new cracks appeared in the interior longitudinal about one foot from the junctions with the exterior transversals. At 4400 lbs. and 4600 lbs.

cracks continued to open up at the center. At a load of 4780 lbs. new cracks occurred at the junctions of the interior and exterior beams.

At this point, yielding under load was very great and it was difficult to reach 5000 lbs. It was decided to try loading at increments of 400 lbs. This involved continuous pumping and a load of 5380 lbs. was reached. However, this load could not be held and the load dropped down to 5000 lbs. At 5380 lbs. cracks appeared in two locations on the exterior members. Torsional cracks appeared on the exterior beams at junctions with the interior beams, and several cracks appeared at the corners of the exterior grid. Gauges 6, 7 and 8 were reset and loading was again attempted. A load of 5080 lbs. was achieved but it dropped off very rapidly. Upon further loading, a load of only 4980 lbs. could be achieved.

At this point gauge readings were discontinued. Jacking was continued and deflection increased considerably. The test continued until the two bottom bars of the interior transversal broke at a point directly under the load. A reading was taken on the hydraulic point gauge and the total deflection was 0.854 ft. Increased deflection could not be achieved, as the jack had reached its full length of travel.

The above constituted the first part of test no. 1 and the entire sequence of events can be traced in Figures 28 to 33 inclusive, pages 49 to 51. Load-deflection curves for several gauge positions appear in Figure 27, page 48. Test data is listed in Appendix B, page 112. Rotation of the exterior beams was negligible to this point in the test. It was decided that observation of further deflection might be useful and the jack was reset as described earlier. The second section of test no. 1 proceeded from this point.

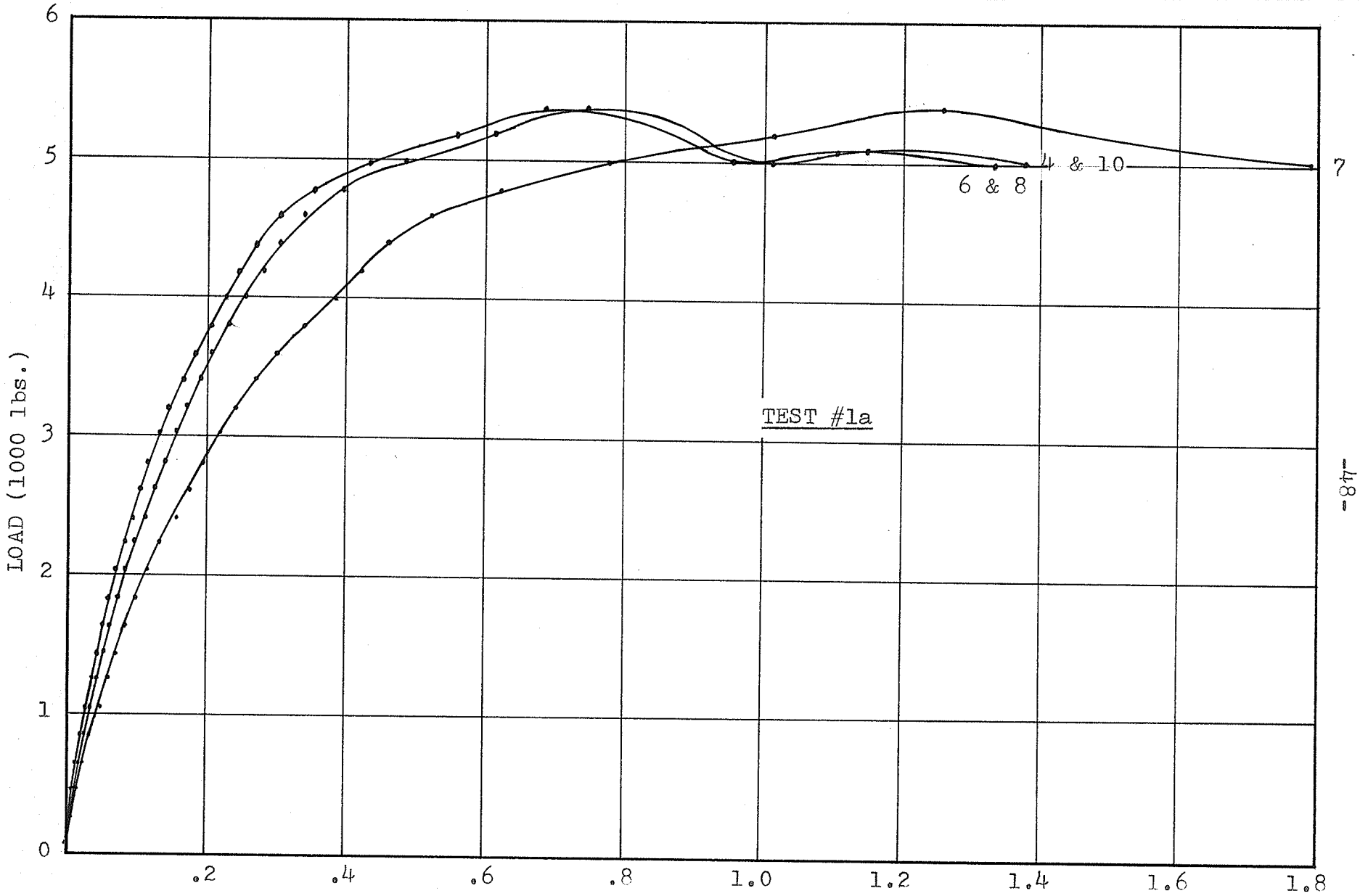

Figure 27. Load-Deflection Curves for Several Gauge Locations.

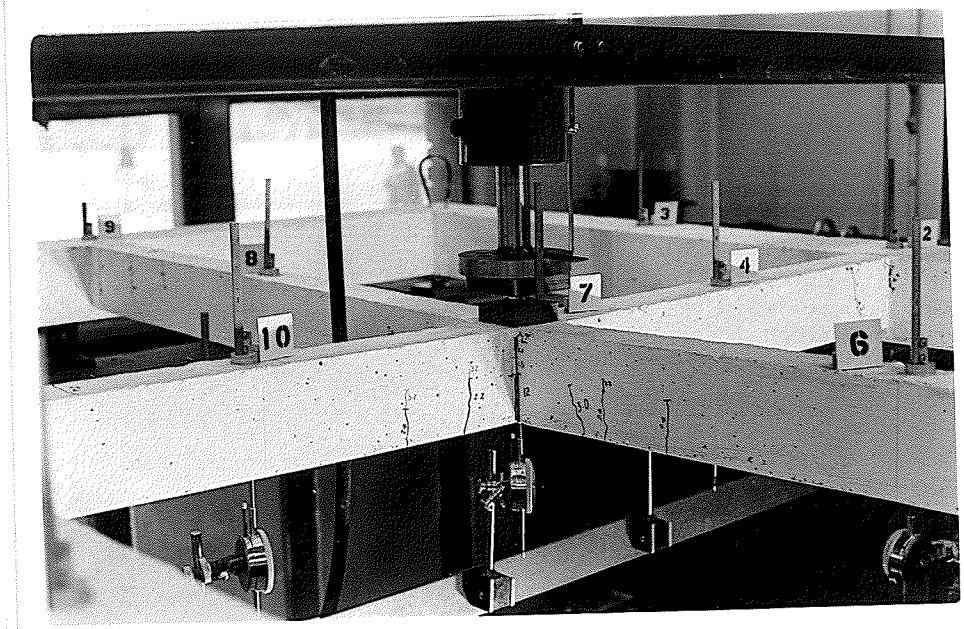

Figure 28. Early Crack Development.

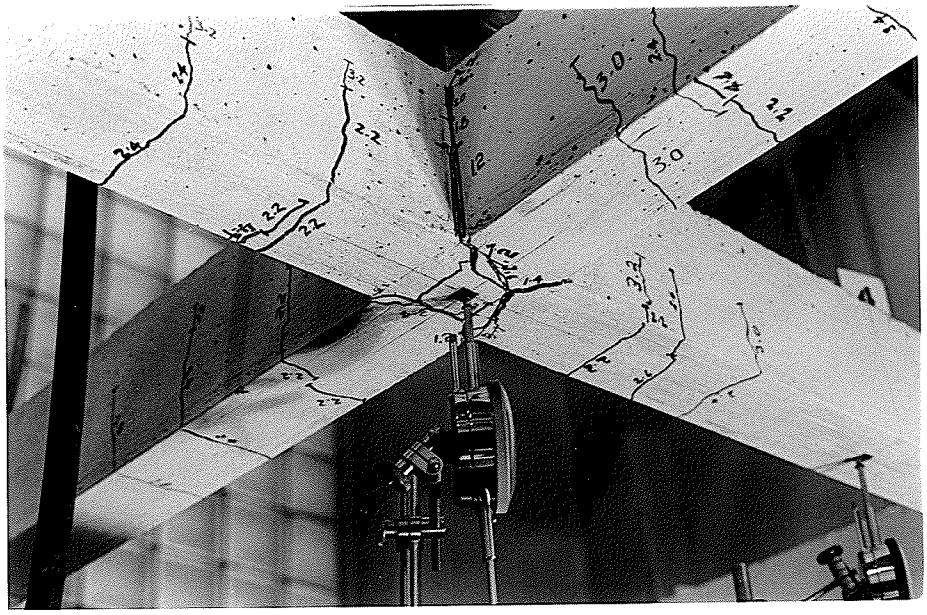

Figure 29. Cracking on Underside of Grillage.

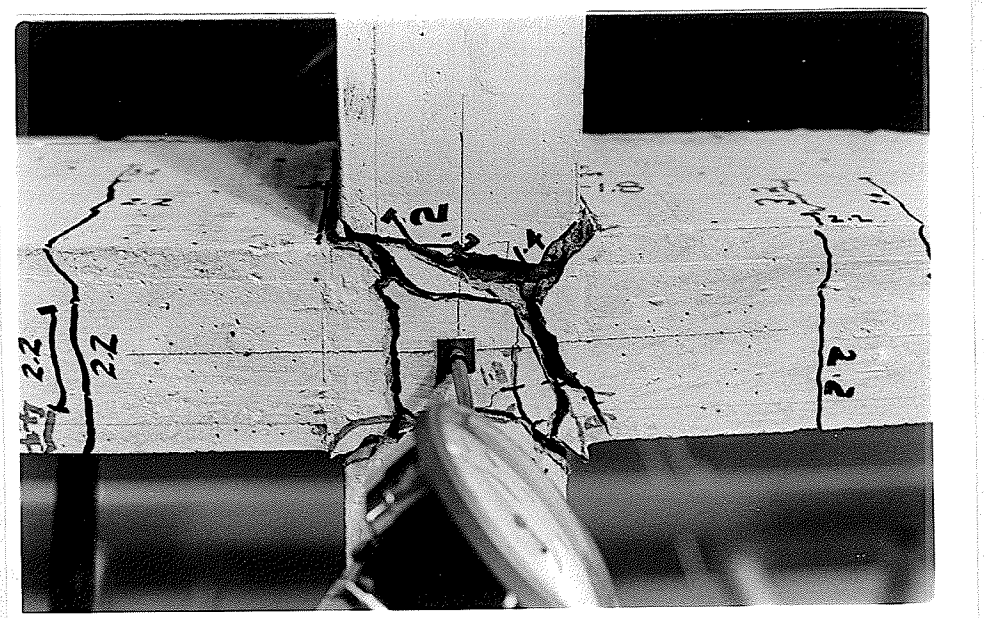

Figure 30. Crack Development Directly Under Load.

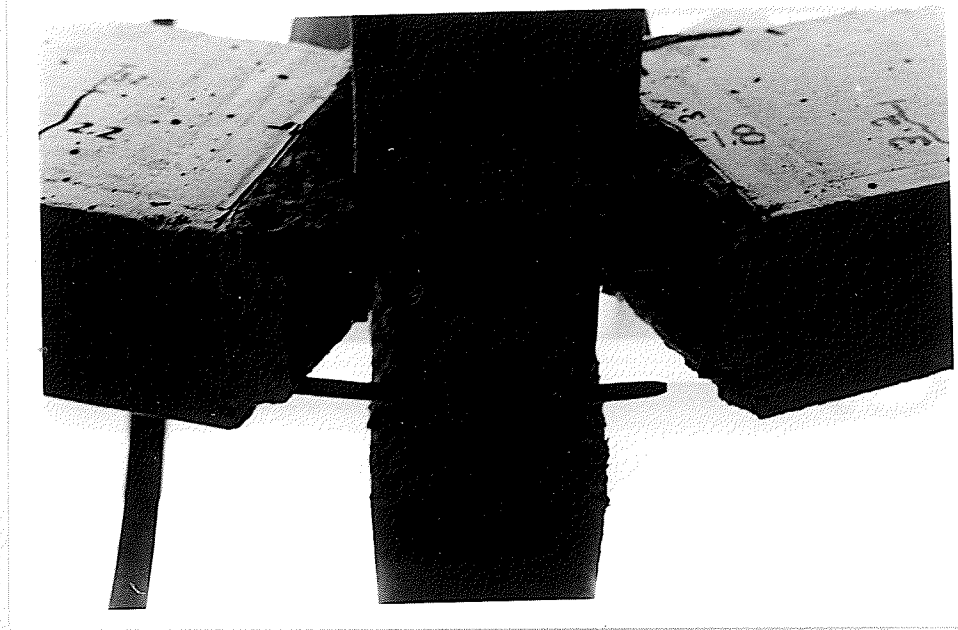

Figure 31. Broken Transversal Bars.

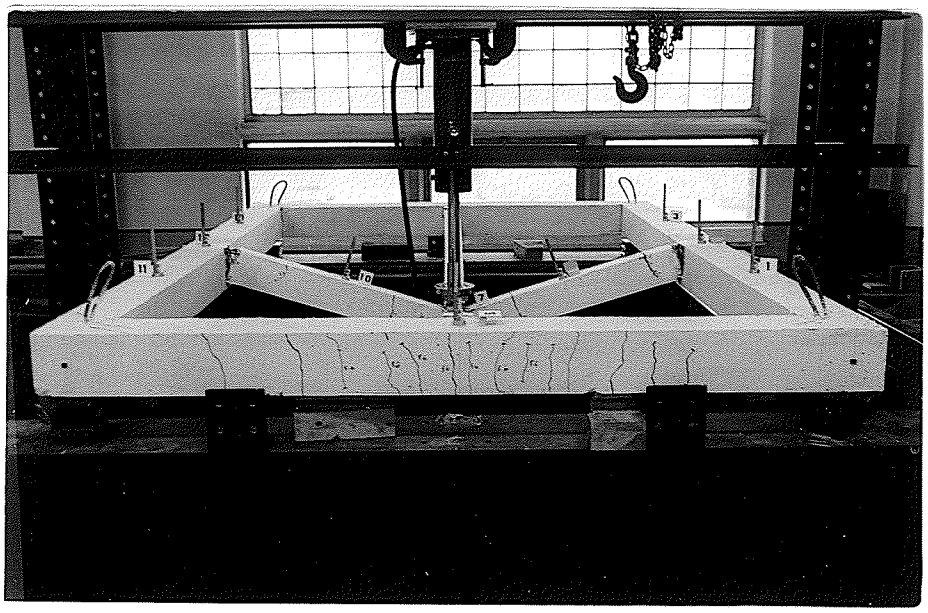

Figure 32. End View at End of Test #1a.

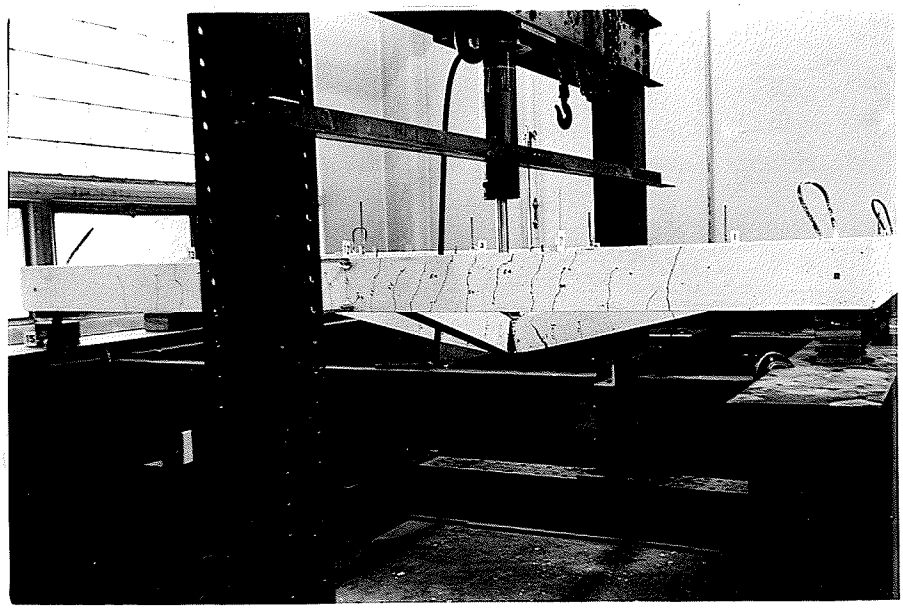

Figure 33. Side View at End of Test #1a.

4.2.2. Observations from Test #1b.

When the steel beam was inserted between the base of the jack and the portal frame, and extra blocking was inserted between the head of the jack and the roller bearing resting on the grillage, testing proceeded as before. Deflection readings were taken with the hydraulic point gauge. These readings could only be considered approximate as the gauge was "zeroed" for the second run according to the total deflection of the first run. That is to say that rebound upon unloading was not taken into account.

As load was applied, center deflection continued to increase and the cracks continued to open. As the deflection increased, load again began to increase. At a load of about 6100 lbs. the deflection was .923 ft. This load remained quite steady and yielding seemed to be taking place.

Load, after remaining steady for some time, again began to increase. At a load of 7100 lbs. the deflection increased from .961 ft. to .984 ft. Load then increased again to 7700 lbs. as the deflection reached 1.021 ft.

Up to this point no observable rotation of the exterior beams was noticed. However, yielding again seemed to be taking place and the load at a deflection of 1.045 ft. was 7500 lbs.

As the grillage center deflection increased, the model again began to take increased load. At a deflection of 1.076 ft. the load climbed to 8300 lbs. Under this loading the structure again began to yield. Several interesting developments occurred at this time. On the interior transversal definite hinge action had developed on either side of the load point. This phenomenon was observed earlier but it was more pronounced at this time. This development can be traced in Figure 35, page 56, and Figure 41, page 59.

At this load of 8300 lbs. slight rotation and lateral displacement of the exterior longitudinals was observed for the first time. However, the exterior transversals still did not show any rotation or vertical displacement. With the load holding and the deflection increasing a sharp report was heard at a deflection of 1.097 ft. The load immediately dropped off to 5900 lbs. and eventually to 5000 lbs. The loud noise was a result of a top bar breaking in the interior transversal at the beam junction near gauge 12. The bar which broke can be seen in Figure 36, page 56, and shows all the signs of a typical tension failure. Necking is quite visible in the photograph.

After dropping off rapidly, the load again began to increase. At a deflection of 1.108 ft. the load was holding at 7200 lbs. After a short while, the load again began to increase and at a deflection of 1.129 ft., the load reached 7800 lbs. At this point new cracks appeared around the midpoints of the interior longitudinals and the old cracks continued to widen and spread. No increase in the exterior longitudinal rotation could be detected at this point.

The load continued to climb, and when it again reached the previous maximum of 8300 lbs., both bottom bars of the interior longitudinal broke. The load dramatically dropped off to 4750 lbs. and the deflection reading at this point was 1.168 ft. The two broken bars of the interior longitudinal can be seen in Figure 38, page 57. No increase in exterior longitudinal rotation was observed.

Load again was applied, and at a deflection of 1.208 ft. the load reached 5900 lbs. This load remained steady as deflection increased to 1.264 ft. At this point a bar or bars broke inside one of the interior beams and the load dropped to 2400 lbs. Jacking continued and load again began to increase as deflection increased. At a load of 4600

lbs. and a deflection of 1.308 ft. internal cracking was heard in the interior longitudinal. As load continued to increase along with the deflection, spalling of concrete occurred on the interior transversal between gauge positions 2 and 4. The rotation of the exterior longitudinals also remained quite small as before.

Load continued to increase until it reached 5900 lbs. at a deflection of 1.454 ft. when a report was heard and the load dropped off to 4800 lbs. It was not apparent what bar had broken. The load continued to fluctuate and again began to increase. At 5700 lbs. and a deflection of 1.481 ft. the top bar of the interior longitudinal broke under the load point with a sharp report and the load dropped to 3600 lbs.

The structure was still able to take renewed loading and at a load of 4800 lbs., the other top bar of the interior longitudinal broke at a deflection of 1.569 ft. The load then dropped off to 0 lbs. when the top bars of the interior longitudinal were completely broken.

At this point the load plate tilted and no further loading was possible. The grillage was shifting on its supports as the load was being applied at an angle. If the load plate had not tilted, more deflection could perhaps have been obtained until the interior transversal bars had broken completely. Nevertheless, the final point gauge reading showed a total deflection of 1.613 ft. Figures 35 to 42, pages 56 to 59, show the progress of the grillage collapse quite well.

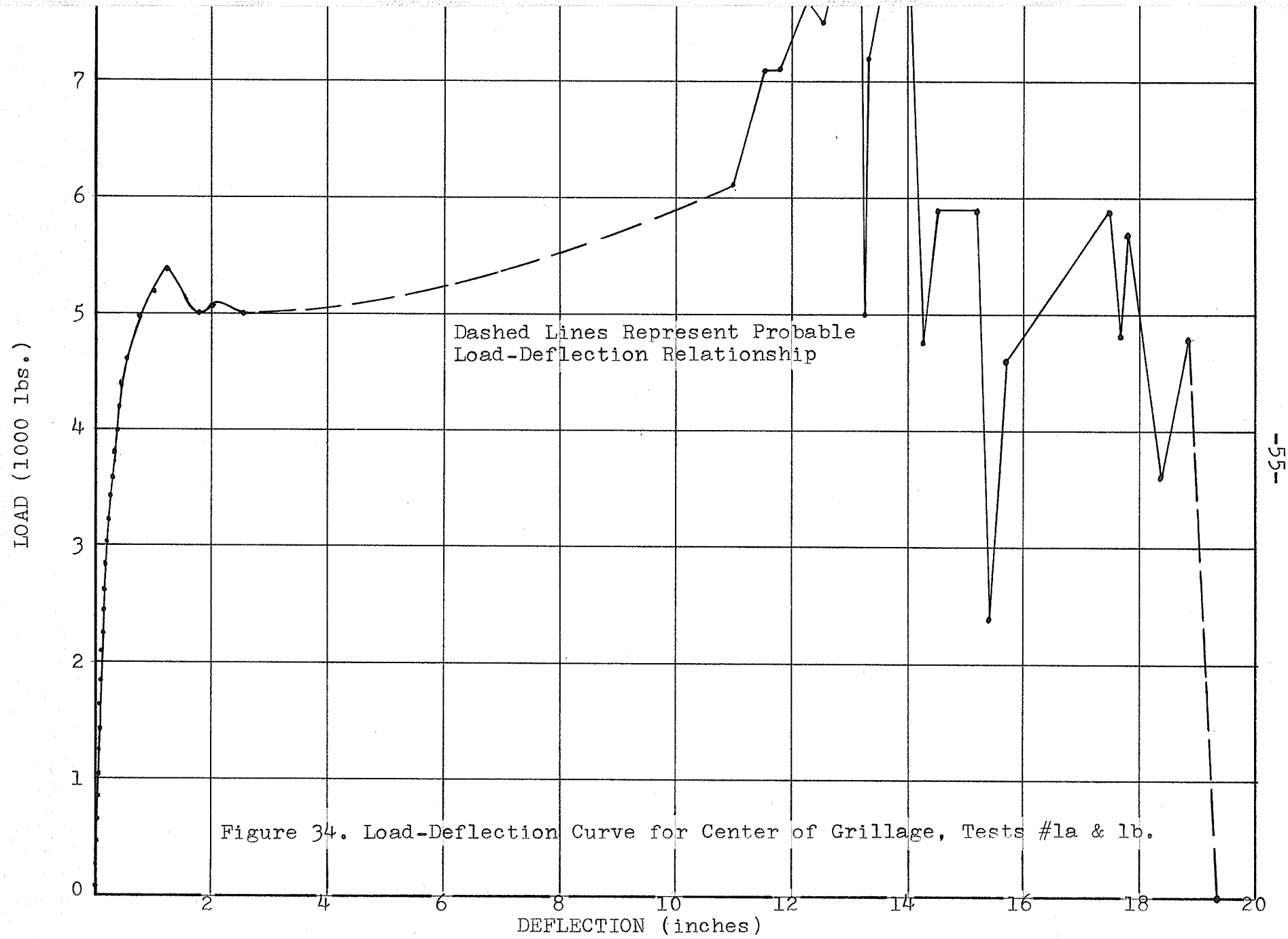

Figure 34. Load-Deflection Curve for Center of Grillage, Tests #1a & 1b.

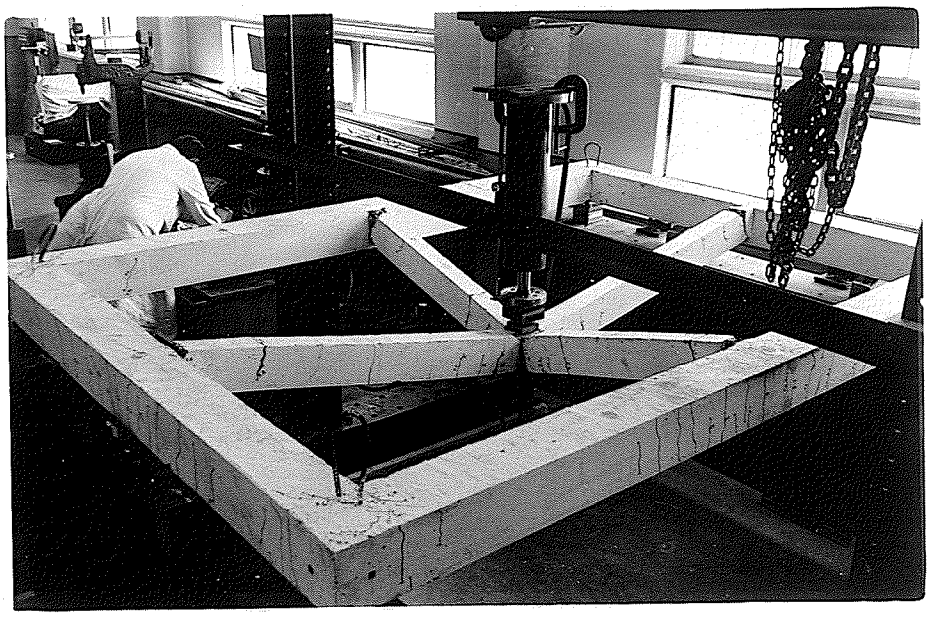

Figure 35. Testing Arrangement for Test #1b.

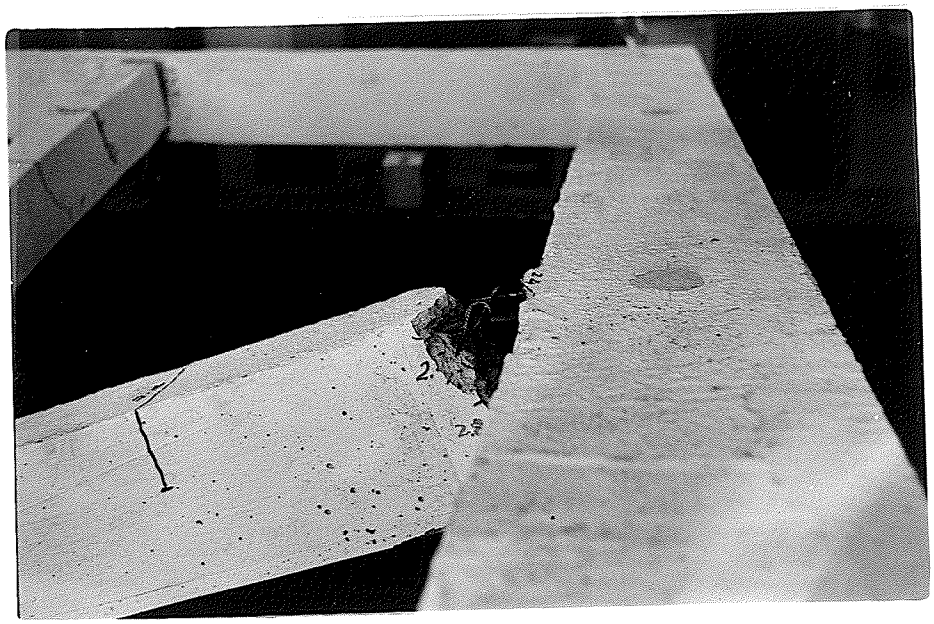

Figure 36. Broken Top Bar Near Gauge #12 Location.

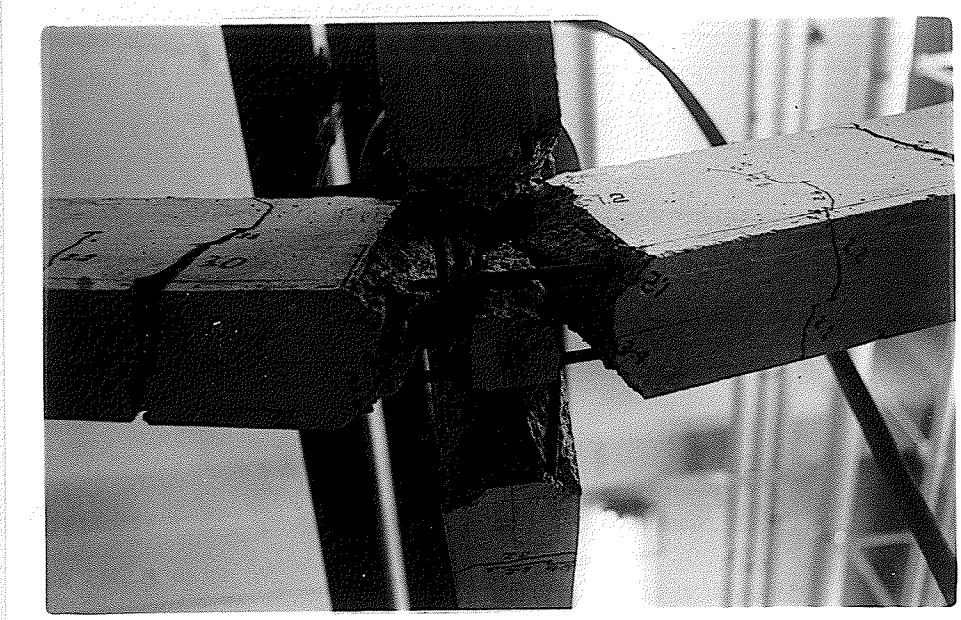

Figure 37. Broken Bars Directly Under Load.

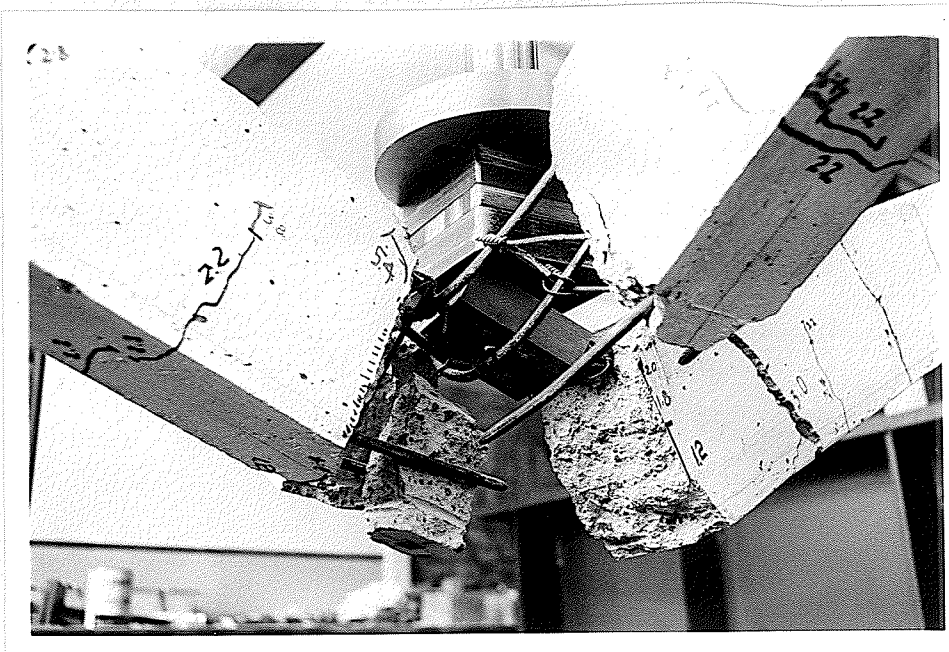

Figure 38. Tilted Load Plate at Completion of Test.

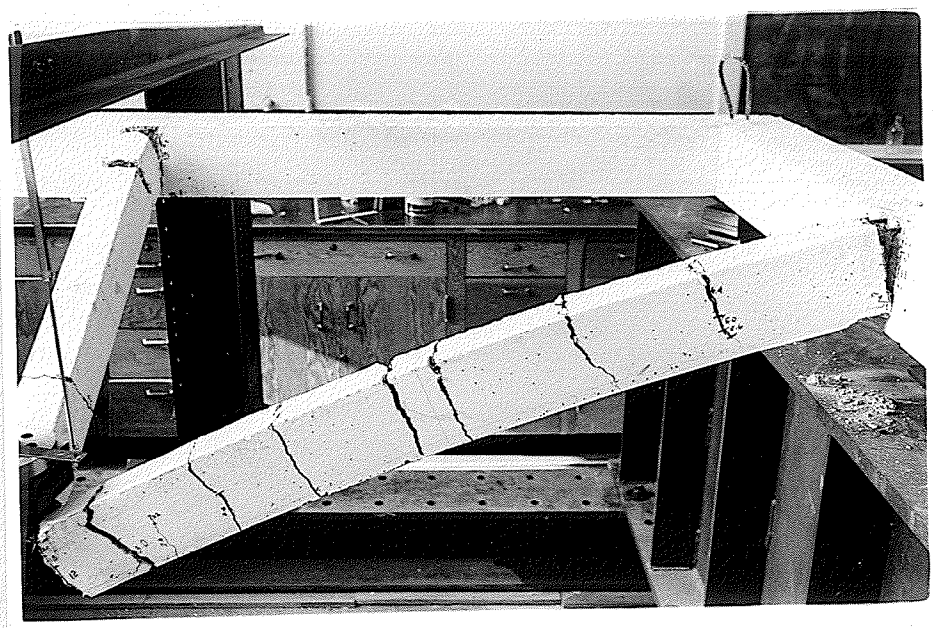

Figure 39. Section of Longitudinal at End of Test.

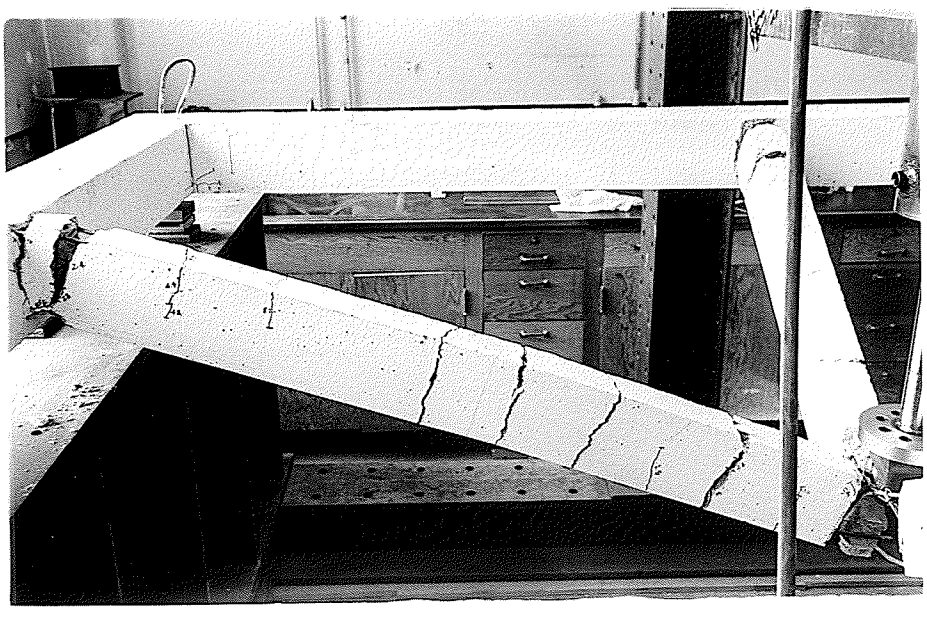

Figure 40. Section of Longitudinal at End of Test.

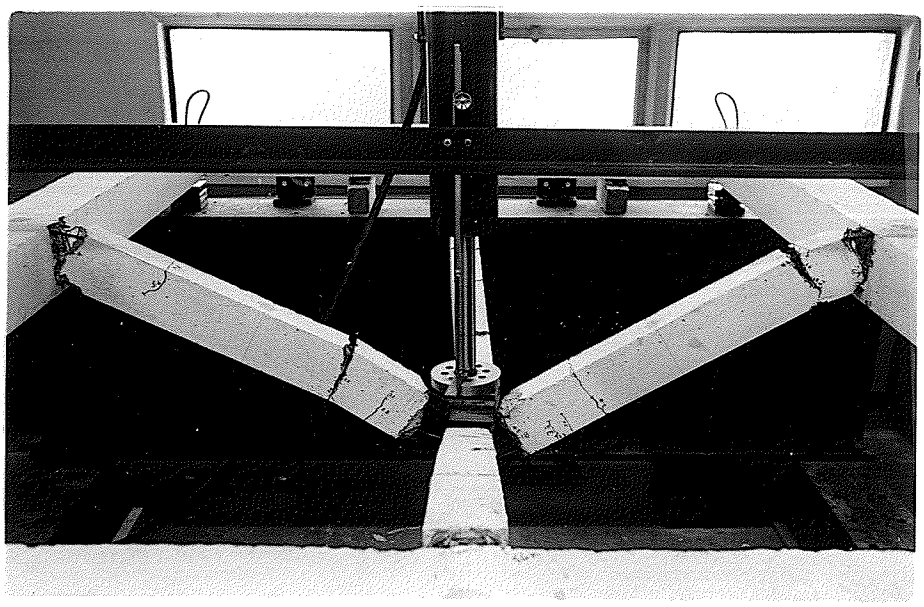

Figure 41. Transversal at Completion of Test.

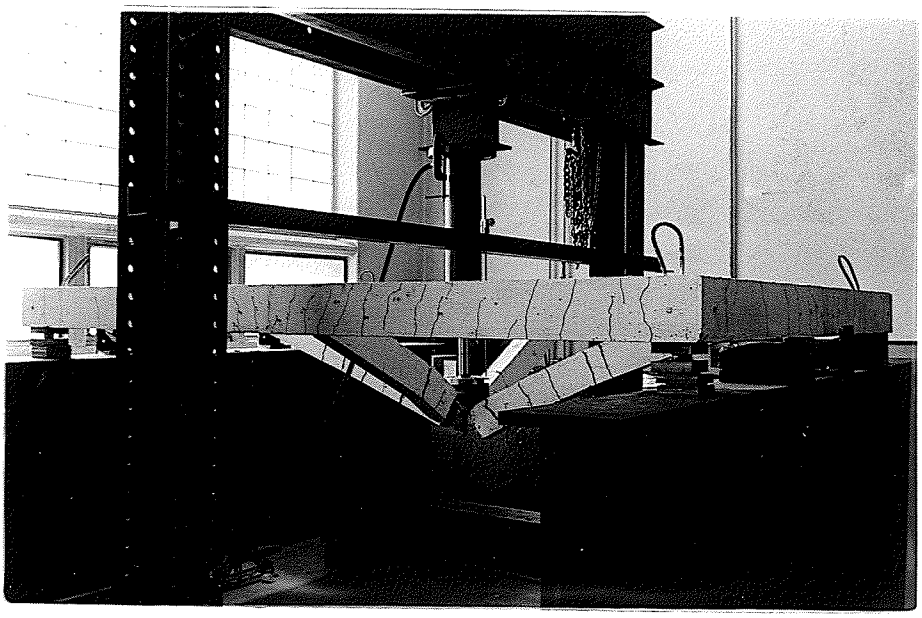

Figure 42. Side View of Grillage at End of Test.

4.3 Observations from Test #2.

When the first test was completed, it was thought that no new information would be gained by loading the second grillage in the same manner as the first. A system of two concentrated loads, acting upon the interior longitudinal, was finally decided upon. This loading arrangement was previously shown in Figures 19 and 20 on page 35.

The jack loading increment varied during the test. At the beginning of the test the increment was 400 lbs. This meant that each of the concentrated loads increased by one-half of this amount or 200 lbs. During the test the jack loading increment was reduced to 200 lbs. for a short time and then increased again to 400 lbs. In the following discussion the loads referred to are the concentrated load values and not the total load upon the grillage.

Initial loading progressed smoothly. The grillage sat well upon its supports and it was not until a load of 530 lbs. that the first crack appeared under the load at gauge position 9. At a load of 725 lbs. a crack appeared on the interior transversal on one side of its junction with the interior longitudinal. Cracks appeared near the load at gauge position 7 at 925 lbs., as well as on the interior transversal on the other side of its junction with the interior longitudinal. Between loads of 925 and 1315 lbs. the existing cracks continued to propagate.

At 1315 lbs. several new cracks appeared on the interior beams. On the interior longitudinal, cracks appeared at the center as well as at the junction with the exterior transversal near gauge location 11. On the interior transversal cracks appeared at the junctions with the exterior longitudinals. As the load reached 1515 lbs. more cracks appeared on the interior transversals near the center and

cracking occurred at the junction of the interior longitudinal and exterior transversal near gauge 5.

At 1610 lbs. new cracks appeared on the interior transversal between gauge locations 12 and 8 and between gauge locations 8 and 4. At the same time the cracks, at all of the interior beam junctions with the exterior beams, propagated from the top of the interior beams toward the bottom. These cracks continued to lengthen when the load reached 1710 lbs. New cracks also appeared on all of the interior beams approximately 6 inches from their junctions with the exterior beams. These cracks started at the top of the beams and progressed down the sides.

All existing cracks continued to propagate as loading proceeded and at 2000 lbs. the first torsional cracks appeared on the exterior beams. As load increased to 2300 lbs. new cracks were developing under the load points and near the center of the grillage.

The grillage continued to take load well, and the only developments as the load increased from 2300 to 2890 lbs. were some new cracks on the interior transversal between gauge locations 8 and 14. When the load reached 2890 lbs., yielding was observed as the load dropped off considerably at this time.

After some yielding, the grillage again began to take increased loading. When the load reached 3550 lbs. the grillage again began to yield considerably. As deflection increased, the load again began to increase. When the load reached 3850 lbs., many new cracks developed. Increased cracking was evident at the center of the grillage and the exterior members showed increased torsional cracks both at midspan and at the corners. Figure 45 shows cracking near the load points. See page 66.

Deflection continued to increase as the load reached 4100 lbs. At this load new torsional cracks appeared on the exterior beams and new cracks appeared at the junctions of the interior transversals and the exterior longitudinals. With the load remaining at this level, deflection continued to increase markedly.

The cracks continued to open under the load points and at the beam junctions. Although deflection continued to increase, the torsion cracks on the exterior beams no longer appeared to propagate. The predicted collapse mechanism had formed and can be seen in Figure 46, page 66.

The load continued to fluctuate and from the previous high of 4100 lbs., the load began to drop first to 3725 lbs. and then to 3285 lbs. Upon reaching that low, the load again began to rise. At first it reached 3385 lbs. and continued to increase. At 4900 lbs. the collapse mechanism began to change in appearance. The interior longitudinal between the loads no longer remained straight, but started to bend up at the center where it joined with the interior transversal. This development indicated that the failure mechanism was changing mode. Figure 47, page 67, shows this new collapse mode.

The load continued to increase and at a load of 6000 lbs. the new mode of failure was clearly developing. At 7800 lbs. the interior longitudinal was 1 3/4 inches higher at the center than at the load points. At 8390 lbs. the bottom steel in the interior longitudinal broke in the vicinity of gauge 9. Figure 49, page 68, shows the broken bars directly under the load point. At this time the spreader-beam, by which loading was being carried out, was bearing at the center of the grillage and further loading was considered to be too difficult to analyze. The final deflections for the interior longitudinal were 9.125 inches at

the center and 12.25 inches at the load points. The state of the grillage at the completion of the test can be observed in Figures 48 to 54 on pages 67 to 70.

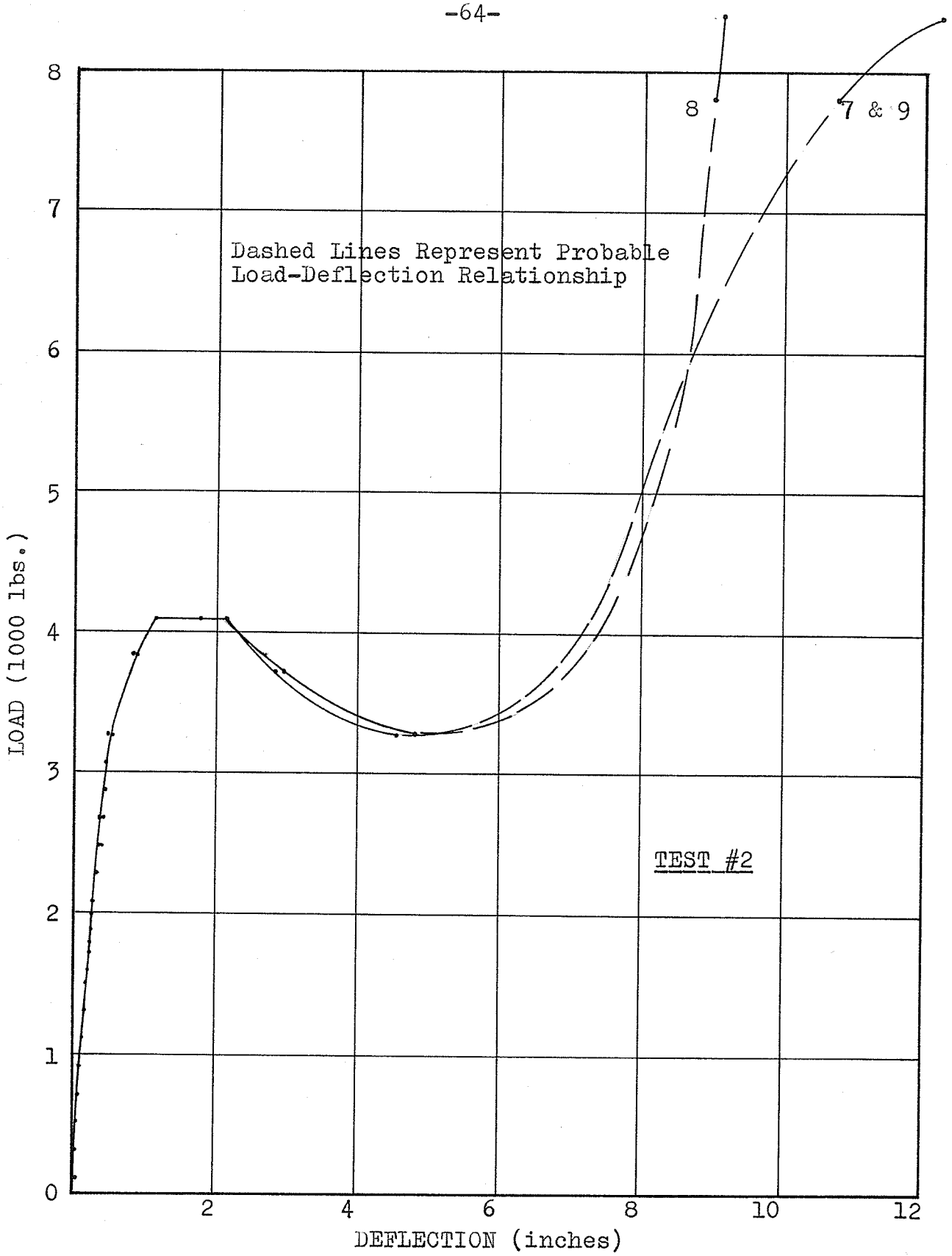

Figure 43. Load-Deflection Curves for Several Gauge Locations.

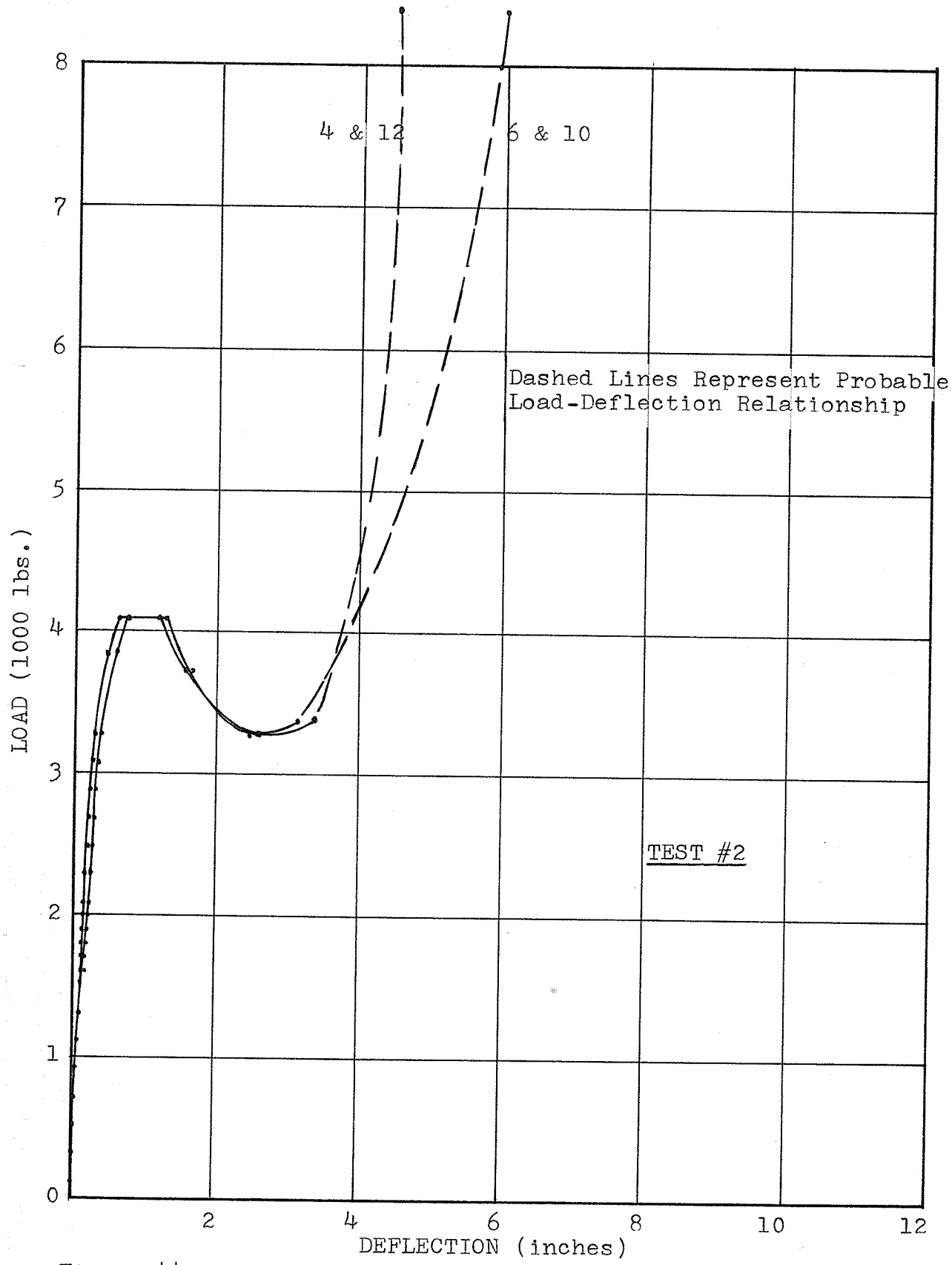

Figure 44. Load-Deflection Curves for Several Gauge Locations.

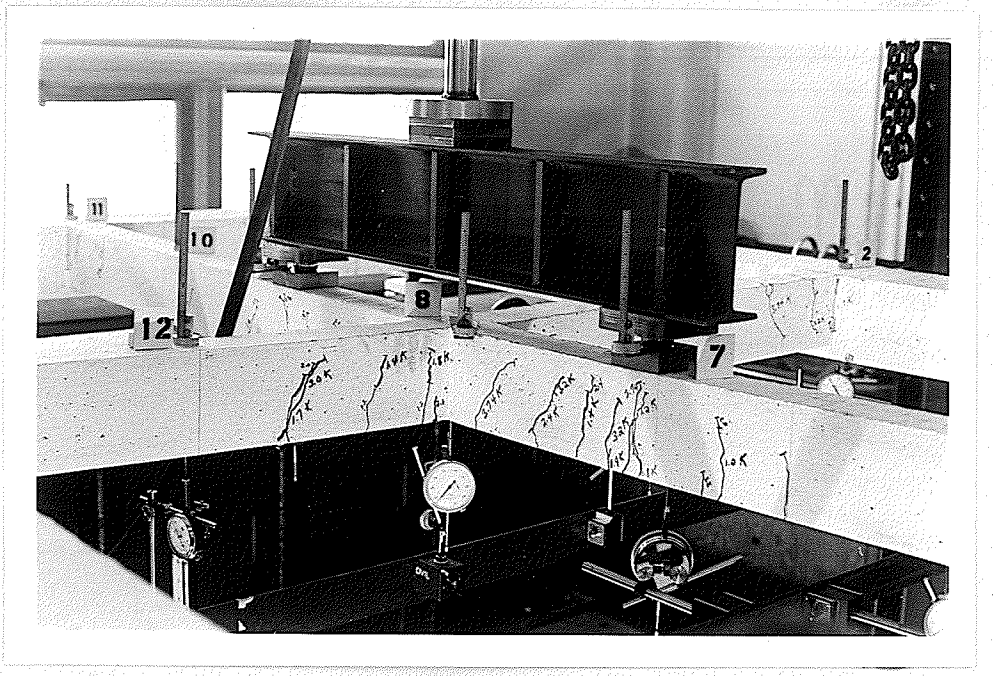

Figure 45. Early Crack Development.

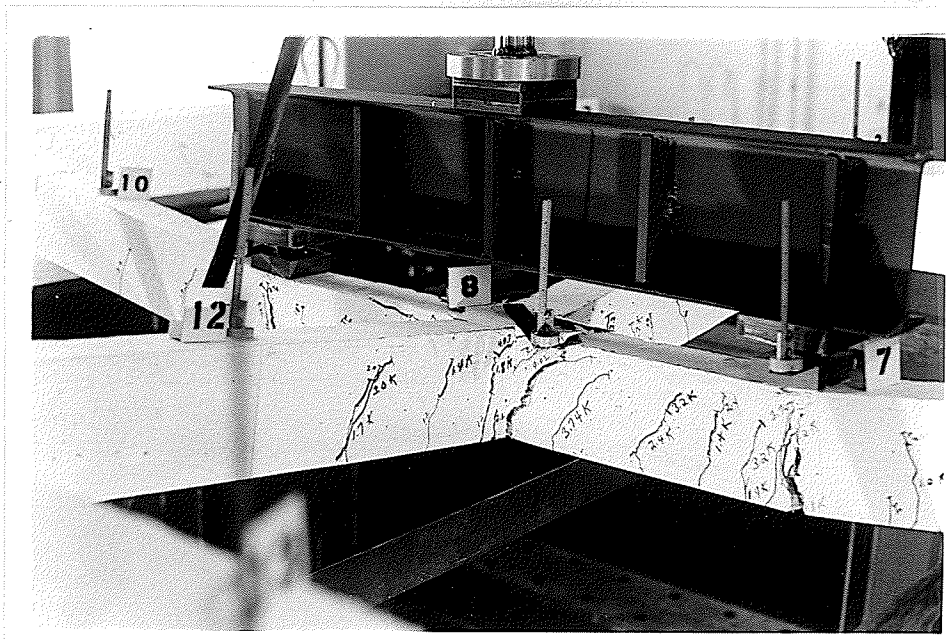

Figure 46. Further Crack Development.

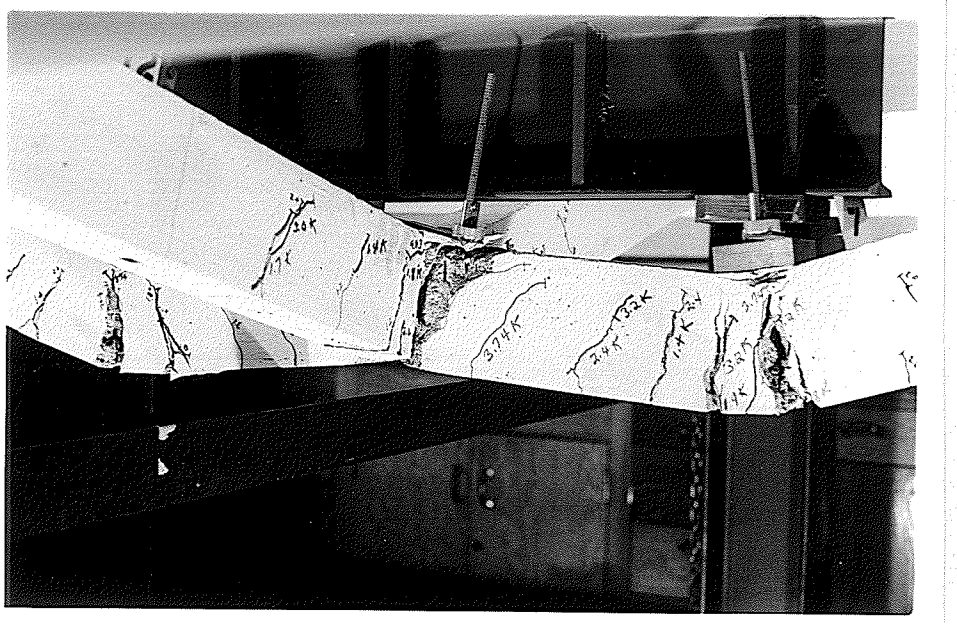

Figure 47. Change in Cracking Pattern.

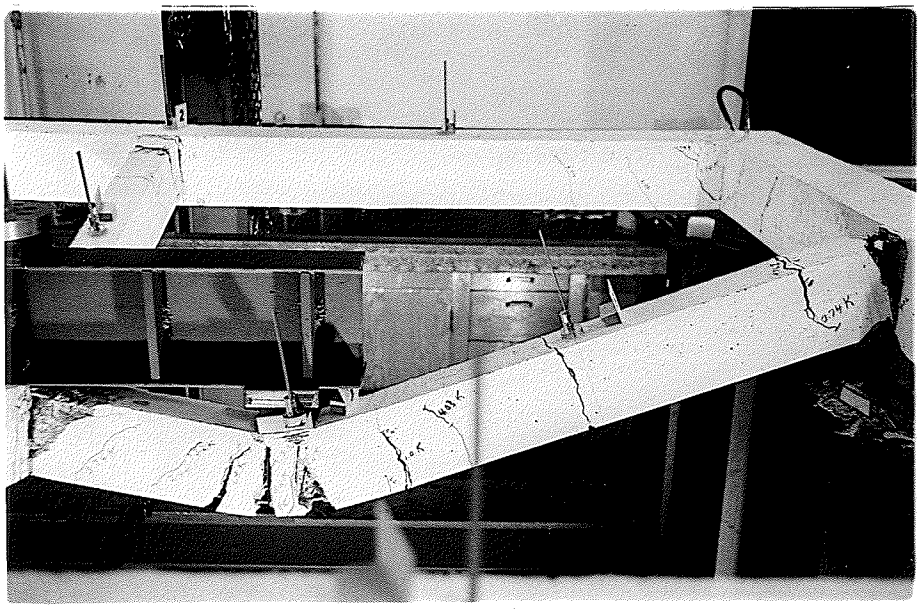

Figure 48. Section of Longitudinal at End of Test.

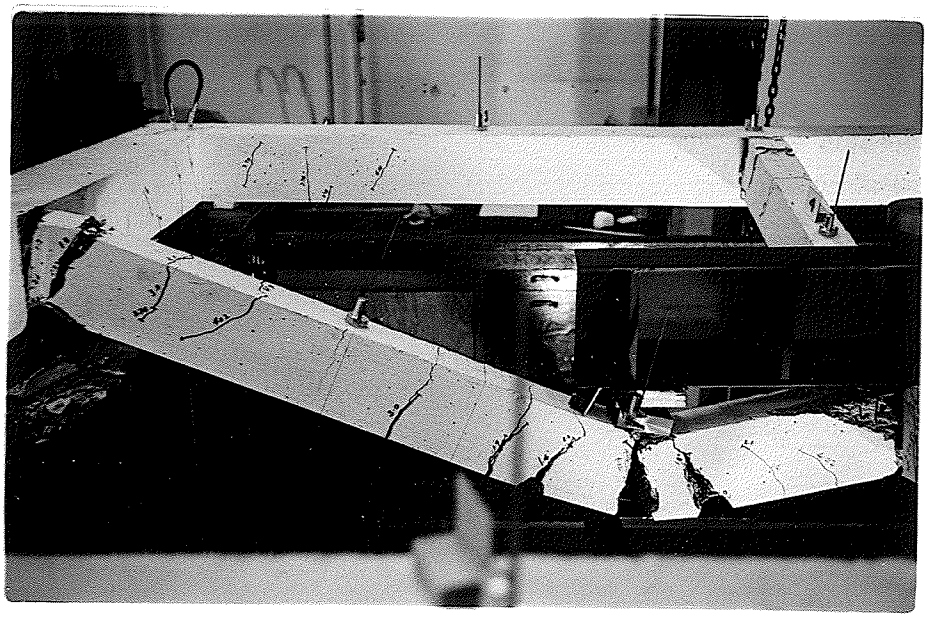

Figure 49. Section of Longitudinal at End of Test.

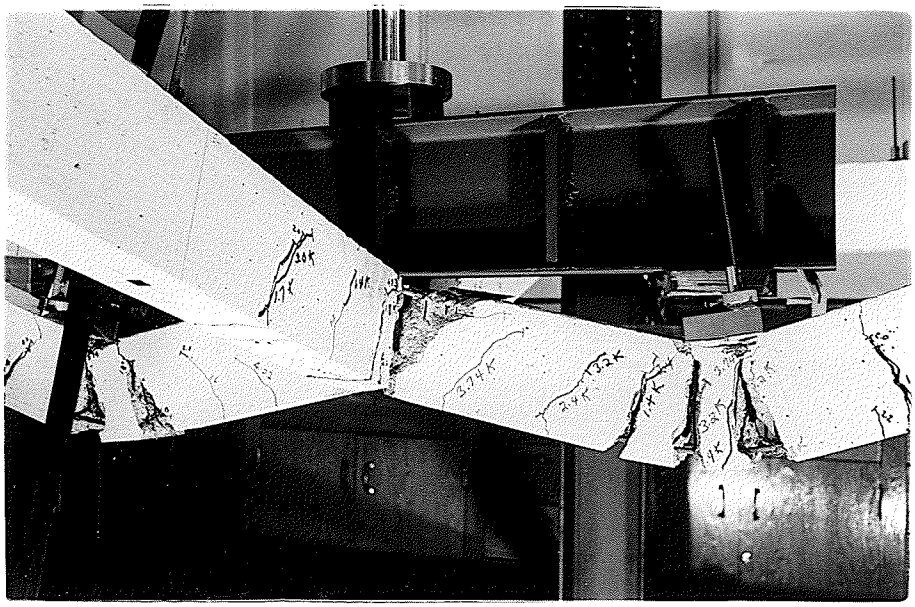

Figure 50. Final Collapse Configuration.

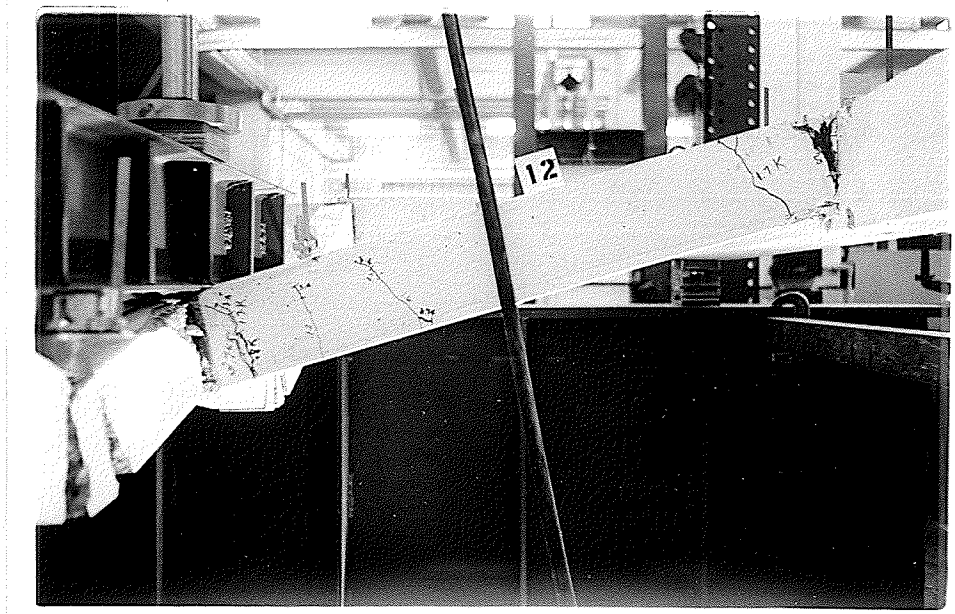

Figure 51. Section of Transversal at End of Test.

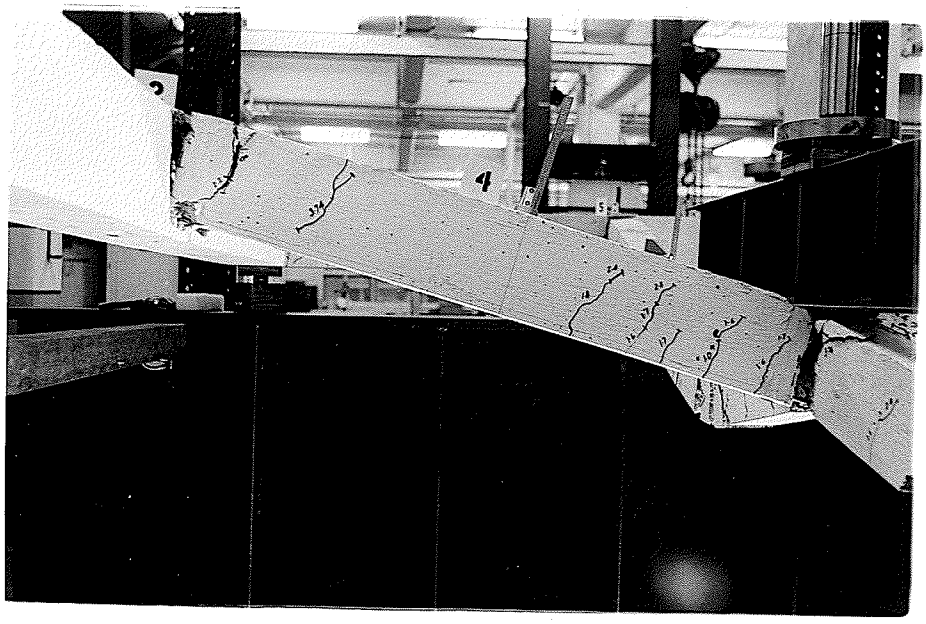

Figure 52. Section of Transversal at End of Test.

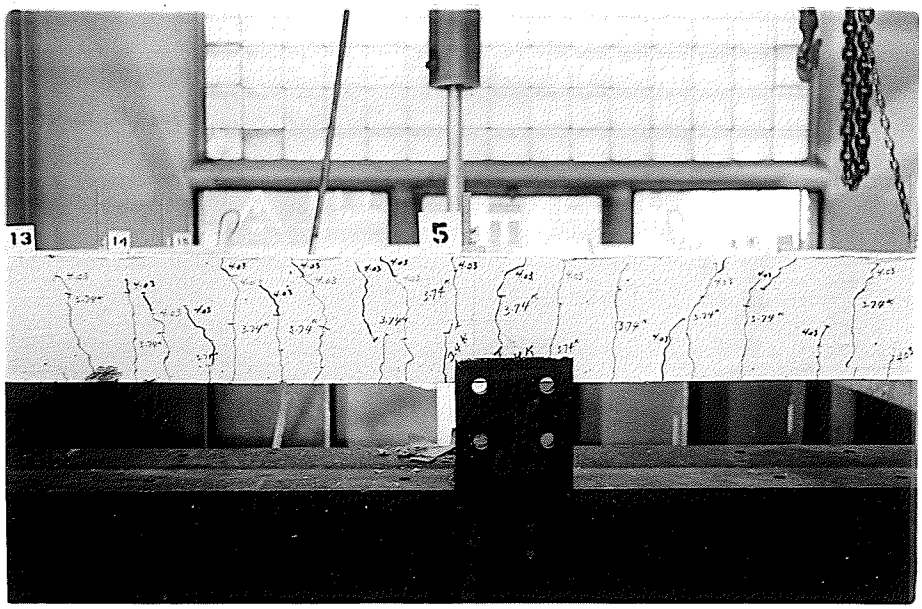

Figure 53. Torsion and Flexure Cracks on Exterior Transversal.

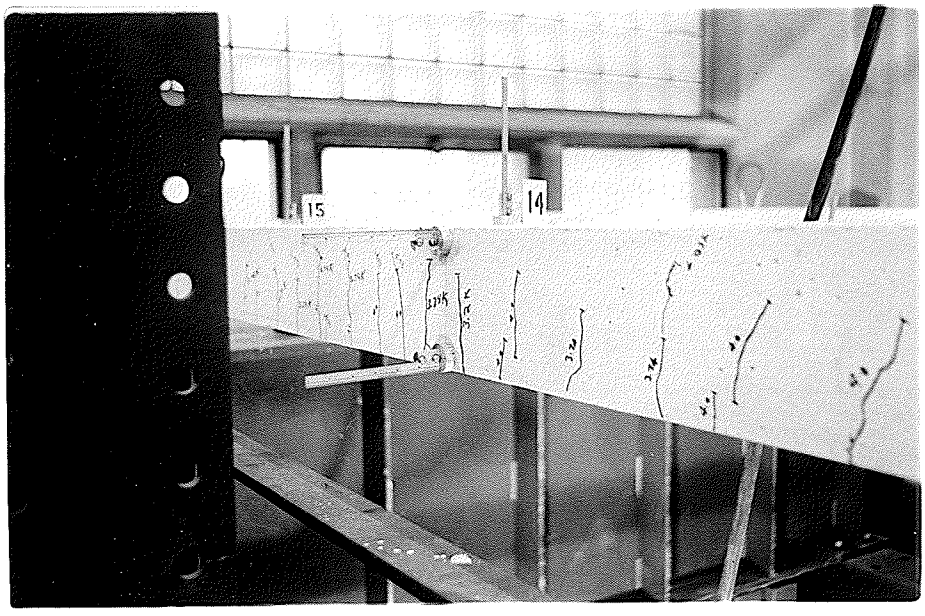

Figure 54. Torsion and Flexure Cracks on Exterior Longitudinal.

CHAPTER V

ANALYSIS OF THE GRILLAGES

The two grillages were analyzed using a combination of ultimate strength and plastic hinge theories. Even though the manner of loading each of the grillages was different, the same principles of analysis were used in investigating the ultimate load of each structure. In the theoretical analysis the calculations consisted of finding the plastic moment of the beams, finding the torsional moment of the beams and finding the ultimate load based on the combined ultimate load and plastic hinge theories. Various modes of collapse were investigated and the mode giving the smallest ultimate load was considered the critical mode.

5.1 Plastic Bending Moment.

The method used to analyze the grillage beams for their ultimate flexural strength was basically the British method as explained by Jones[7]. The various ultimate strength theories vary in their approach to the distribution of the concrete compressive stress, however, most theories which predict the ultimate moment are essentially the same and generally the following assumptions are made:

(a) The distribution of the concrete compressive stresses can be defined. Usually this is done by means of coefficients from which the average compressive stress and position of the centre of pressure can be assessed.

(b) The beam will fail when the maximum compressive strain in the beam reaches a particular value.

(c) The distribution of the concrete strain is linear (which is the same as saying that the strain at any level

varies directly as the distance from the neutral axis).

(d) The average strain in the steel has the same value as the strain in the concrete at the same level.

(e) The concrete does not resist tension.

The equations set down by Jones for the calculation of the ultimate moment in doubly reinforced beams are:

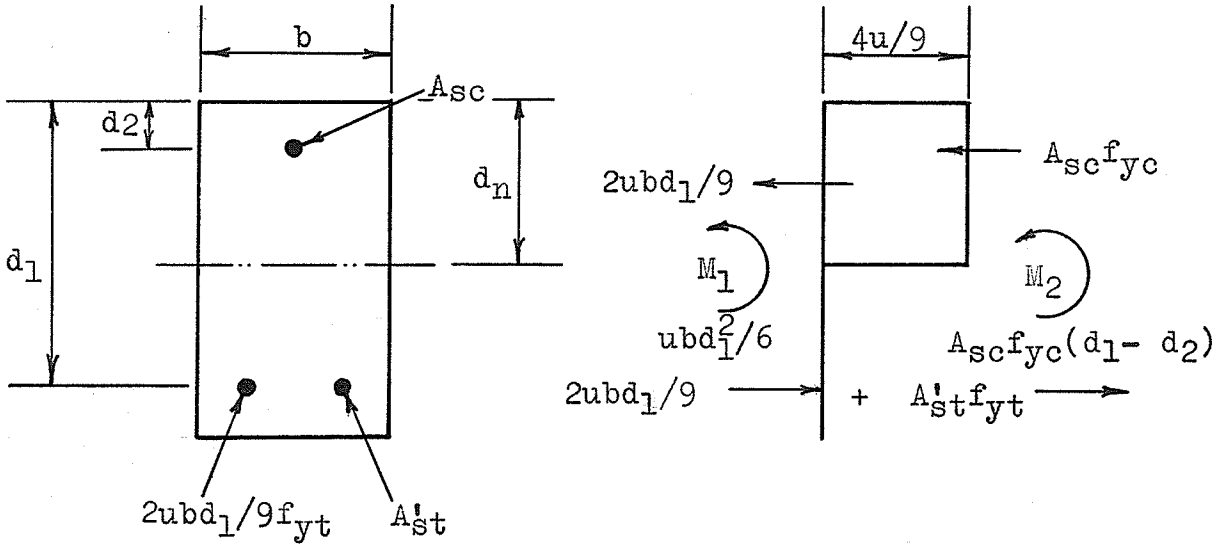

If longitudinal forces are equated and we initially assume that the steel is yielding,

$$A_{st}f_{yt} = A_{sc}f_{yc} + 4/9\ ubd_n$$

or $$d_n = 9/4ub\ (A_{st}f_{yt} - A_{sc}f_{yc}).$$

By taking moments about the tensile steel,

$$M_u = 4/9\ ubd_n(d_1 - \tfrac{1}{2}d_n) + A_{sc}f_{yc}(d_1 - d_2),$$

the value of d_n having been found by the previous equation.

It is quite obvious, from the cross-section of the main beams used in the grillage, that too much compression steel has been used. In reality the compression steel would probably not reach the yield point, but the value of the ultimate moment would not be materially affected. Basically, the reason why so much compression steel was used in the exterior beams was to provide adequate torsional rigidity. The interior beams, on the other hand, had a minimum of tensile and compressive reinforcement. This steel, in conjunction with closed lateral hoops, provided a symmetrical reinforcing cage.

Example calculations of the ultimate moment capacity of the grillage beams is shown in Appendix A, page 107.

5.2 Torsional Moment.

The method used to find the torsional moment of the exterior beams in the grillages was established by Lansdown[8]. The equations suggested by Lansdown are for beams subjected to pure torsion. These equations were considered quite satisfactory by the author, as tests by Nylander[9] as well as Cowan and Armstrong[10] indicated that small amounts of bending increased the torsional strength of a beam. It is believed that the "self-prestressing" effect in a cracked beam affects favourably the torsional strength of the member, raising it to the same order of strength as that of the uncracked member.

In general, the Lansdown theory deals with helical transverse reinforcement as this system is of a more fundamental nature. A reinforcing cage of longitudinal bars and transverse hoops is conceeded to be a more practical

system and is dealt with in the following manner. The contribution of longitudinal bars and hoops to the strength of a concrete member may be estimated by transforming the actual reinforcement into an equivalent helix and then proceeding as for the case of helical reinforcement.

For a rectangular beam and helical reinforcement Lansdown has found that the torque contributed by the steel (and its associated concrete stress) is:

$$M_{T_{st}} = \frac{5}{3} A_{cage} \frac{n_x F_{yx} \sin\beta}{C} (K_1 + K_s)$$

where A_{cage} is the area enclosed by the reinforcing cage (b'. d'). This equation is applicable to square as well as rectangular sections in which case K_1, as the proportion of steel on the long sides of a beam, is the same as K_s, the proportion of steel on the short sides.

The torque developed cannot be far from that predicted by the yielding of the whole length of helical bars, and a good approximation results if one sets $K_1 = K_s = 1$. Substituting one obtains

$$M_{T_{st}} = \frac{10}{3} A_{cage} \frac{n_x F_{yx} \sin\beta}{C} .$$

In transforming a system of longitudinal bars and closed hoops or stirrups, Lansdown has found that the actual reinforcement may be replaced with an equivalent 45-degree helical cage, having a steel ratio equal to the lesser of the longitudinal or transverse ratios, and the "surplus" steel ignored.

It was found convenient for purposes of calculation, to work in terms of the equivalent yielding force per unit length, R, developed by the reinforcements. Thus n long-

itudinal bars in a member have an equivalent yielding force of

$$R_L = \frac{nF_{yL}}{C}$$

per unit length of circumference, where F_{yL} is the yielding strength of one longitudinal bar, whereas hoops at pitch, p, have an equivalent yielding force of

$$R_T = \frac{F_{yT}}{p}$$

per unit of beam. The equivalent helix force then becomes the lesser of R_T and R_L , i.e. R_{min}.

The transformation to the equivalent 45 degree helical reinforcement is completed by noting that

$$n_x F_{yx} = C \cdot R_{min} .$$

By noting this and knowing $\sin\beta = .707$ (as $\beta = 45^o$), the torsional moment reduces to

$$M_T = 2.536\ A_{cage}\ R_{min} .$$

An example calculation for the exterior grillage beams is shown in Appendix A, page 107.

5.3 Grillage No. 1.

Analysis.

The loading on the first grillage consisted of a single point load at the center. The high bending strength of the main beams and the relative weakness of the interior beams,

suggested that the failure would probably be confined to the interior beams. Three various modes of collapse were investigated to find the ultimate load that the grillage could take.

The first mode of collapse investigated consisted of plastic hinges forming at the center of the three grillage longitudinals.

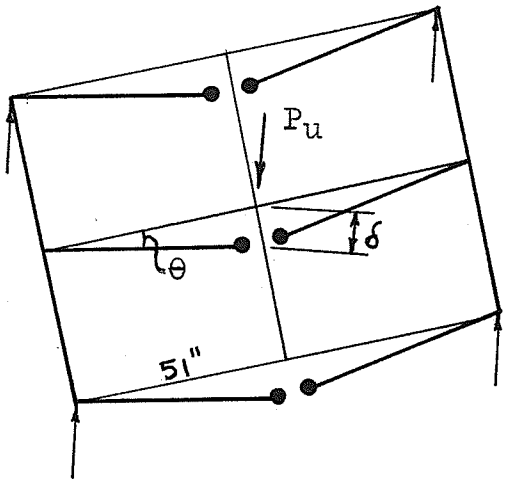

A virtual work equation was found to be the quickest and simplest form of calculation.

$$P_u\delta = 4M_{EP}\theta + 2M_{IP}\theta$$

$$\delta = 51\ \theta$$

$$51\phi P_u = 4M_{EP}\phi + 2M_{IP}\phi$$

$$P_u = \frac{4M_{EP}}{51} + \frac{2M_{IP}}{51}$$

$$= \frac{4 \times 153{,}000}{51} + \frac{2 \times 16{,}170}{51}$$

$$= 12{,}000 + 634$$

$$P_u = \underline{12{,}634 \text{ lbs.}}$$

The second mode of collapse investigated took into account the possible formation of torsional hinges in the exterior members.

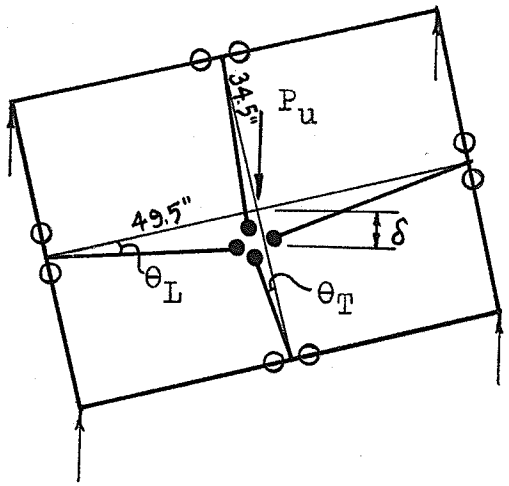

○ Torsional Hinge

● Bending Hinge

$$P_u\delta = 4M_{ET}\theta_L + 4M_{ET}\theta_T + 2M_{IP}\theta_L + 2M_{IP}\theta_T$$

$$\theta_L = \frac{\delta}{49.5} \qquad \theta_T = \frac{\delta}{34.5}$$

$$P_u\delta = 4M_{ET}\frac{\delta}{49.5} + 4M_{ET}\frac{\delta}{34.5} + 2M_{IP}\frac{\delta}{49.5} + 2M_{IP}\frac{\delta}{34.5}$$

$$= \frac{4M_{ET}}{49.5} + \frac{4M_{ET}}{34.5} + \frac{2M_{IP}}{49.5} + \frac{2M_{IP}}{34.5}$$

$$= \frac{4 \times 30,700}{49.5} + \frac{4 \times 30,700}{34.5} + \frac{2 \times 16,170}{49.5} + \frac{2 \times 16,170}{34.5}$$

$$= 2,480 + 3,560 + 653 + 937$$

$$P_u = \underline{7,630 \text{ lbs.}}$$

The third and final mode of collapse investigated, considered the possibility of all of the plastic hinges forming in the interior beams. This mode of collapse was the one generally anticipated and the grillage beams were originally so proportioned, that this mode would be the probable collapse mode.

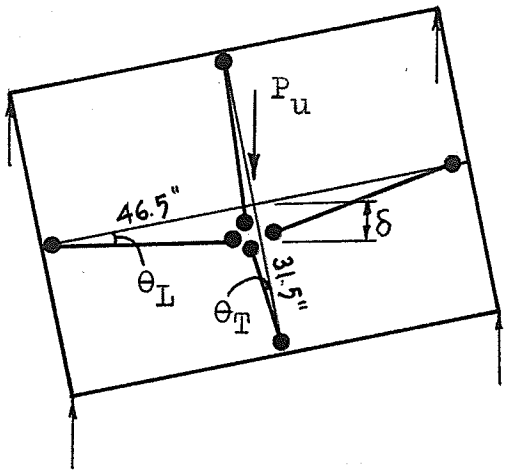

$$P_u\delta = 4M_{IP}\theta_L + 4M_{IP}\theta_T$$

$$\theta_L = \frac{\delta}{46.5} \qquad \theta_T = \frac{\delta}{31.5}$$

$$P_u\delta = 4M_{IP}\frac{\delta}{46.5} + 4M_{IP}\frac{\delta}{31.5}$$

$$= \frac{4 \times 16{,}170}{46.5} + \frac{4 \times 16{,}170}{31.5}$$

$$= 1{,}390 + 2{,}050$$

$$P_u = \underline{3{,}440 \text{ lbs.}}$$

Assuming that the third mode is the failure mode an equilibrium check of the grillage reveals:

F.B.D. of the Interior Longitudinal

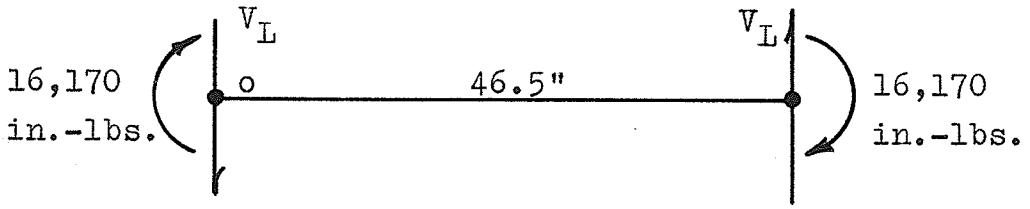

$$\Sigma M_o = 0$$

$$= 16{,}170 + 16{,}170 - 46.5V_L = 0$$

$$\therefore V_L = \frac{32{,}340}{46.5} = 695 \text{ lbs.}$$

F.B.D. of the Interior Transversal

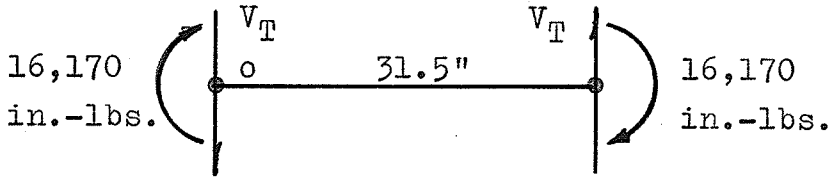

$$\Sigma M_o = 0$$

$$= 16{,}170 + 16{,}170 - 31.5V_T = 0$$

$$\therefore V_T = \frac{32{,}340}{31.5} = 1{,}025 \text{ lbs.}$$

At the center

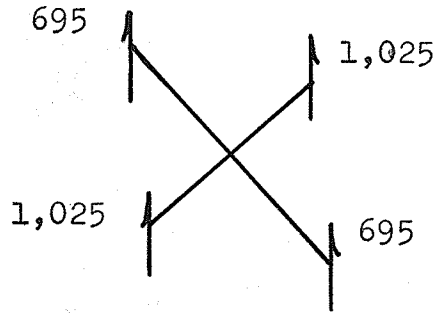

Total

695
695
1,025
1,025
3,440 lbs. ✓

F.B.D. of the External Longitudinals

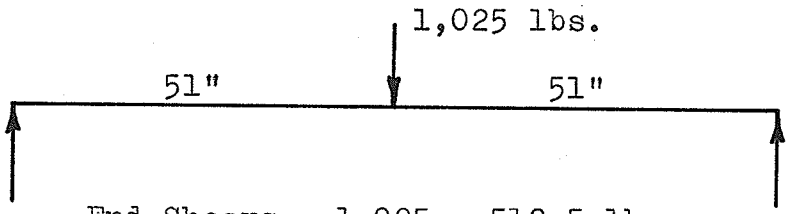

End Shears = $\frac{1,025}{2}$ = 512.5 lbs.

M @ center of beam = 512.5 x 51 = 26,150 in.-lbs.

F.B.D. of the External Transversals

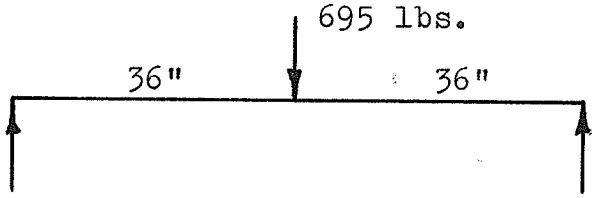

End Shears = $\frac{695}{2}$ = 347.5 lbs.

M @ center of beam = 347.5 x 36 = 12,500 in.-lbs.

Reaction at one corner

= 347.5 + 512.5 = 860 lbs.

Check of total reaction

= 4 x 860 = 3,440 lbs. ✓

Moment Diagram.

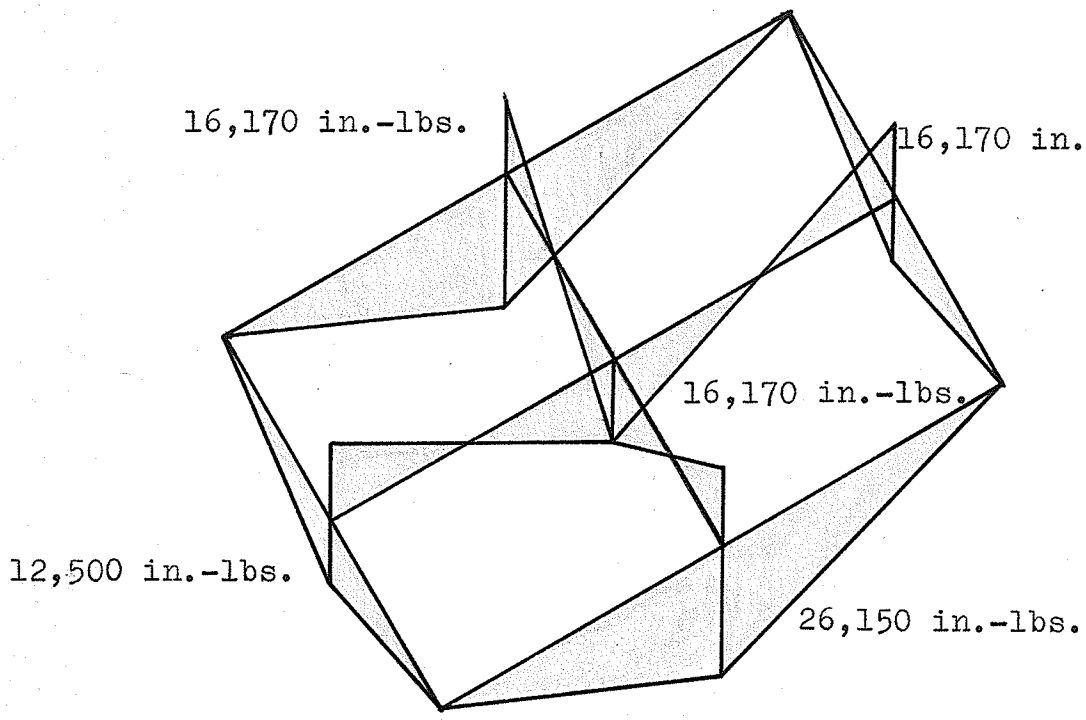

Shear Diagram.

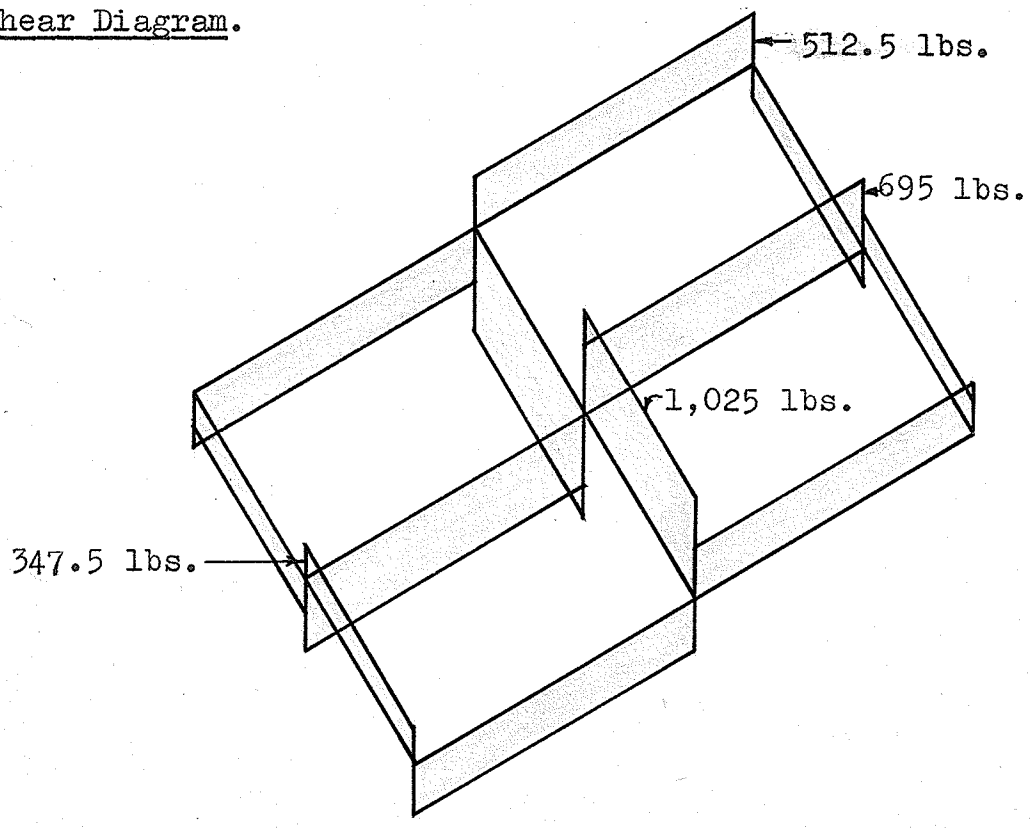

5.4 Grillage No. 2.

Analysis.

The second grillage was identical to the first in all respects. The loading of the grillage differed, however, as two concentrated loads were placed on the interior longitudinal instead of one concentrated load at the center.

Two modes of failure were considered for the second grillage. Each of the collapse modes confined the plastic hinges to the interior beams as suggested by the collapse of grillage no. 1.

The first mode of collapse investigated considered a failure similar to the first grillage.

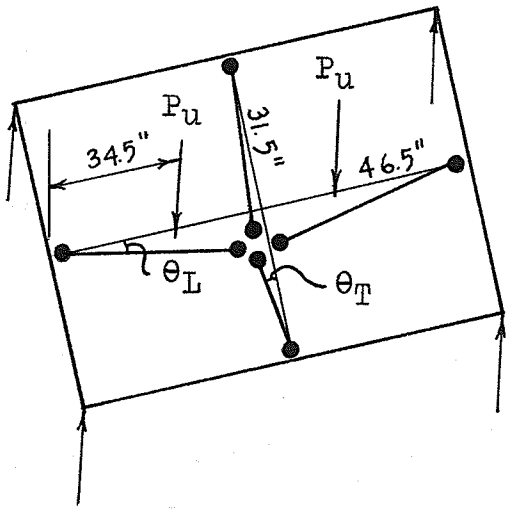

$$\theta_L = \frac{\delta}{46.5} \qquad \theta_T = \frac{\delta}{31.5}$$

Deflection under the loads = $\frac{34.5}{46.5}\delta = 0.742\,\delta$

$$2(.742\delta P_u) = 4M_{IP}\theta_L + 4M_{IP}\theta_T$$

$$.742P_u\delta = 2M_{IP}\frac{\delta}{46.5} + 2M_{IP}\frac{\delta}{31.5}$$

$$.742P_u = \frac{2 \times 16{,}170}{46.5} + \frac{2 \times 16{,}170}{31.5}$$

$$= 695 + 1{,}025 = 1{,}720 \text{ lbs.}$$

$$\therefore P_u = \frac{1{,}720}{.742} = \underline{\underline{2{,}320 \text{ lbs.}}}$$

The second mode of collapse considered plastic hinges forming directly under the loads.

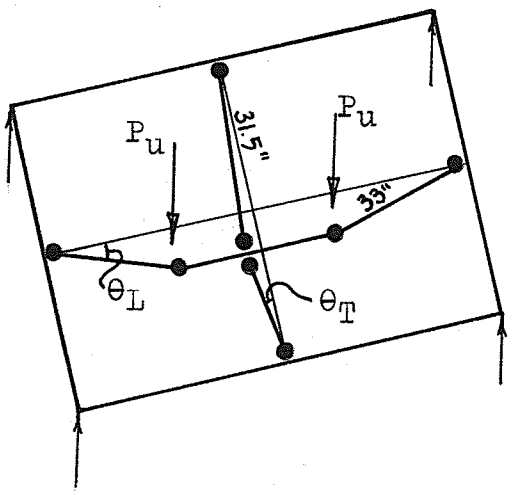

$$\theta_L = \frac{\delta}{33} \qquad \theta_T = \frac{\delta}{31.5}$$

$$2(P_u\delta) = 4M_{IP}\theta_L + 4M_{IP}\theta_T$$

$$P_u\delta = 2M_{IP}\frac{\delta}{33} + 2M_{IP}\frac{\delta}{31.5}$$

$$P_u = \frac{2 \times 16{,}170}{33} + \frac{2 \times 16{,}170}{31.5}$$

$$= 980 + 1{,}025$$

$$P_u = \underline{\underline{2{,}005 \text{ lbs.}}}$$

Assuming that the second collapse mode is the failure mode, an equilibrium check reveals:

F.B.D. of the Interior Longitudinal

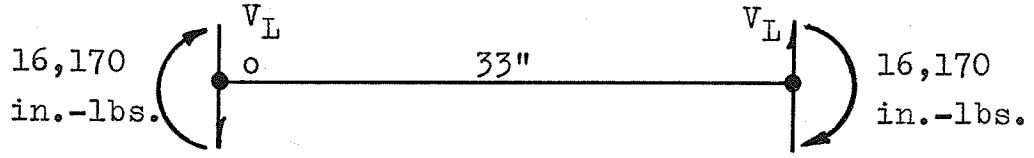

$$\Sigma M_o = 0$$

$$= 16{,}170 + 16{,}170 - 33V_L = 0$$

$$\therefore V_L = \frac{32{,}340}{33} = 980 \text{ lbs.}$$

F.B.D. of the Interior Transversal

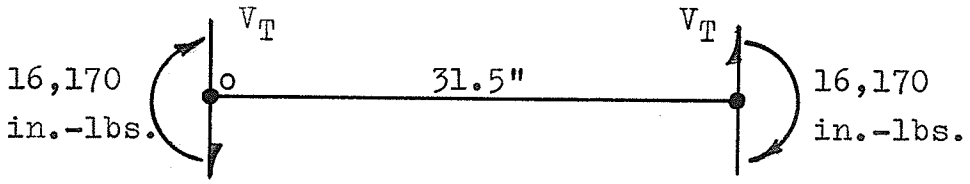

$$\Sigma M_o = 0$$

$$= 16{,}170 + 16{,}170 - 31.5V_T = 0$$

$$\therefore V_T = \frac{32{,}340}{31.5} = 1{,}025 \text{ lbs.}$$

At the center

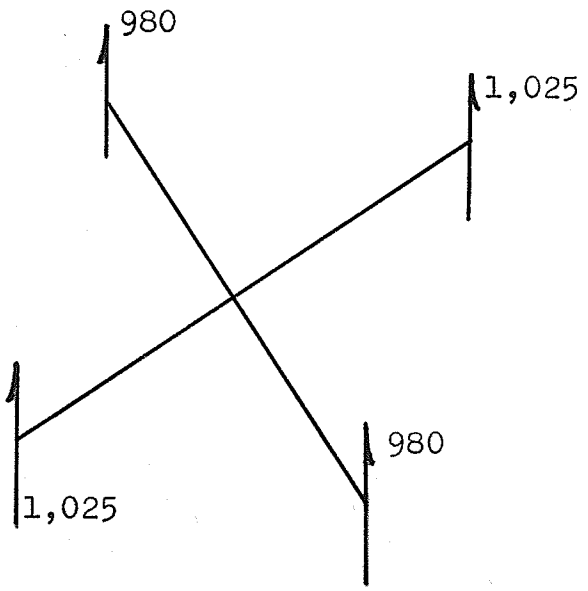

Total	980
	980
	1,025
	1,025
	4,010 = $2P_u$

$\therefore P_u$ = 2,005 lbs. ✓

F.B.D. of the External Longitudinal

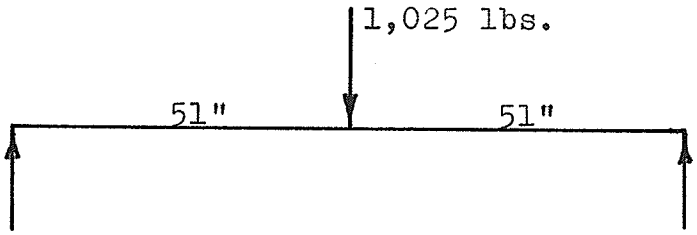

End Shears = $\frac{1,025}{2}$ = 512.5 lbs.

M @ center of beam = 512.5 x 51 = 26,150 in.-lbs.

F.B.D. of the External Transversal

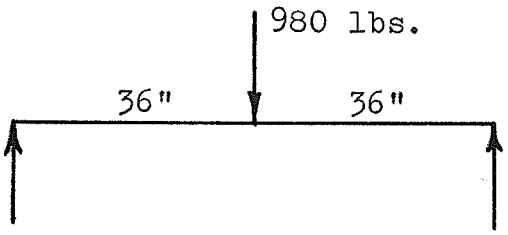

End Shears = $\frac{980}{2}$ = 490 lbs.

M @ center of beam = 490 x 36 = 17,630 in.-lbs.

Reaction at one corner

= 490 + 512.5 = 1,002.5 lbs.

Check of total reaction

= 4 x 1,002.5 = 4,010 lbs. ✓

Moment Diagram.

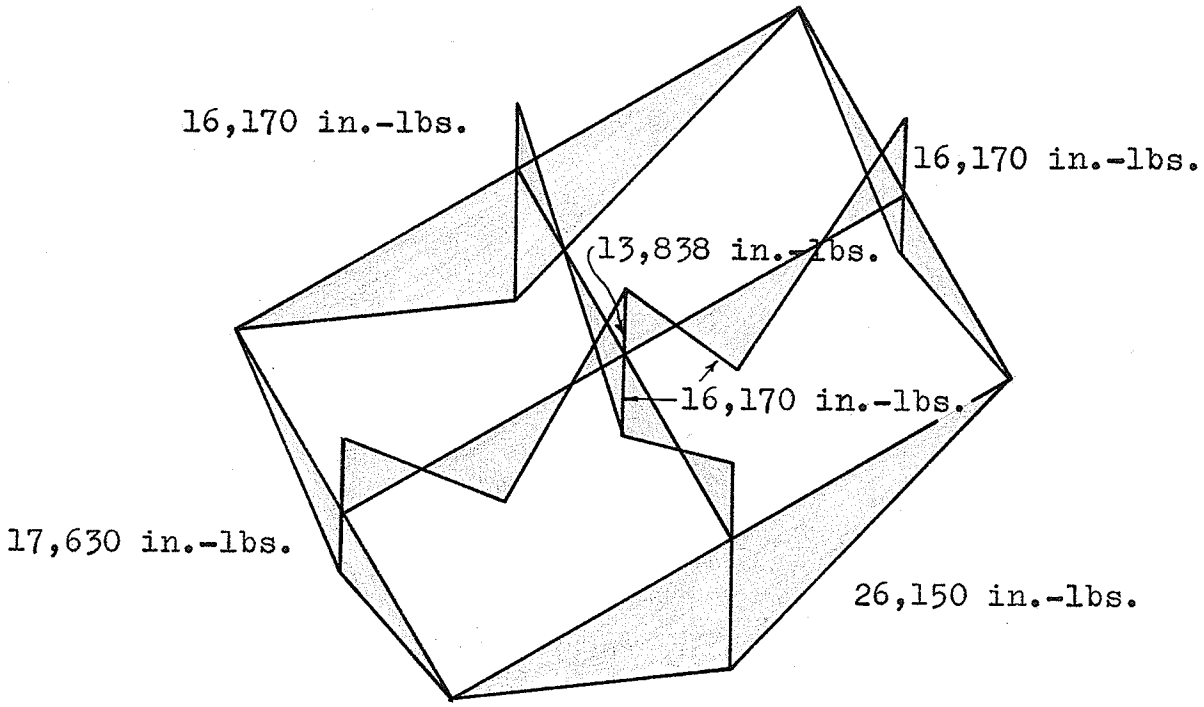

Shear Diagram.

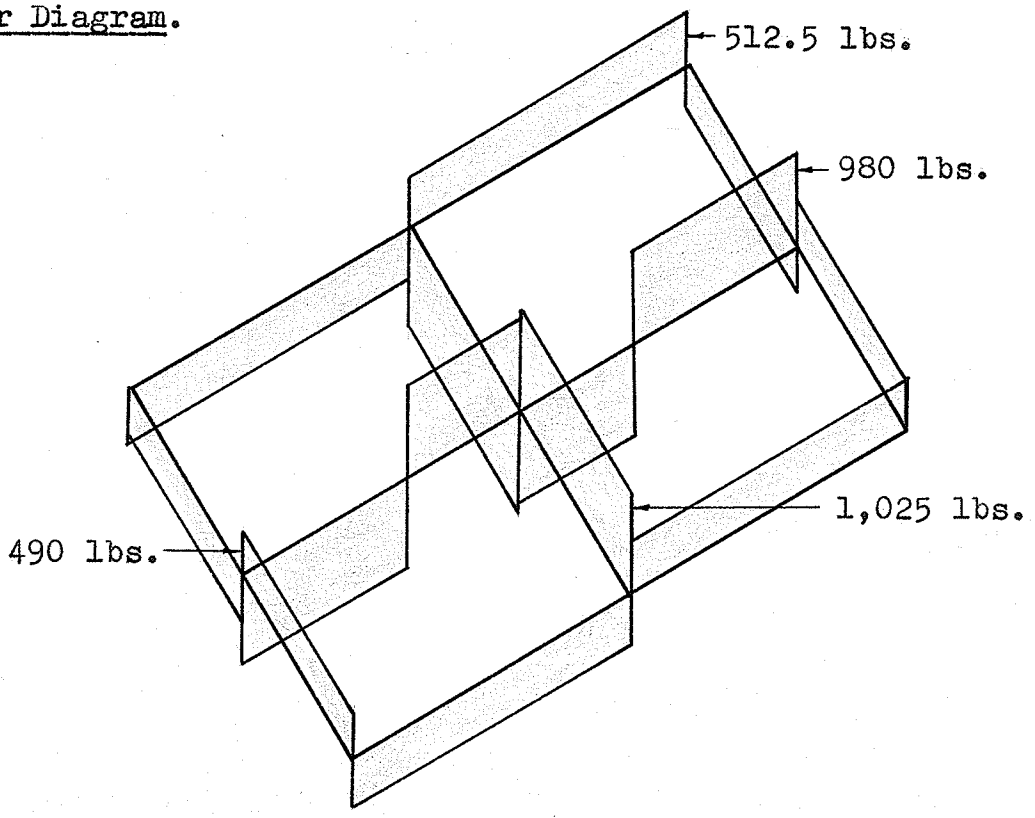

5.5 Test Results and Discussion.

(a) Grillage No. 1.

It is of interest to note, before going into a detailed discussion of test results, the criterion of failure or collapse for concrete beams. Two main types of failure exist. Concrete beams can fail either by primary crushing of the concrete or by failure initiated by the yielding of the steel. If the failure is a primary concrete failure it is usually called a compression failure, and if the failure is initiated by the yielding of the steel it is called a tension failure. In the first grillage test, a flexural failure initiated by the yielding of steel best describes the mode of collapse.

The maximum load resisted by grillage no. 1, in the two part test performed upon it, was 8300 lbs. By the above definition of failure this could hardly be construed as the failure or collapse load. Both yielding of steel, as witnessed by the broken bars, and crushing of concrete had occurred before this point. The final deflection, 1.613 ft., also could not be tolerated in a working structure. It can be seen, however, in Figure 34, page 55, that two distinct stages of failure occurred. The first stage is the one most readily associated with concrete failure--namely yielding of steel and crushing of concrete. The second stage of failure of the grillage is associated with catenary action of the reinforcing steel or a hanging reinforcement network at large deflections. A detailed examination of increased loading with large deflections will be dealt with in the general discussion.

Studying Figure 27, page 48, shows that the probable yield or collapse load for the grillage was in the region of 5380 lbs. This load yields a ratio of observed to cal-

culated strength of 1.56. The pattern of cracks, developed at this point, indicates that the collapse mechanism is the same as the predicted mode of failure. It is also interesting to note that torsional cracks began to appear in the exterior members when the load reached the 5180 lb. value.

In the observations of the first grillage test, it was mentioned that there may have been some yield when the load reached 2630 lbs. From the load-deflection curves, there does not seem to be any yield plateau at this load. It does appear, however, that yield began near the 5000 lb. mark for the center portion of the grillage. Load continued to increase to 5380 lbs. and then dropped off again to the 5000 lb. level where it remained fairly constant.

Several reasons could explain the larger than anticipated collapse load of 5380 lbs. First of all, a greater concrete strength than the design value undoubtedly added to the increased load. Second, the steel strength had to be greater than indicated. Table II, page 28, shows that the average yield stress of the $\frac{1}{4}$" $\emptyset$ steel, for the first grillage, was 38,400 psi. The same table shows that the average yield stress of the $\frac{1}{4}$" $\emptyset$ steel for the second grillage, was 65,300 psi. The large discrepancy indicates that an error in testing the steel of the first grillage may have occurred, as the steel used in both grillages came from the same bundle of bars. An increased yield point would definitely account for some of the increase in the collapse load. If an analysis is made with the yield strength of the $\frac{1}{4}$" $\emptyset$ steel at 48,000 psi. or 20 percent greater than the previously assumed value, the ratio of observed to calculated strength becomes 1.30.

A third reason for the larger collapse load may have been the effect of membrane action in the interior beams. In composite beam and slab structures, it has been indica-

ted in tests at the University of Manitoba that membrane forces in conjunction with arching action can increase the yield load of a structure as much as 1.77 times the indicated load[11]. Tests by Kani[12] at the University of Toronto indicate that concrete beams, subject to flexural loading, transform into a tied arch and that the capacity of the remaining arch may be higher than that anticipated for the beam.

Tests of transversally loaded reinforced concrete plates revealed that actual load-deflection relationship differs from that of the yield line theory [23]. One of the factors responsible for this fact is the membrane action induced as a result of finite deformation. At early stages of loading the membrane action is compressive and, depending upon the boundary conditions, may result in a significant increase of the collapse load over the limit load rendered by the yield line theory. As deflection increases, the membrane action changes from a compressive to a tensile one. Continuation of plastic deformation produces significant changes in geometry of the structure and the slab is transformed into a "plastic" or "tensile membrane". This results in an increase of load with increasing deflections. In this case the strength of the structure lies in the hanging network of reinforcement. The strength of this "tensile membrane" is limited only by the limit of plastic elongation of the reinforcement. Both compressive and tensile membrane actions are dependent, however, on the restraint offered by the surrounding structure. The exterior beams of the grillage were rigid enough to promote this type of membrane action in the interior grillage beams.

This "tensile membrane" or hanging network action of reinforcement could explain the manner in which the grillage resisted loading beyond the first stage maximum of 5380 lbs.

From observation during the test, it was fairly obvious that a hanging network of reinforcement resisted the load. The concrete under the load gradually broke away and the load plate eventually rested directly on the reinforcing bars. A precise analysis of the stresses in the steel would be impossible. Several bars had broken and the manner in which stresses had redistributed could only be assumed. In addition, localized areas of very high strain concentration existed at the junctions of the interior and exterior beams as well as directly beneath the load.

The development of cracking under loading was previously described in the observations of Tests no. 1a and 1b. However, the exact nature of the cracks was not previously given. In the first part of Test no. 1, the initial cracks that developed were tension cracks due to moment. As the load and deflection increased, these cracks tended to widen considerably in the areas of high stress concentration--namely at the junctions with the main beams and directly beneath the load. It is interesting to note that only one diagonal crack appeared on the interior beams. This crack can clearly be seen on the interior longitudinal in Figure 33, page 51, and subsequent pictures. Near the completion of this phase of the test, torsional cracks appeared on the exterior beams. These, however, were not of a very severe nature. Crack development in the first part of Test no. 1 can be traced in Figures 28 to 33, on pages 49 to 51.

In the second portion of Test no. 1, vertical cracks due to moment continued to form on the interior beams. These cracks eventually opened and a pronounced bending or hinging took place on the transversal at a point approximately 9 inches from the junctions with the main beams and the same distance from the load point. Figure 41, page 59, shows this development. Crushing and spalling of concrete

also took place in this part of the test. Towards the end of the test, the load plate rested upon the reinforcing bars rather than upon the concrete. Figure 38, page 57, shows this situation clearly.

Deflection and rotation readings for the exterior beams were recorded only in the first part of Test no. 1. The largest deflection of a main beam was 0.230 inches at gauge location 12. The rotation at the centers of the main longitudinals was 4 degrees 10 minutes or 0.07272 radians. Severe cracking was not observed on the exterior beams.

The small values for deflection and rotation could be expected for the heavy exterior beams because of their high ultimate bending and torsional strengths. Increased concrete and steel strengths further increased the exterior beam capacity to resist load. Tests performed on sections of grillage no. 1 and outlined in Appendix C, page 117, show that the bending strength was approximately 92 percent greater than the original calculated strength. If actual concrete strength, actual steel yield strengths and action of dowel bars are taken into account, the increase in strength is in the order of 24 percent. The action of the dowel bars, used to anchor the interior beam steel, increased the bending strength of the exterior beams substantially. The ultimate moment capacity of the exterior beams, taking into account the actual concrete and steel strengths of grillage no. 1, was 189,200 in.-lbs. The ultimate moment capacity taking into account the action of the dowel bars in the center portion of the beams as well, was 237,100 in.-lbs. This figure compares to the observed value of 294,000 in.-lbs. The effect of the dowel bars was not fully considered in the original analysis.

Torsion tests conducted on sections of grillage no. 1 revealed an average yield strength of 30,650 in.-lbs. This compares very favorably with the original calculated value

of 30,700 in.-lbs. If actual yield strengths for the longitudinal and tie steel are used in recalculating predicted torsional strength, the yield or ultimate strength becomes 26,150 in.-lbs. The ratio of actual to predicted strengths now becomes 1.17.

By viewing pictures of Tests 1a and 1b, it can be seen that shear and diagonal tension did not influence the collapse mode of the structure. It appears that the precautions taken to avoid shear problems proved adequate.

(b) Grillage No. 2.

In the second test the collapse or failure load of 4100 lbs. was slightly more than twice the predicted collapse load of 2005 lbs. However, if the concrete strength at testing, as well as the yield strength of the $\frac{1}{4}$" $\emptyset$ steel in the second grillage are used as design data, the predicted collapse load becomes 3330 lbs. Using this figure, the actual collapse load to predicted collapse load ratio is 1.23. This ratio gives a more realistic comparison between test and theoretical values. As mentioned previously in the discussion of the first test, the other portion of the load increase may have been due to compressive and tensile membrane action combined with arching action in the interior grillage beams.

As in the first test, the grillage was able to withstand a load greater than that normally considered the failure load, or in other words two stages of collapse were in evidence. After the predicted failure mode was achieved, loading was continued. At first the load dropped off to 3300 lbs. and then began to climb again. Figures 43 and 44, on pages 64 and 65, show that the maximum load achieved was 8390 lbs. This figure represents one of the concentrated loads, so that the total load withstood, was 16,780 lbs.

It is possible that this load could have been greater, as the test was terminated before total destruction. When the spreader-beam, separating the loads, came to rest upon the concrete at the center of the grillage, loading was discontinued. This, in effect, would have constituted a third point load, and analysis of such a loading system would have been very difficult. It is believed, as in the first test, that a hanging network of reinforcement or "plastic membrane" enabled the load to achieve such magnitude. Accurate analysis of stresses would again be most difficult, as several bars had broken and stress redistribution without strain gauges would be impossible to determine.

Crack development proceeded as expected in the second grillage test. Flexural cracks developed under the load points as well as at the junctions of the interior and exterior beams. As loading increased, the cracks increased in both length and width and the compressive zone of the beams gradually decreased. The increased stress in the compressive zone eventually reached the compressive strength of the concrete and the destruction of the compressive zone brought about flexural failure of the grillage.

At failure, the plastic hinges that formed at the junction of the interior transversal and interior longitudinal proved very interesting. The bending hinges formed exactly at the junction with the interior longitudinal and the cracking that developed could almost be classified as torsional. In any manner, the weakening of the interior longitudinal at these hinge locations, along with transformation of the interior beams into a "plastic" or "tensile membrane", led to a change of collapse mode as loading reached 4900 lbs. As mentioned earlier, this increased loading at large deflections will be more fully discussed in the general discussion.

Torsional cracks began appearing on the exterior beams at a load of 3200 lbs. These cracks were not of a severe nature just as in the first test. Again cracks due to bending were not severe on the exterior beams.

Deflection and rotation of the exterior beams was again small. The maximum deflection of an exterior beam was 0.268 inches at gauge location 2. Rotation at the center of the exterior longitudinals was 5 degrees 21 minutes or 0.09340 radians.

From the photographs of the test, it can be seen that shear and diagonal tension did not play a great role in the collapse of the structure at 4100 lbs. As loading progressed beyond this point some of the diagonal cracks that had formed earlier did open up and propagate. Flexural, not diagonal, failure was responsible for the collapse of the structure.

(c) General Discussion.

Collapse for both grillages tested, followed the same general pattern. Each grillage showed two distinct failure stages. In the first grillage the two stages were fully developed, whereas, in the second grillage only the first stage was clearly defined and further loading would have been necessary to develop the second stage.

As mentioned earlier, it is believed that both grillages resisted initial loading by bending action in combination with compressive membrane action. At this point in the loading the steel strains in the interior beams, at their junctions with the exterior beams, were tensile at the top and compressive at the bottom.

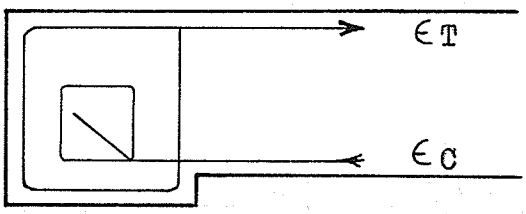

As deflection of the center portion of the interior beams increased, the membrane action changed from a compressive to a tensile one. At this point in loading, strains in the top and bottom steel were both tensile. The top steel in the interior beams probably had a large tensile strain, and stress in the steel would in all probability be the yield stress. The bottom steel, however, would have a smaller tensile strain as it was changing from a compressive to a tensile strain and the stress in the bars would be less than the yield stress. At this point the beams still possessed some bending resistance.

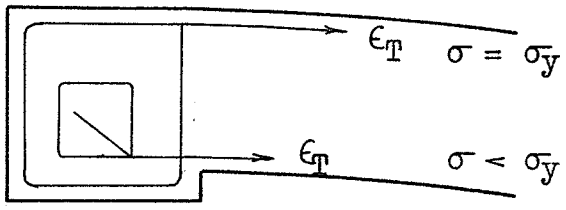

Continuation of deflection gradually produced changes in the geometry of the structure and the interior beam system was gradually transformed into a hanging network of reinforcement or a "tensile membrane". This phenomenon resulted in an increase of load with increasing deflection until the failure stress of the reinforcement bars was reached.

This development can be traced in the following simplified explanation.

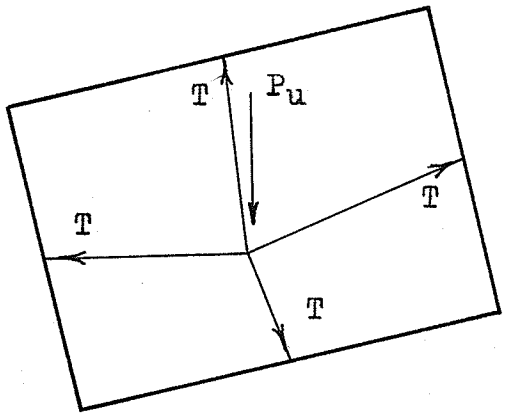

Taking a free body diagram of one of the members.

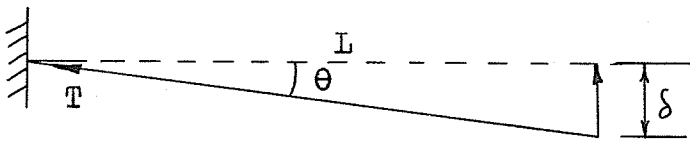

$$P_u = P_{conventional} + P_{additional}$$

$P_{conventional}$ represents the load that the structure is able to withstand by bending. In the early stages of loading, deflection is small and $P_{conventional}$ dominates the right hand side of the above equation. At this stage there is only a very small tensile force in the members so the vertical component of T is negligible. However, as deflection increases the load is resisted by a hanging network of reinforcement and the tensile force in the bars becomes significant. At this stage, $P_{additional}$, the vertical component of the tension forces in the members begins to dominate the right hand side of the equation and $P_{conventional}$ due to bending gradually disappears.

As deflection becomes quite large the length of the members increases due to strain and the following situation arises.

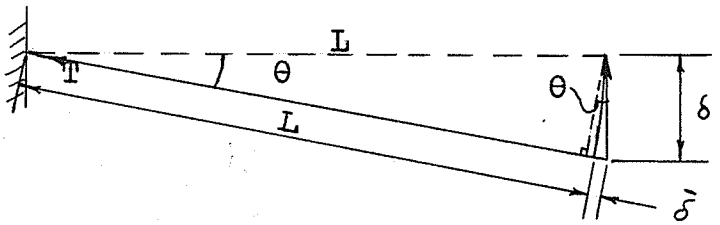

$$T = f(\delta)$$

As θ and δ increase, $\bar{\delta}$ increases as $\bar{\delta} = L(\sec\theta - 1)$ or

$$\bar{\delta} \cong \delta \sin\theta$$

Also $\bar{\delta} = \frac{TL}{AE}$ where $A = A_s$ and $E = E_s = 29{,}000{,}000$ psi.

$\therefore T = \frac{\bar{\delta}AE}{L}$ but $E = \frac{\sigma}{\epsilon}$, $\sigma =$ steel stress

and $\therefore T = \frac{\bar{\delta}A_s\sigma}{L\epsilon}$ as $\bar{\delta} = L\epsilon$

σ can now be σ_y or greater as in the strain hardening range.

Now $T = \frac{A_sE\bar{\delta}}{L} \cong \frac{A_sE\,\delta\sin\theta}{L}$ and

$$P_{additional} = T \sin\theta$$

Therefore, as the rotation of the beams increases, the tension force in the steel increases until the steel stress reaches its failure value. Thus $P_{additional}$ becomes larger as deflection increases and the ultimate load reaches the second failure stage or the ultimate strength of the hanging reinforcement network.

In order for this type of "tensile membrane" or "plastic membrane" to form, the beams must be restrained by rigid edge beams but they must also be free to rotate. This theory of increased loading with increased deflection helps to explain the two stages of failure for the grillages tested.

(d) Summary of Discussion.

Table IV offers a summary of experimental and analytical values (corrected for known beam strengths).

Table IV. Summary of Results.

Model	P_u Theoretical (lbs.)	P First Phase (lbs.)	Factor	P Second Phase (lbs.)
Grillage No. 1	4,140	5,380	1.30	8,300
Grillage No. 2	3,330	4,100	1.23	8,390

In general, both grillage models resisted loading in the same manner. In the first stage of failure, the grillage strength was due to bending action in conjunction with compressive and tensile membrane action. This membrane action was found to influence the ultimate load significantly in each of the models. As deflection became quite large, the structure was transformed into a "plastic membrane" and loading increased as deflection increased. This action accounted for the second phase of collapse which was evident in both grillage tests.

CHAPTER VI

CONCLUSIONS AND SUGGESTIONS FOR FURTHER RESEARCH

It may be concluded from the material presented in this study that the method of combined ultimate strength and plastic hinge theories is valid and safe when it is used in the analysis of reinforced concrete grillages. Although concentrated loads were used in this investiagation, any method of loading, concentrated loads, distributed loads or combinations of the two can be applied to any form of grillage and a collapse mechanism can be found fairly readily.

In the design of reinforced concrete sections, it is generally accepted that the plastic design method is a more logical and economical one than the elastic method. However, when the ultimate strength and plastic hinge theories are applied to a structure, the analyst must bear in mind certain limitations pertaining to the properties of materials, their relation to one another and limitations which arise in cases of extremely severe types of loading. The accuracy of this method of analysis is dependent to a great extent of the accuracy with which the ultimate strength of the separate elements can be predicted under various loading conditions.

One of the most difficult areas in which a prediction must be made is that of shear and diagonal tension. In the tests conducted for this study, the individual members were over-designed for shear and the problem of a premature shear failure did not occur. Another area to guard against is the formation of "brittle hinges" in which case failure would be catastrophic.

Another important factor upon which the ultimate

strength and plastic hinge theories depend is the availability of ductility in areas of the structure where plastic hinges may form. Too little or too much steel may affect the ductility of a section and the plastic moment may not be reached. Visual evidence during the tests showed that there was adequate ductility in the grillages tested and this indicates that rotations at plastic hinges do not necessarily have to be calculated for similar grillages.

Both grillage models had two stages of collapse. For the first stage, the actual collapse loads were larger than the predicted loads. Larger than design concrete and steel strengths accounted for a portion of the increased loads. Compressive and tensile membrane forces acting in conjunction with arching action were proposed as other factors affecting the failure load. Increased loading occurred after the first stage of collapse as the deflections of the interior members increased. To explain this phenomenon, it was suggested that the structures had become "plastic" or "tensile membranes". A characteristic of this type of hanging reinforcement network is that its strength is limited only by the limit of plastic elongation of the reinforcement. The strength exhibited by this system is greatly in excess of that found by ultimate strength analysis.

In the original analytical analysis of the exterior members of both grillages, the bending strengths were underestimated. Dowel bars, used at the centers of all exterior members to anchor interior beam steel, were found to influence ultimate moment to a fairly large degree. Increased concrete and steel strengths also added to greater moment capacity. Actual torsional strengths of exterior grillage members agreed fairly well with predicted values even though the yield strength of the tie reinforcing was slightly below the assumed value.

It is the author's considered opinion that further research into the behaviour of grillages will yield valuable information in making the ultimate strength and plastic hinge theories a useful tool for the analysis of composite concrete structures. Further grillage tests should attempt to duplicate as closely as possible actual practical designs. In the tests conducted by the author, the exterior members were deliberately made excessively strong so that failure modes could readily be predicted. Although the tests proved successful and provided needed preliminary results, more research is required in similar as well as more complicated grillages.

Work in this field is at present going ahead at the University of Manitoba. Several concrete beam and slab structures have already been tested and at this writing a relatively complicated grillage system is being tested.

Two other areas of research could contribute to grillage frame use and knowledgeable application. These areas are the effects of repeated loads and the predictability of limit design techniques.

This study provides only preliminary findings in a very complex field of research. It is hoped that the data gathered here, used in conjunction with other research, will eventually lead to a valid method of predicting the ultimate strength of composite concrete structures.

BIBLIOGRAPHY

1. Whitney, C.S. — "Plastic Theory of Reinforced Concrete Design". Proc. A.S.C.E., Dec. 1940; Trans. A.S.C.E. v.107, 1942, pp.251-282.

2. Evans, R.H. — "The Plastic Theories for the Ultimate Strength of Reinforced Concrete Beams". Jour. I.C.E. v.21, n.2, Dec. 1943, pp.88-121.

3. Baker, A.L.L. — "Further Research in Reinforced Concrete, and its Application to Ultimate Load Design". Proc. I.C.E. v.2, Pt.III, Aug. 1953, pp.269-310.

4. Hognestad, E., Hanson, N.W. and McHenry, D. — "Concrete Stress Distribution in Ultimate Strength Design". Jour. A.C.I., v.27, n. 4, Dec. 1955 (Proc. v.52), pp.455-479.

5. Baker, J.F., Horne, M. R. and Heyman, J. — "The Steel Skeleton". Vol. 2: "Plastic Behaviour and Design". (Cambridge University Press. 1956.) p.408.

6. Ernst, G.C. — "Moment and Shear Redistribution in Two Span Continuous Reinforced Concrete Beams". A.C.I. Jour., v.30, n.5, Nov. 1958, pp.573-589.

7. Jones, L.L. "Ultimate Load Analysis of Reinforced and Prestressed Concrete Structures". Chatto and Windus Ltd., London, 1962.

8. Lansdown, A.M. "An Investigation into the Ultimate Behaviour of Reinforced Concrete Beam and Slab Structures, in particular Bridge Decks". Ph.D. Thesis, University of Southampton, June 1964.

9. Nylander, H. "Torsion and Torsional Restraint of Concrete Structures". Statens Kommitte for Byggnadsforskning, Meddelanden No. 3, 1945, pp.138.

10. Cowan, H.J. and Armstrong, S. "Experiments on the Strength of Reinforced and Prestressed Concrete Beams and of Concrete-Encased Steel Joists in Combined Bending and Torsion". Magazine of Concrete Research, v.7, n.19, March 1955, pp.3-20.

11. Yih, J.C. "Model Studies of Reinforced Concrete Skew Slab and Beam Bridges Under Ultimate Loads". M.Sc. Thesis, University of Manitoba, March 1967.

12. Kani, G.N.J. "The Riddle of Shear Failure and Its Solution". Journal A.C.I., v. 61, n. 4, April 1964, pp.441-467.

13. Teerachaichayuti, S. "A Study of Reinforced Concrete Beam and Slab Bridge Decks Under Ultimate Loads". M.Sc. Thesis, University of Manitoba, April 1968.

14. Cowan, H.J. "Reinforced and Prestressed Concrete in Torsion". Edward Arnold Publishers Ltd., London, 1965.

15. ACI Committee 438, Torsion. "Torsion of Structural Concrete". A.C.I. Publication SP-18, 1968.

16. ACI Committee 318. "Building Code Requirements for Reinforced Concrete". (A.C.I. 318-63), June 1963.

17. Chan, W.W.L. "The Ultimate Strength and Deformation of Plastic Hinges in Reinforced Concrete Frameworks". Magazine of Concrete Research, n. 21, Nov. 1955, pp.121-132.

18. Pfrang, E.O., Siess, C.P. and Sozen, M.A. "Load-Moment-Curvature Characteristics of Reinforced Concrete Cross Sections". Journal A.C.I., v. 61, n. 7, July 1964, pp.763-778.

19. ACI-ASCE Committee 326. "Report on Shear and Diagonal Tension". Journal A.C.I., v. 59, n. 1, Jan. 1962, pp.1-30; n. 2, Feb. 1962, pp.277-333; n. 3, Mar. 1962, pp.353-395.

20. Reese, R.C. "CRSI Design Handbook, Working Stress Design, Revised". Concrete Reinforcing Steel Institute, Chicago, 1965.

21. Reese, R.C. "Floor Systems By Ultimate Strength Design". Concrete Reinforcing Steel Institute, Chicago, 1968.

22. Mattock, A.H. "Rotational Capacity of Hinging Regions in Reinforced Concrete Beams". Flexural Mechanics of Reinforced Concrete, ASCE-1965-50, ACI SP-12.

23. Wood, R.H. "Plastic and Elastic Design of Slabs and Plates". Thames and Hudson, London, 1961.

APPENDIX A

DESIGN OF GRILLAGE BEAMS

1) Reinforcement for Exterior Beams.

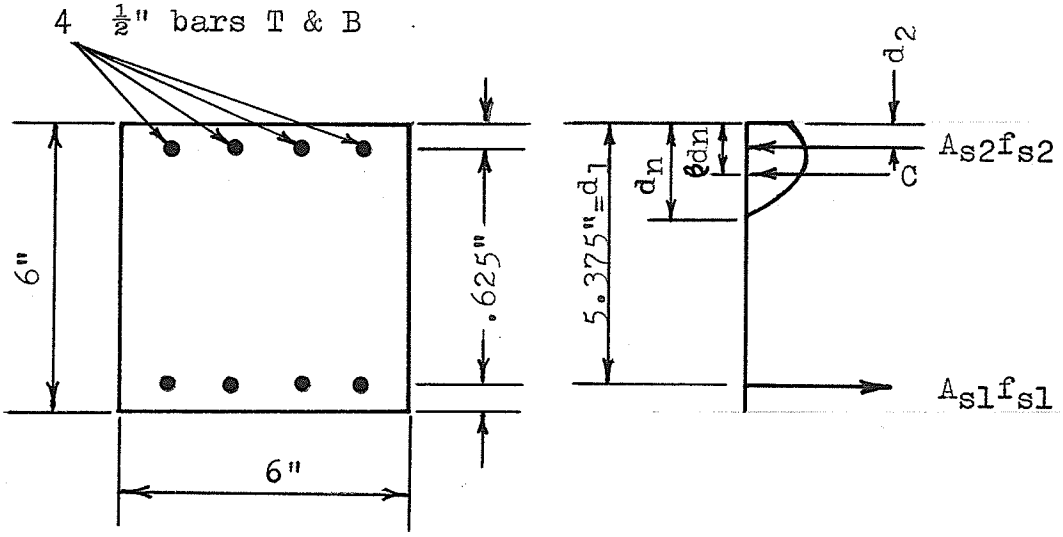

BEAM SECTION FORCE DIAGRAM

For f'_c = 3,000 psi.

$$f_{pr'} = 0.85\ f'_c \qquad u = \frac{f'_c}{.78}$$

$$A_{s1}f_{s1} = \alpha u b d_n + A_{s2}f_{s2}$$

u = 3,850 psi.
αu = 2,380 psi.
β = 0.462
ε_c = 0.00353

$A_{s1}f_{s1} = A_{st}f_{st}$ $\qquad$ $A_{s2}f_{s2} = A_{sc}f_{sc}$

f_{yt} = 40,000 psi. f_{yc} = 36,000 psi.

$$d_n = \frac{9}{4ub} (A_{st}f_{yt} - A_{sc}f_{yc})$$

$$= \frac{9}{4 \times 3{,}850 \times 6} (.8 \times 40{,}000 - .8 \times 36{,}000)$$

$$= \frac{9}{4 \times 3{,}850 \times 6} (32{,}000 - 28{,}800)$$

$$= \frac{9}{96{,}200} (3{,}200)$$

$$= 0.3 \text{ inches}$$

$$M_u = \frac{4}{9} ubd_n (d_1 - \tfrac{1}{2}d_n) + A_{sc}f_{yc} (d_1 - d_2)$$

$$= \frac{4}{9} \times 3{,}850 \times 6 \times .3 (5.375 - .150) + .8 \times 36{,}000(4.75)$$

$$= 16{,}100 + 136{,}900 = \underline{153{,}000 \text{ in.-lbs.}}$$

2) Reinforcement for Interior Beams.

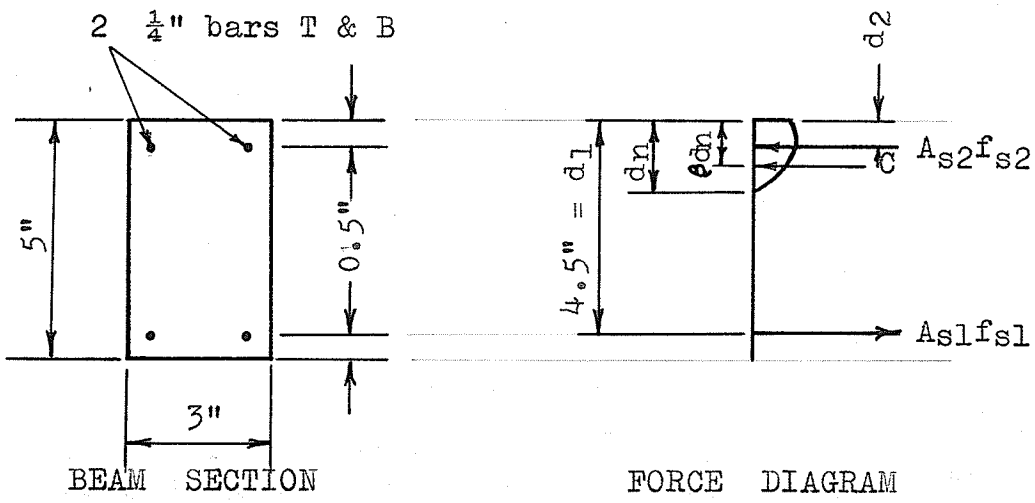

For f'_c = 3,000 psi.

$$f_{pr'} = 0.85f'_c \qquad u = \frac{f'_c}{.78}$$

$$A_{s1}f_{s1} = \alpha u b d_n + A_{s2}f_{s2}$$

$$u = 3{,}850 \text{ psi.}$$
$$\alpha u = 2{,}380 \text{ psi.}$$
$$\beta = 0.462$$
$$\varepsilon_c = 0.00353$$

$$A_{s1}f_{s1} = A_{st}f_{st} \qquad A_{s2}f_{s2} = A_{sc}f_{sc}$$

$$f_{yt} = 40{,}000 \text{ psi.} \qquad f_{yc} = 36{,}000 \text{ psi.}$$

$$d_n = \frac{9}{4ub}\left(A_{st}f_{yt} - A_{sc}f_{yc} \right)$$

$$= \frac{9}{4 \times 3{,}850 \times 3}\left(.1 \times 40{,}000 - .1 \times 36{,}000 \right)$$

$$= \frac{300}{3{,}850} = 0.078 \text{ inches}$$

$$M_u = \frac{4}{9} u b d_n \left(d_1 - \tfrac{1}{2}d_n \right) + A_{sc}f_{yc}\left(d_1 - d_2 \right)$$

$$= \frac{4}{9} \times 3{,}850 \times 3 \times 0.078 \left(4.422 \right) + 0.1 \times 36{,}000 \left(4 \right)$$

$$= 1{,}770 + 14{,}400$$

$$= \underline{16{,}170 \text{ in.-lbs.}}$$

3) Calculation of Torsional Moment for Exterior Beams.

With calculation based on the Lansdown Method and referring to previous discussion on page 75,

$$M_T = 2.536\ A_{cage}\ R_{min}\ .$$

For both grillages:

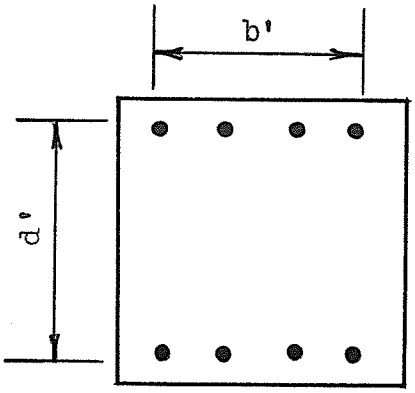

$A_{cage} = 5.5 \times 5.5 = 30.25 \quad in.^2$

$C = 2(b' + d') = 2(5.5 + 5.5) = 22$ in.

pitch = p = 1 in.

$F_{YL} = 40{,}000$ psi. $\qquad F_{YT} = 40{,}000$ psi.

Area of #11 gauge wire = 0.010 $in.^2$

$$\therefore R_L = \frac{nF_{YL}}{C} = \frac{8 \times 0.20 \times 40{,}000}{22} = 2{,}910 \text{ lb/in.}$$

where n = number of longitudinal bars

$$R_T = \frac{F_{YT}}{p} = \frac{0.010 \times 40{,}000}{1} = 400 \text{ lb/in.}$$

The equivalent helix force then becomes the lesser of R_T and R_L , i.e. $R_{min.}$, therefore $R_T = R_{min.}$

$$\therefore M_T = 2.536\ A_{cage}\ R_{min}$$

$$= 2.536 \times 30.25 \times 400$$

$$= \underline{30{,}700 \text{ in.-lbs.}}$$

APPENDIX B

LOAD-DEFLECTION READINGS

TESTS 1a and 2.

Dial Gauge Readings in Inches, Load Readings in Pounds.

Gauge / Load	1	2	3	4	6	7	8	10	11	12	13	Lat. Defl'n. 14	Lat. Defl'n. 15
0													
90	0	0	0	0	0	0	0	0	0	0	0	0	0
270	.003	.003	0	.005	.005	.007	.009	.005	.003	.003	.002	0	0
470	.005	.006	0	.011	.010	.014	.010	.011	.006	.006	.005	0	0
660	.008	.010	.002	.017	.015	.021	.016	.017	.008	.010	.007	0	0
870	.010	.013	.005	.023	.020	.029	.021	.023	.010	.013	.009	0	0
1060	.013	.018	.008	.034	.030	.047	.030	.034	.014	.018	.012	0	.001
1260	.016	.022	.011	.042	.036	.058	.037	.043	.017	.022	.016	.001	.001
1450	.019	.026	.014	.050	.044	.069	.045	.051	.020	.027	.019	.001	.002
1650	.023	.031	.018	.059	.052	.083	.052	.061	.024	.032	.022	.001	.002
1850	.026	.036	.021	.070	.060	.096	.061	.071	.028	.038	.026	.002	.003
2050	.030	.041	.037	.081	.070	.113	.070	.083	.032	.043	.029	.002	.003
2250	.034	.047	.038	.096	.083	.134	.085	.099	.036	.048	.033	.002	.004
2430	.039	.054	.038	.111	.096	.155	.098	.115	.041	.055	.037	.002	.005
2630	.043	.060	.038	.125	.107	.173	.112	.120	.045	.062	.042	.003	.005
2830	.048	.066	.043	.139	.118	.192	.123	.142	.050	.069	.047	.003	.006
3030	.052	.072	.047	.155	.133	.216	.137	.158	.055	.075	.051	.003	.007
3220	.056	.078	.051	.169	.148	.239	.151	.174	.060	.082	.056	.004	.007
3420	.061	.085	.056	.187	.166	.268	.169	.192	.065	.089	.060	.005	.008
3600	.065	.090	.061	.206	.184	.298	.187	.211	.070	.095	.065	.005	.008
3800	.070	.097	.066	.229	.204	.338	.208	.234	.076	.104	.071	.006	.009
4000	.078	.106	.074	.256	.229	.381	.233	.262	.083	.113	.077	.007	.010
4200	.082	.113	.078	.278	.248	.418	.252	.284	.088	.120	.082	.007	.011
4400	.088	.120	.084	.303	.271	.459	.275	.308	.094	.128	.088	.008	.012
4600	.093	.127	.091	.337	.302	.519	.305	.342	.100	.137	.095	.008	.013
4780	.101	.137	.099	.395	.354	.620	.356	.398	.108	.147	.102	.009	.014
4980	.109	.148	.107	.482	.435	.775	.436	.484	.115	.156	.109	.010	.016
5180	.118	.160	.118	.610	.560	1.013	.561	.613	.124	.166	.118	.010	.016
5380	.126	.170	.125	.745	.687	1.255	.686	.745	.134	.179	.128	.011	.016
5000	.134	.181	.135	1.009	.957	1.784	.956	1.027	.143	.210	.138	.010	.015
5080	.139	.185	.132	1.102	1.150	1.962	1.037	1.117	.146	.219	.140	.010	.015
4980	.140	.187	.133	1.373	1.331	2.517	1.342	1.382	.150	.230	.143	.009	.013

Steel Scale Readings in Inches, Load Readings in Pounds.

Gauge / Load	1	2	3	4	5	6	7	8	9	10	11	12	13
0													
90	0	0	0	0	0	0		0	0	0	0	0	0
270	0	.01	0	.01	0	0		.01	0	0	0	.01	0
470	0	.01	0	.01	0	.01		.01	0	.01	.01	.01	.01
660	.01	.01	0	.02	0	.01		.02	0	.01	.01	.01	.01
870	.01	.02	.01	.03	0	.02		.02	0	.02	.01	.02	.01
1060	.01	.02	.01	.04	0	.03		.03	0	.03	.01	.02	.01
1260	.02	.03	.02	.05	0	.04		.04	.01	.04	.02	.03	.02
1450	.02	.03	.02	.05	.01	.04		.05	.01	.05	.02	.03	.02
1650	.02	.04	.02	.06	.01	.05		.05	.01	.06	.02	.04	.02
1850	.03	.04	.03	.07	.01	.06		.06	.01	.07	.03	.04	.03
2050	.03	.05	.03	.08	.01	.07		.07	.01	.08	.03	.05	.03
2250	.04	.05	.03	.10	.01	.08		.09	.01	.09	.04	.05	.03
2430	.04	.06	.04	.12	.01	.09		.10	.01	.11	.04	.06	.04
2630	.04	.06	.04	.13	.01	.11		.11	.02	.12	.04	.07	.04
2830	.05	.07	.05	.15	.02	.12		.13	.02	.13	.05	.07	.05
3030	.05	.08	.05	.16	.02	.13		.14	.02	.15	.06	.08	.05
3220	.06	.09	.05	.17	.02	.15		.15	.02	.17	.06	.09	.06
3420	.06	.09	.06	.19	.02	.16		.17	.03	.18	.07	.09	.06
3600	.07	.10	.06	.21	.02	.18		.19	.03	.20	.07	.09	.06
3800	.07	.10	.07	.23	.03	.20		.20	.03	.22	.07	.10	.06
4000	.08	.11	.07	.26	.03	.23		.23	.04	.25	.08	.11	.07
4200	.08	.12	.08	.28	.03	.24		.25	.04	.27	.08	.12	.08
4400	.09	.13	.09	.31	.04	.27		.27	.04	.29	.09	.12	.08
4600	.09	.13	.09	.34	.04	.30		.30	.04	.33	.09	.14	.09
4780	.10	.14	.10	.40	.04	.35		.35	.04	.38	.10	.14	.09
4980	.11	.15	.10	.49	.05	.43		.44	.05	.46	.11	.15	.11
5180	.12	.16	.12	.62	.05	.55	1.013	.56	.05	.59	.12	.16	.11
5380	.12	.17	.12	.76	.06	.68	1.253	.69	.06	.72	.13	.17	.12
5000	.13	.19	.13	1.05	.06	.96	1.783	.95	.06	.99	.13	.18	.13
5080	.13	.18	.13	1.15	.06	1.05	1.953	1.15	.07	1.08	.14	.18	.13
4980	.14	.19	.14	1.45	.07	1.34	2.493	1.32	.07	1.35	.14	.18	.13

Table VII. Load-Deflection Readings, Test No. 2.

Dial Gauge Readings in Inches, Load Readings in Pounds.

Gauge / Load	1	2	3	4	6	7	8	9	10	12	13	14	15
0	0	0	0	0	0	0	0	0	0	0	0	0	0
135	0	.005	.003	.008	0	.008	.009	.042	.004	.008	.003	.004	.002
330	0	.012	.008	.019	0	.051	.022	.042	.013	.019	.008	.009	.007
530	0	.019	.013	.029	.003	.063	.036	.045	.019	.029	.011	.016	.011
725	.002	.026	.018	.041	.012	.077	.051	.060	.029	.041	.017	.023	.016
925	.009	.037	.025	.061	.033	.102	.077	.085	.041	.059	.024	.032	.023
1125	.019	.050	.034	.086	.047	.132	.109	.118	.063	.084	.032	.043	.031
1315	.029	.062	.042	.110	.066	.164	.140	.146	.084	.108	.039	.055	.040
1515	.037	.074	.051	.137	.085	.196	.177	.183	.104	.135	.048	.066	.047
1610	.043	.081	.056	.150	.095	.212	.194	.200	.114	.148	.052	.072	.052
1710	.047	.087	.060	.163	.104	.226	.209	.215	.124	.159	.056	.077	.056
1800	.052	.093	.065	.176	.114	.240	.226	.231	.133	.171	.060	.084	.061
1900	.057	.100	.070	.188	.123	.255	.241	.246	.143	.183	.064	.089	.065
2000	.061	.105	.073	.199	.131	.268	.256	.260	.151	.194	.068	.094	.070
2100	.067	.114	.079	.215	.143	.287	.276	.278	.162	.209	.073	.101	.073
2300	.075	.126	.088	.239	.163	.319	.308	.308	.182	.233	.082	.112	.082
2490	.086	.140	.098	.268	.185	.354	.345	.344	.206	.260	.092	.126	.091
2690	.094	.151	.108	.291	.204	.382	.376	.373	.222	.284	.100	.136	.099
2890	.105	.165	.117	.321	.227	.420	.415	.413	.250	.313	.109	.149	.109
3090	.113	.176	.124	.347	.248	.454	.451	.446	.271	.338	.117	.159	.116
3285	.120	.186	.131	.376	.274	.499	.499	.496	.300	.369	.123	.168	.122
3850	.158	.237	.168	.555	.436	.777	.806	.810	.474	.553	.159	.215	.158
4100	.178	.261	.186	.716	.587	1.045	1.097	1.108	.636	.719	.176	.238	.175
4100					1.005	1.666	1.768	1.769	.705				
4100	.197	.285	.202	1.272	1.204	2.036	2.148	2.128	.895	1.269	.190	.254	.187
3725	.198	.285	.202	1.650	1.581	2.766	2.899	2.832	1.257	1.644	.188	.250	.283
3285	.189	.268	.191	2.549		4.456	4.733	4.556		2.563	.178	.235	.274

Table VIII. Load-Deflection Readings, Test No. 2.

Steel Scale Readings in Inches, Load Readings in Pounds.

Gauge / Load	1	2	3	4	5	6	8	10	11	12	13	14	15
0	0	0	0	0	0	0	0	0	0	0	0	0	0
135	.01	.01	0	.01	0	0	0	.01	0	.01	0	.01	.01
330	.01	.02	.01	.02	.01	.01	.015	.01	0	.02	.01	.02	.01
530	.01	.02	.01	.03	.01	.02	.031	.02	0	.03	.01	.02	.02
725	.02	.03	.02	.04	.01	.03	.047	.04	.01	.04	.02	.02	.02
925	.03	.04	.02	.06	.01	.04	.078	.05	.01	.06	.03	.04	.03
1125	.04	.05	.03	.09	.02	.06	.109	.07	.01	.08	.03	.05	.03
1315	.05	.07	.04	.11	.02	.08	.141	.08		.10	.04	.06	.05
1515	.06	.08	.05	.14	.03	.10	.172	.10		.13	.05	.07	.05
1610	.06	.09	.05	.15	.03	.11	.188	.12		.14	.05	.08	.06
1710	.07	.09	.06	.17	.03	.12	.203			.15	.06	.08	.06
1800	.07	.10	.07	.17	.04	.13	.219			.17	.06	.09	.06
1900	.08	.11	.07	.19	.04	.14	.234			.18	.06	.09	.07
2000	.08	.11	.08	.20	.04	.15	.250			.19	.07	.10	.08
2100	.09	.12	.08	.22	.04	.16	.266		.04	.20	.07	.10	.07
2300	.09	.12	.08	.24	.04	.17	.297	.19	.04	.22	.08	.11	.08
2490	.10	.14	.10	.27	.05	.20	.344	.21	.05	.25	.09	.12	.09
2690	.11	.15	.10	.29	.05	.22	.375	.23	.05	.28	.10	.14	.10
2890	.12	.16	.11	.32	.06	.24	.406	.26	.06	.30	.10	.15	.11
3090	.13	.17	.12	.34	.06	.26	.438	.28	.06	.33	.11	.16	.12
3285	.14	.19	.14	.38	.07	.29	.500	.32	.07	.37	.13	.17	.13
3850	.18	.24	.17	.56	.10	.45	.797	.49	.10	.55	.16	.22	.17
4100	.20	.27	.20	.72	.11	.60	1.078	.65	.11	.71	.18	.24	.19
4100													
4100	.22	.29	.21	1.28	.13	1.14	2.203	1.19	.12	1.25	.19	.26	.20
3725	.22	.29	.21	1.68	.13	1.52	2.953	1.55	.11	1.61	.19	.25	.20
3285	.21	.27	.21	2.66	.12	2.47	4.703	2.46	.11	2.54	.18	.24	.18

APPENDIX C

TESTS OF GRILLAGE ELEMENTS

When the two grillage tests were completed, the exterior beams of both grillages were still in good condition. One grillage was then cut apart using an electrical power saw with a diamond tip blade. The two exterior transversals were used in torsion tests, while the two exterior longitudinals were subjected to flexural tests.

FLEXURAL TESTS.

The loading configuration for the flexural tests was as appears in the following diagram.

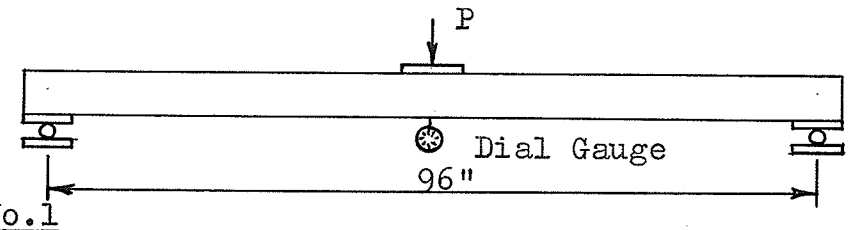

BEAM No.1

Load (lbs.)	Deflection (in.)	Load (lbs.)	Deflection (in.)
2,000	0	11,300	2.040
4,000	0.139	11,500	2.460
5,000	0.202	11,600	2.672
6,000	0.268	11,700	2.870
7,000	0.326	11,600	3.360
8,000	0.398	11,700	3.630
9,000	0.475	11,900	3.850
10,000	0.576	11,800	4.140
10,040	0.717	11,000	4.678
10,900	1.345	11,400	4.894
11,000	1.446	11,450	5.265
11,000	1.615	11,450	5.528
11,100	1.930	Max. Load = 11,900 lbs.	

BEAM No.2

Load (lbs.)	Deflection (in.)	Load (lbs.)	Deflection (in.)
2,000	0	12,000	2.791
4,000	0.144	12,260	2.836
5,000	0.179	12,560	2.900
6,000	0.242	12,000	3.036
7,000	0.304	12,170	3.177
8,000	0.364	12,280	3.265
9,000	0.432	12,470	3.346
10,000	0.514	11,790	3.555
11,000	0.674	12,250	3.598
11,180	0.997	12,320	3.654
11,220	1.203	12,250	3.774
11,420	1.360	12,400	3.872
11,540	1.603	12,040	4.066
12,000	1.775	12,380	4.126
12,000	1.897	12,590	4.233
12,000	2.194	12,000	4.468
12,140	2.250	12,080	4.684
11,900	2.460	12,470	4.778
12,000	2.483	12,000	5.019
12,170	2.523	11,800	5.263
12,280	2.584	12,450	5.339
11,820	2.759	Max. Load = 12,590 lbs.	

The average maximum load = $\frac{11,900 + 12,590}{2}$ = 12,245 lbs.

$\therefore$ The average $M_u = \frac{Pl}{4} = \frac{12,245 \times 96}{4}$ = 294,000 in.-lbs.

Ratio of Actual to Originally Predicted Moment = $\frac{294,000}{153,000}$ = 1.92

Reasons for the large difference in values were increased concrete strength, increased steel strength and the effect

of the four #4 dowel bars present at the center of the exterior beams for interior beam steel anchorage. In the original analysis the dowel bars were not considered in moment calculations. If increased concrete strength, increased steel strength and the effect of dowel bars are considered, the following ratio exists.

$$\text{The Ratio of Actual to Predicted Moment} = \frac{294,000}{237,100} = 1.24$$

This figure presents a more realistic value between predicted and test values. A typical exterior beam after testing can be seen in Figure 55, page 121.

TORSIONAL TESTS.

The two exterior transversal bars were tested in a torsion machine. The test setup can be seen in Figure 56, page 121.

BEAM No. 1

Moment (in.-lbs.)	Degrees of Rot.	Comments
30,000		First cracks appear and apparent yield.
45,880	28	Max. moment; cracks opening and concrete spalling off.
	90	Max. rotation.

BEAM No. 2

Moment (in.-lbs.)	Degrees of Rot.	Comments
31,300		First cracks appear and apparent yield.
44,800	25	Max. moment; cracks opening and concrete spalling off.
	82	Max. rotation.

The average yield moment = $\frac{30,000 + 31,300}{2}$ = 30,650 in.-lbs.

Ratio of Actual to Predicted Moment = $\frac{30,650}{30,700}$ = .999

If actual yield strengths for the longitudinal and tie steel are used in recalculating predicted torsional strength, the yield or ultimate moment becomes 26,150 in.-lbs. The ratio of actual to predicted strenghts now becomes 1.17. The two ratios show excellent agreement between predicted and actual values. The two transversals tested can be seen in Figures 57 and 58 on page 122.

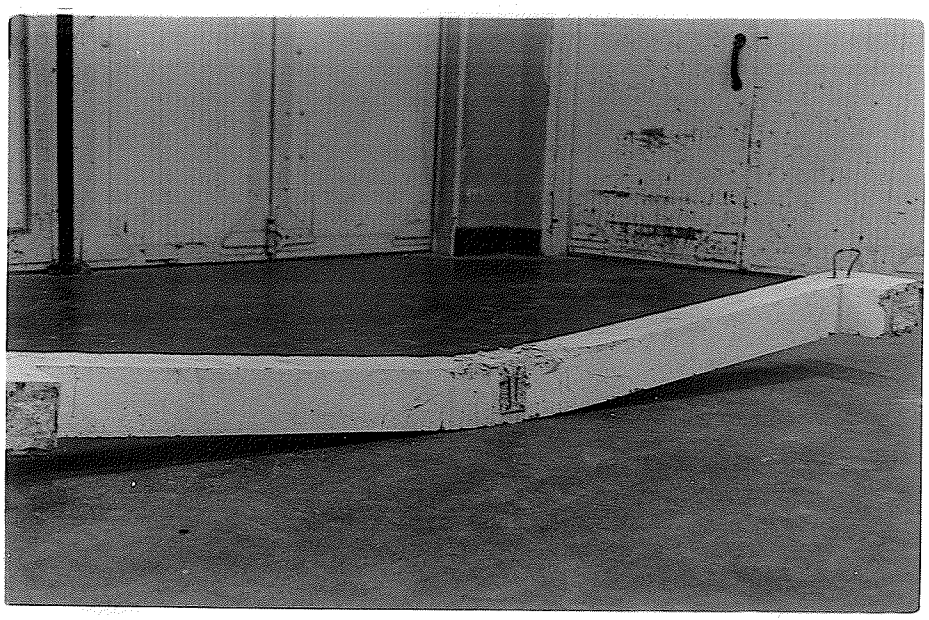

Figure 55. Longitudinal at End of Flexural Test.

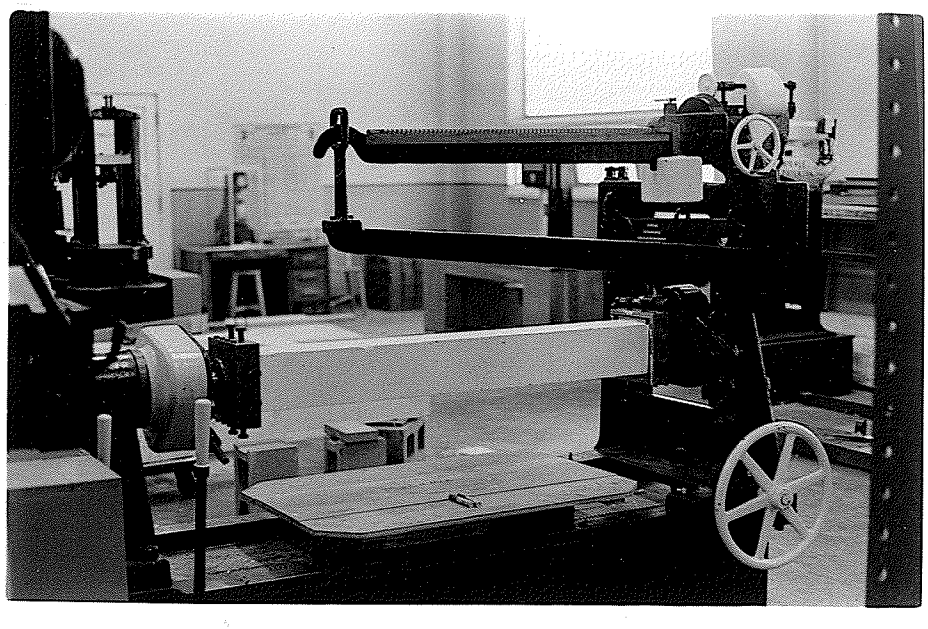

Figure 56. Testing Apparatus for Torsion Test.

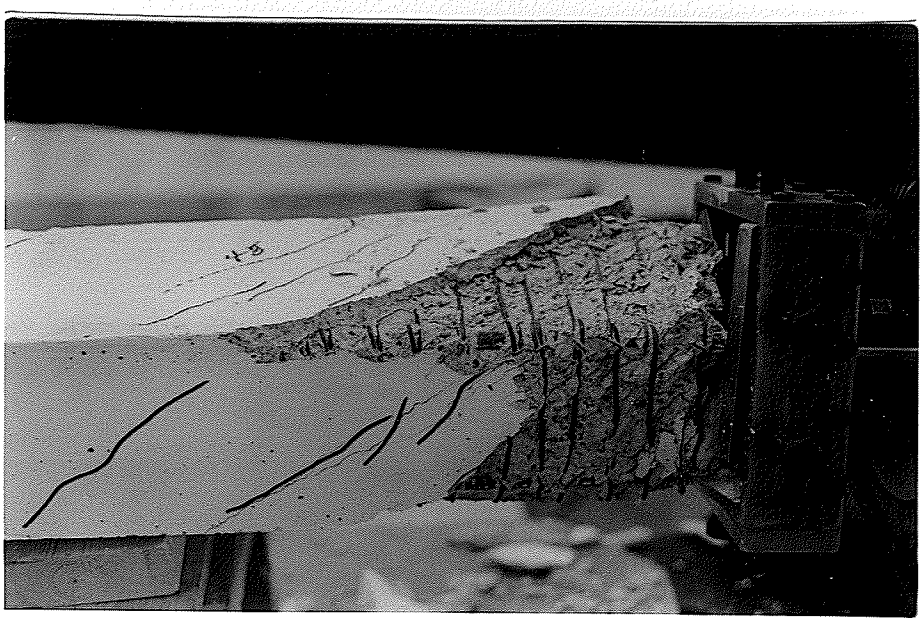

Figure 57. First Beam at End of Torsion Test.

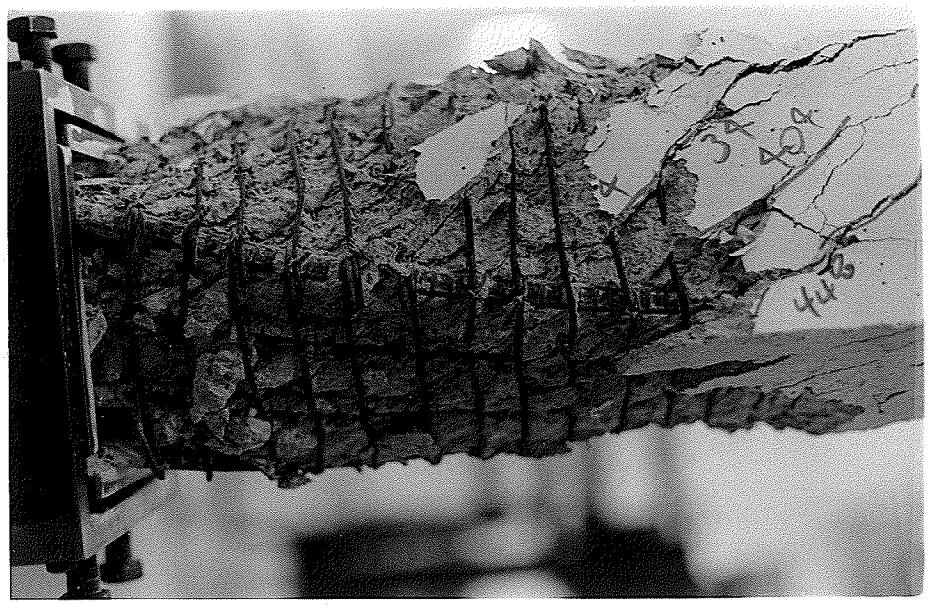

Figure 58. Second Beam at End of Torsion Test.